Stable Isotopes in Oceanographic Studies and Paleotemperatures

SPOLETO 1965

EDITOR E. TONGIORGI

CONSIGLIO NAZIONALE DELLE RICERCHE
LABORATORIO DI GEOLOGIA NUCLEARE - PISA

Deuterium and oxygen 18 variations in the ocean and the marine atmosphere

H. CRAIG and L. I. GORDON

Department of Earth Sciences and Scripps Institution of Oceanography, University of California, La Jolla, California

« The sea is the source of the waters, and the source of the winds. Without the great sea, not from the clouds could come the flowing rivers or the heaven's rain: but the great sea is the father of clouds, of rivers and of winds ».

Xenophanes of Colophon, ca. 500 B.C.
(translated by Aubrey de Selincourt)

INTRODUCTION

This paper describes the experimental and theoretical results we have obtained in our study of the variations of the hydrogen and oxygen isotopic abundances in the sea and the atmosphere. The principal stable molecular species are present in the following proportions:

H_2O^{16}	1,000,000
HDO	320
H_2O^{18}	2000

these being the approximate molecular parts per million in mean sea water. The varying proportions of these molecules in sea water provide an oceanographic tracer like salinity, but with an extra degree of freedom: salt is a tracer for the oceanic fluid, but the isotopic composition is a tracer specifically for the water component of the fluid. Of course if the molecules always occur in the same proportions relative to the salinity they would be no

more useful than one of the elements comprising the « compound » we refer to as salinity. That this is not the case was shown in the first mass spectrometric investigations of these isotopes in the sea: the oxygen 18 study of EPSTEIN and MAYEDA (1953) and the deuterium study of FRIEDMAN (1953). In particular, EPSTEIN and MAYEDA observed that the oxygen-18/oxygen-16 ratio was different in regions of considerable melt water influx from the ratio, for waters of the same salinity, in open ocean areas.

The emphasis in these first studies was on the range and nature of the isotopic variations rather than on interpretation in terms of the meteorological and oceanographic processes established by classical research; the importance of their work was the demonstration that the isotopic variations were sufficiently great to provide an excellent tracer for oceanographic and meteorological research. In the ocean for example, we can write three mixing equations in any particular application, for mass, salinity, and enthalpy or temperature. Carbon 14 has added another variable, and BOLIN and STOMMEL (1961) have used this isotope to form systems of four equations for the study of deep water genesis. However, the distribution of this isotope is at present not at all well understood, particularly in the southern oceans. Also the use of temperature as a variable requires a term for the enthalpy influx from the bottom into the deep water masses, and the carbon 14 concentrations in surface and intermediate waters have been changing in an uncertain manner due to production of this isotope in nuclear tests. We are also studying the use of the rare gases in sea water as oceanographic tracers, but the accurate measurement of these gas concentrations is very difficult, as is shown by the discrepancies between the results of MAZOR, WASSERBURG and CRAIG (1964) and those of BIERI, KOIDE and GOLDBERG (1964).

If we examine the precision of measurement of different tracers relative to the magnitude of the differences between deep water masses, we find that temperature and salinity can be measured to about 1-2 percent of the differences, while the D/H and O^{18}/O^{16} ratios can be measured to about 10 percent of the differences. Carbon 14 also falls in the 10 percent class, while the precision on rare gases at present would be about 30-40 percent.

Considering the ease of measurement, the sample collection problems, the analytical equipment required, and the size of the ocean and the amount of work involved in synoptic studies, we believe the hydrogen and oxygen isotopes offer the best possibility for development as a routine oceanographic tool which can be used by a number of institutions. This is not to say that the work is anywhere as easy as the routine measurements of temperature and salinity, which the oceanographers have developed to a very high order of precision and dependability; a sizable investment of time and highly trained technicians are required in order to get the necessary precision for isotopic measurements. Despite this drawback, they offer a promising method for oceanographic studies; the hydrogen and oxygen isotopes are the variables most intimately related to the actual water in the sea, and they furnish a direct link to the water in the atmosphere and on the continents, and to the evaporation and precipitation cycle which causes the salinity variations.

In our work to date we have concentrated principally on the oxygen 18 variations because of the direct relationship to paleotemperature studies which require a knowledge of the oxygen isotope variations in the sea in space and time. Our work on deuterium to date has been principally on understanding the ocean-atmosphere exchange of water and we shall discuss both isotopic species in this context.

The latter half of this paper, dealing with the evaporation-exchange theory, was presented in detail at the 1964 Spoleto Conference on Isotopic Variations in Natural Waters. It is published in this volume with the oceanic work in order to provide a single paper on our studies of the ocean-atmosphere isotope effects.

EXPERIMENTAL METHODS

The isotopic ratios are always compared to those in a standard material on the mass spectrometer as this results in much greater precision than a direct analysis of the absolute ratios. It is necessary to define a standard for expressing the data; the standard in general use is the SMOW (standard mean ocean water) defined in

terms of a water standard distributed by the National Bureau of Standards (CRAIG, 1961b). The isotopic data are expressed as delta units defined by:

$$R/R_{SMOW} = 1 + \delta$$

where R refers to the isotope ratio D/H or O^{18}/O^{16}. The delta values are tabulated in per mil units like salinity. Thus $\delta_{SMOW} = 0$ ‰.

We shall discuss the precision with principal reference to oxygen analyses, as we are most concerned here with defining the delta values for the deep water masses which differ only by small amounts in isotopic composition. EPSTEIN and MAYEDA (1953) reported a probable error in δO^{18} of $\pm$ 0.1‰ corresponding to a standard deviation of 0.15 per mil. Since, as we shall show, the total difference between North Atlantic Deep Water and Pacific Deep Water in O^{18} content is less than 0.3 per mil, it was evident that the analytical precision would have to be pushed to the limit in order to study deep ocean waters.

For sea water oxygen 18 analyses we use the EPSTEIN-MAYEDA technique of equilibrating CO_2 with 25 ml of water and analyzing successive aliquots of the CO_2 taken about two days apart to ensure that equilibrium has been reached between the isotopic composition of the two phases. (This isotopic equilibrium is attained via the carbonic acid and bicarbonate chemical equilibria). Although we use much smaller water samples (down to 0.1 ml) for analyzing water vapor, the large sample size for sea waters ensures effectively against contamination and vapor loss effects during analysis. Our improvements in analytical technique consist principally of very careful attention to detail. The mass spectrometer performance has been improved by using transistorized and carefully selected electronic components. More importantly, we use CO_2 equilibrated against a laboratory standard water close to SMOW in composition, rather than CO_2 derived from carbonate by acid reaction, as a mass spectrometer standard. The working gas standard for ratio comparisons, flowing through the standard inlet valve, is several hundred ml of such gas, but the actual standard from which the data are calculated consists of the mean of a set of five samples of CO_2 equilibrated against the laboratory standard water and analyzed, one a day, by introduction into the spectrometer through the *sample* system. The standard analyses are plotted vs. analysis

number, and the delta values of the samples are calculated relative to the observed mean delta of the set of standards. This method removes the error due to fluctuation of individual standards, which is especially great in the case of carbonate standards, and cancels the slight fluctuations in the machine working standard which sometimes occur.

Using this system the average difference between successive aliquots of CO_2 equilibrated against a sample is consistently 0.03 per mil. At least two aliquots are taken for each sample in order to be sure that equilibrium has been reached. During the past year we analyzed 21 samples of our standard water (which has been adjusted to the chlorinity of normal sea water) independently of its use as an operational standard; the standard deviation of these data is $\pm$ 0.020 per mil. This water, our LJ-2 standard, has a delta value of —.39 vs. SMOW and a very accurately known chlorinity so that evaporation can readily be detected. It is a useful check standard close to SMOW and we have a supply of sealed ampoules which we have been furnishing to other laboratories on request.

Although the isotopic activity coefficients differ in some highly saline solutions, the salinity of normal sea water has no effect on the analysis by CO_2 equilibration. Duplicate analyses of distilled water before and after addition of NaCl to sea water chlorinity gave delta values of —14.84, —14.86 before, and —14.84, —14.87 after the addition.

Deuterium analyses are performed on H_2 produced from water by reaction with uranium metal and analyzed on a separate mass spectrometer; standard controls are the same as for oxygen. The standard deviation for our deuterium data is presently about 0.2 per mil.

It should be noted that the standard deviations of 0.02 and 0.2 per mil for oxygen and hydrogen stated here apply to laboratory samples with no errors from sampling and storage effects, and for samples close in isotopic composition to the standard water. The analytical errors include uncertainties in various correction factors for spectrometer characteristics which enter as a percentage of the measured delta value and increase the uncertainties in delta at larger values.

Processes affecting the isotopic composition of sea water

Precipitation

In order to understand the variations in isotopic composition in sea water it is first necessary to establish the nature of the variations in the precipitation, continental runoff, and polar meltwater entering the sea. The results of a worldwide survey of such waters are shown in figure 1, from the work of Craig (1961a). We have since extended the range of variation down to δ values of —50 per mil for oxygen 18, these very light values being found in ice at the South Pole. The deuterium and oxygen data show a very good linear correlation over the entire range, the relationship being:

$$\delta D = 8\ \delta O^{18} + 10$$

when the delta values are in per mil. In figure 1, the values which fall markedly off of the straight line are waters subjected to evaporation after precipation.

Figure 1. — *Deuterium and oxygen 18 variations in precipitation and meteoric waters, relative to the SMOW standard (from* H. Craig, 1961a).

It was first pointed out by Kirshenbaum (1951) that in the precipitation process the heavier isotopic species HDO and H_2O^{18} will rain out preferentially because their saturation vapor pressures are lower than that of H_2O^{16} so that they concentrate in the liquid phase. Thus the process resembles a batch distillation in which the initial material, in this case the atmospheric water vapor, is steadily depleted in the heavy isotopes. The extent of the depletion for each isotope is governed by the fractionation factor between liquid (or solid) and vapor at equilibrium:

$$\alpha^+ = (R_{liquid}/R_{vapor})_{eqlb.} = p_{H_2O^{16}}/p_i = 1 + \varepsilon^+$$

where p_i is the saturation vapor pressure of either heavy isotopic species. The fractionation factor α^+ is greater than one, the value of ε^+ being 74 per mil for deuterium (as HDO) and 9.2 per mil for oxygen 18 at 25°C. (Deuterium vapor pressure data throughout this paper are from the work of Merlivat, Botter, and Nief (1963); oxygen 18 vapor pressure data are from measurements of Y. Horibe in our laboratory).

Several authors have discussed the precipitation variations in terms of a simple model of the atmosphere containing only a vapor phase. Such a model does not reproduce well the actual observed effects and it is necessary to treat the two-phase system. The variation of either heavy isotope in such a system, assumed to be closed except for removal of precipitation, is given by:

$$\frac{d\lambda}{d\ln f} = \frac{\varepsilon^+}{1+\alpha^+ L} \qquad (1)$$

where:

$$\lambda = \ln\ (1+\delta) \approx \delta,$$

L is the mean ratio of liquid (or solid) phase to vapor phase during the precipitation process, and f is the fraction of original moisture remaining in the system at any time. The value of the slope in figure 1 is fixed by the isotopic vapor pressures at the various precipitation temperatures and by the mean ratio of condensate to vapor in the air mass.

The first precipitation from an air mass over the sea has about the isotopic composition of sea water; in higher latitudes or at high altitudes within the continents the precipitation is progressively

depleted in deuterium and O^{18} according to (1). Thus we find the mean precipitation in tropical and sub-tropical regions to range from about 0 to —5 per mil in oxygen 18, from about —5 to —15 in temperate regions, and still lower in the polar regions. This large variation in the composition of precipitation has much to do with the different relationships between salinity and isotopic composition in different parts of the ocean.

Evaporation and Molecular Exchange

The evaporation and exchange at the sea surface constitute the most complicated and most interesting portion of the isotopic cycle. Previous workers have stated that the vapor evaporating from the sea will be that in isotopic equilibrium with the sea surface or, in fact, even much lower in D and O^{18}. Yet it has been clear from the earliest measurements that the mean precipitation over the sea surface cannot possibly be as depleted in D and O^{18} as the removal of such vapor would require for material balance. A large part of our work to date has therefore been concentrated on this problem, which is discussed in detail in a later section of this paper.

An important part of the problem is the determination of the isotopic composition of the vapor which actually occurs over the sea surface. The development of the techniques for this work has been done in collaboration with Dr. Y. Horibe in our laboratories and the details will be published elsewhere. In figure 2 we show the oxygen 18 variations in vapor over the N. Pacific on Monsoon Expedition (the track is shown in figure 6). The isotopic composition of the surface water is also shown, together with a dashed line showing the composition of vapor which would actually be in isotopic equilibrium with the sea surface at the observed temperatures.

It is seen that rather large and varying departures from isotopic equilibrium occur. The maximum deviation of about 4.5 permil is found in latitude 18-26° in the northern part of the trade winds belt, the area of maximum evaporation. The relative humidity data shown are calculated relative to air temperature rather that sea surface temperature; when reduced to the latter temperature, the humidity and isotopic curves correlate rather well.

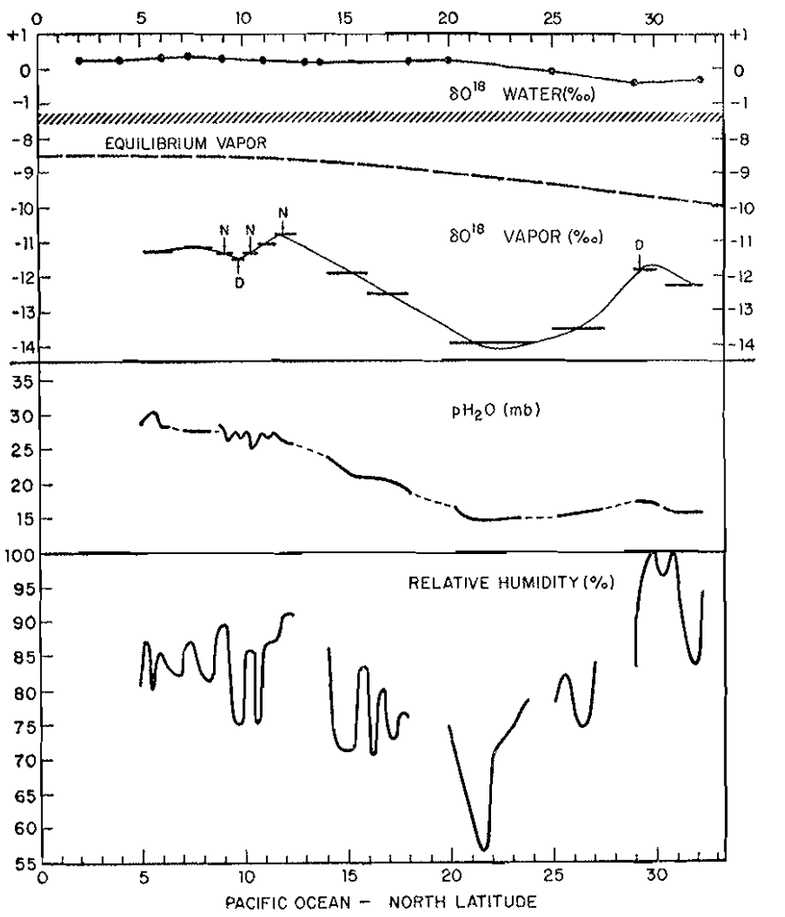

FIGURE 2. — *Oxygen 18 variations in vapor collected at mast height in the North Pacific (Expedition Monsoon, track shown in figure 6). At the top of the figure the variations in the surface water are shown, and a dashed line for the composition of the vapor which would be in isotopic equilibrium with the observed surface water.*

Figure 3 shows the vapor collected along an east-west track across the N. Atlantic (Zephyrus Expedition) at about 20° N. latitude. Except for edge effects at the boundary, the vapor is uniformly about 3 permil lighter than equilibrium vapor. The comparison of these two tracks indicates that meridional variations are much the more pronounced, though of course data from the same oceans are needed to be sure of this.

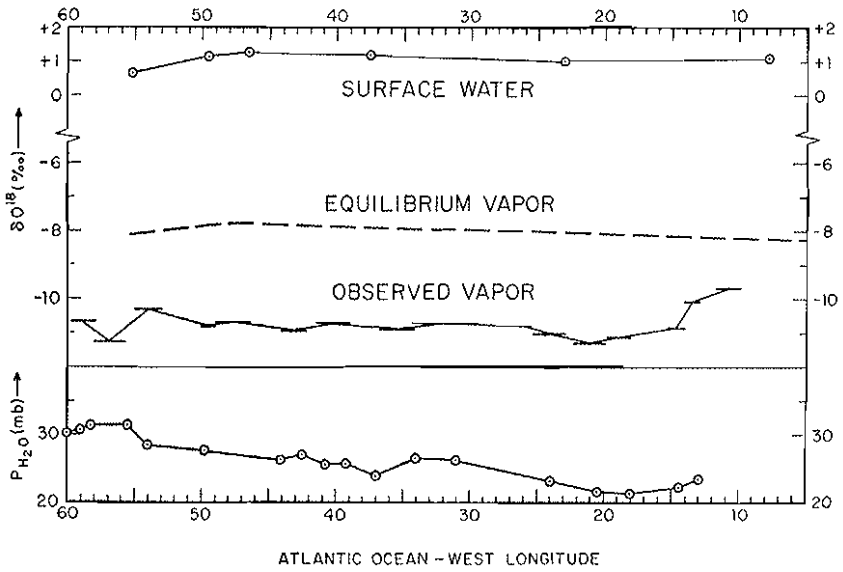

FIGURE 3. — *Isotopic variations in water vapor in the N. Atlantic on an east-west track at about 20° N. latitude. The surface water and equilibrium vapor compositions are also shown.*

Deuterium variations show the same effects of deviation from equilibrium vapor pressure values, and in figure 4 we show a plot of δD vs. δO^{18} for the N. Pacific vapor. The position of equilibrium vapor relative to the surface sea water is also shown. The upper dashed line in this figure indicates the line along which vapor would have to lie to account for the trend of $\delta D - \delta O^{18}$ in surface waters of the open sea and the high salinity lagoons of Baja California (solid points) by simple removal of vapor. It is evident that the vapor follows neither trajectory, but in fact centers on a position on the observed line which marks the relation-

ship in precipitation. The coordinates marking the origin of the precipitation line are thus explained; they are fixed by the original vapor found over the sea. We note that the surface sea water does *not* fall on the precipitation line.

The meridional variation shown is clearly related to the evaporation process. It should be noted that the deviations from

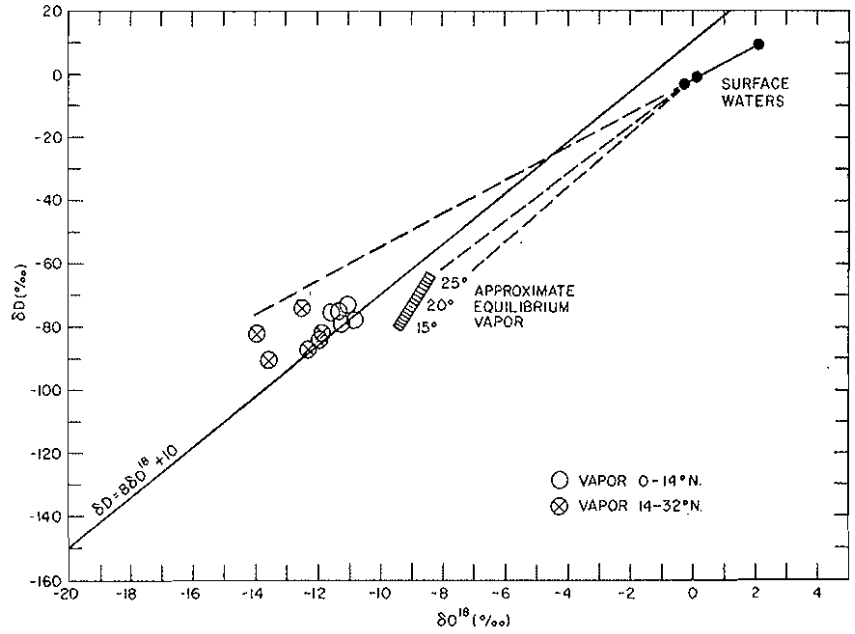

FIGURE 4. — *Deuterium and oxygen 18 values observed in N. Pacific marine vapor collected on Monsoon Expedition. The solid line is the trajectory of precipitation and meteoric waters shown in figure 1. The barred area shows the composition of vapor which would be in equilibrium with the surface sea water.*

equilibrium observed cannot be explained by a multi-stage equilibrium process for precipitation removal from equilibrium vapor; not only is this vapor below cloud base, but the ratio of deuterium to oxygen 18 deviations from single-stage equilibrium are not those which would be observed for an equilibrium process. In fact the mean vapor evaporating from the sea must be much heavier than this vapor and heavier than equilibrium vapor. We shall show in a later section how this comes about.

Freezing and Ice Separation

The final process which affects the isotopic composition of sea water is the formation of ice. We have been studying the ice-water equilibrium; our present results indicate that the oxygen 18 fractionation is such that the ice is about 2 permil heavier than liquid water at equilibrium. This fractionation effect is so small that the freezing process results in an increase of salinity, with essentially no observable effect on the isotopic composition, of the water. FRIEDMAN, REDFIELD, SCHOEN and HARRIS (1964) have observed fractionation effects of about 20 per mil for concentration of deuterium in natural sea ice relative to sea water; since the deuterium delta values are about ten times larger than those for oxygen 18, the effect on the isotopic composition of water is about the same.

DEEP WATER IN PACIFIC TRENCHES

In attempting to define isotopically the major water masses of the oceans, one of our first studies has been a survey of the deep waters in the Pacific trenches sampled on Expedition Proa (locations in figure 6), in order to see how homogeneous the very deep water of the Pacific is. Another point of interest is the comparison of the analytical precision on samples collected at sea and stored in citrate bottles with the standard deviation of 0.02 per mil which can be obtained on laboratory samples. In general the precision will be somewhat worse unless very careful precautions are taken against evaporation and contamination in sample collection. Moreover, we are in general interested in the correlation of salinity with isotopic composition and we have observed salinity errors, both positive and negative, resulting from admixture of salt in or on the bottles or with fresh water contamination. These lead to somewhat indeterminate fluctuations in the observed relationships.

Table 1 lists the results of the analysis of 15 samples from the six trenches sampled, and in addition the results of eight separate analyses made on a composite of these samples after completion of the individual analyses. The standard deviation on the composite

analyses is ±0.016 per mil, about the same as on the individual samples and entirely comparable with the precision on our laboratory standard water. The salinity measurements were made with a bridge and the variations appear to be significant; there is a bare tendency for lighter isotopic values to be associated with the less saline samples but the difference is not enough to be sure of. The individual samples are identical to ±0.02 per mil.

TABLE 1. — *Isotopic composition of the deep water in six Pacific Ocean trenches. Samples from Proa expedition; station locations are shown in figure 6.*

Location	Depth (m)	Salinity	δO^{18} (‰)
Marianas Trench, station H-4.	6781	34.713	—0.15
11°17′N, 142°10′E.	8287	.710	—0.11
	8792	.701	—0.19
Palau Trench, station H-14.	5000	34.696	—0.14
7°44′N, 134°56′E.	7434	.692	—0.16
	7929	.696	—0.16
New Britain Trench, station H-24.	5208	34.711	—0.12
5°58′S, 152°15′E.	6189	.714	—0.14
	8150	.709	—0.14
W. Solomon Trench, station H-34.	5863	34.704	—0.14
6°19′S, 153°45′E.	7839	.700	—0.12
N. New Hebrides Trench, station H-42.	6200	34.696	—0.16
12°17′S, 165°49′E.	8083	.690	—0.16
S. New Hebrides Trench, station H-49.	4624	34.702	—0.16
20°33′S, 168°33′E.	6601	.697	—0.14
Composite trench sample, made from equal aliquots of all the above samples. Eight separate isotopic analyses made over a two month period after completion of individual analyses.	—	(34.702)	—0.18 —0.14 —0.16 —0.14 —0.12 —0.15 —0.15 —0.14
Average, all data			—0.15

These samples were collected routinely by marine technicians rather than by ourselves and brought back on the ship after a long expedition. On examining the citrate bottles it was found that a poor set of gaskets had been used, and many of them had

rotted. All samples with observably poor gaskets were discarded; of the remainder the samples shown in table 1 were analysed isotopically while a separate group from similar depths was reanalysed with a bridge for salinity. The salinity data shown in table 1 are the original analyses made on the ship; the distribution is roughly Gaussian about the calculated mean shown in the table for the composite (34.702). Redetermination of the composite sample gave a salinity of 34.730. In the reanalysed set of samples, the mean change in salinity from the shipboard data was +0.02 per mil, with a range from —0.01 to +0.06 with a roughly Gaussian distribution. That is, these samples had lost 0.08 per cent of their water by evaporation from citrate bottles over a one-year period, while maintaining about the same distribution of relative salinities. We show later in this paper that this amount of evaporation corresponds to an O^{18} enrichment in the sample of 0.01 to 0.02 per mil, depending on whether an equilibrium or non-equilibrium process is assumed and disregarding any effect of diffusion through the gasket. We point this out here because we show in a later section that the trench samples are in fact about 0.02 per mil heavier than the samples from the general deep Pacific water, probably due to this slight evaporation effect. This is a reasonable, though not necessarily correct, explanation for the slight difference in isotopic composition.

Comparison with previous data

In order to use the data of Epstein and Mayeda (1953) together with the data from the present work, their data must be converted to the SMOW scale. The Epstein-Mayeda data are expressed relative to the approximate average of their data as a standard; in order to be expressed on the PDB (Chicago standard) scale their delta values must be corrected by a small multiplying factor for various spectrometer effects and by adding —0.09 per mil to correct for the isotopic composition of their tank CO_2 (Craig, 1957a). The PDB standard is +0.20 on the SMOW scale. Thus the conversion of their data to the SMOW scale is given by (Craig, 1965):

$$\delta_{(\text{vs. SMOW})} = 1.040\ \delta_{\text{E-M}} + 0.11‰$$

where the subscript E-M signifies the δ values recorded by Epstein and Mayeda. (The multiplying factor is one percent larger than estimated previously (Craig, 1957a) due to an additional factor for spectrometer background and mass 44 contribution to mass 46. However the multiplying factor is negligible for ocean waters).

In figure 5 we show a comparison of the Epstein-Mayeda data, expressed on the SMOW scale, with our own data for samples from the same locations or water masses with the same salinity as their samples. The data are shown as their converted and corrected δ values minus our own for the same waters, as a function of salinity of the water. There are three sets of their data for comparison. The Serrano Expedition samples in their paper are the samples with their sample numbers from 26-40, all from the eastern equatorial Pacific, north of the equator; we have used only their surface samples from this set for the comparison shown in

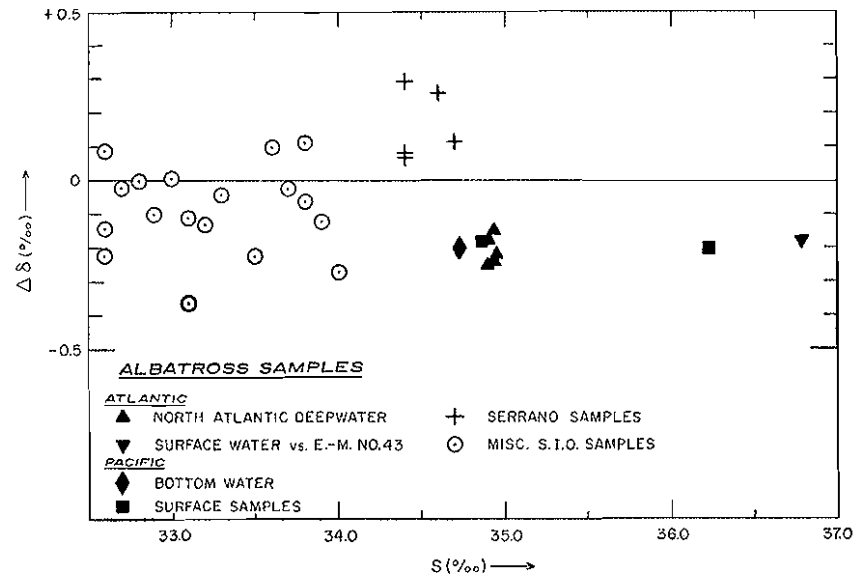

Figure 5. — *Deviations of the δO^{18} values measured by* Epstein *and* Mayeda *(1953) and expressed vs. SMOW from our data on the same waters, plotted as their delta value minus ours, vs. salinity of the water. The inverted solid triangle is an intercomparison of two of their waters (see text). The Albatross expedition samples are uniformly 0.2 per mil light because of HCl solution addition to the samples when collected.*

the figure. These samples were quite old when analyzed and the two samples with positive deviations of about 0.3 per mil may well have been affected by evaporation prior to the isotopic analysis. The samples marked as «miscellaneous SIO samples» in the diagram represent surface water samples from their set of north-east Pacific samples supplied from Scripps. These are from their set of samples from number 61 to 89, using the surface samples only, and comparing their data with the mean value given by our plot of δ vs. salinity for surface waters in the same area (shown later in figure 10). The mean deviation of their values from ours is —0.08 ±0.10 per mil. The range of the deviations relative to the mean is within their standard deviation of about 0.15 per mil and thus corresponds to their analytical precision. The mean deviation is probably not significant, especially as there may even be slight fluctuations in the isotopic composition of surface waters in ten years and there is probably an uncertainty of about 0.05 per mil in the corrections and standard conversions.

The remaining samples, shown as solid points, are samples from the Albatross expedition which include two Pacific surface samples (their numbers 6 and 8), one Pacific bottom water sample (their number 10), and five samples of North Atlantic Deep Water (their sample numbers 3, 4, 17, 22 and 25, from Albatross stations 16, 31, 337, 373, and 400 respectively). The salinity data given by EPSTEIN and MAYEDA for all their Albatross samples differ by amounts ranging up to 0.5 per mil, though generally less, from the final recorded data in the Albatross report, due to their having used a list of preliminary uncorrected salinity data; the samples shown in figure 5 have been plotted with the corrected salinities. The plotted data show that their Albatross data are systematically 0.2 per mil lighter than our data for the same waters; in the case of the North Atlantic and Pacific deep water the comparison is quite good because of the small spread of their data and the impossibility of a change in the isotopic composition of this water. In addition we show one of their samples (number 19, Albatross station 373) of Atlantic surface water plotted vs. another one of their own non-Albatross samples (number 43) from the same location with the same salinity, and it is seen that the same difference is found as in the comparison of the Albatross samples with our data.

The Albatross samples appear to be systematically 0.2 per mil lower in oxygen 18 than other samples of the same sea water. Dr. EPSTEIN (personal communication) informs us that all these samples were mixed with HCl solution when collected as they were intended for later chemical studies; this would have the effect of adding fresh water lower in O^{18} and would not affect the salinities which were measured on other samples. We conclude that +0.2 per mil should be added to all their delta values for Albatross samples (their numbers 1 to 25 inclusive, 58, and 59) in order to correct for this effect.

OCEANOGRAPHIC DATA

Figure 6 shows the station locations from which samples have been taken in the Pacific and Indian oceans. In the Atlantic ocean samples have been obtained from three expeditions: Zephyrus, along a NE-SW track from about 15°N, 60°W to the Straits of Gibraltar; Lusiad, which provided surface samples from about 23°S, 15°W north to the equator and thence westward to 45°W in latitudes 5 to 12°N; and from Eltanin Cruise 12 in the Weddell Sea (March-April, 1964). Additional detailed studies have been made in the Gulf of California, the Mediterranean Sea, and the Red Sea, but these data are not discussed in this paper. Some data from our most recent expedition, Carrousel (SE Pacific to Easter Island and Chile), not shown in figure 6, have been used in the present discussion.

The quality of the different sets of data is somewhat variable, reflecting advances in sampling and analytical techniques since the inception of the work. Most of the samples have been collected personally by the senior author. On our most recent expeditions the samples were drawn from the Nansen bottles and held in large citrate bottles until salinity measurements were completed on the shipboard salinometer after the cast. Using the temperature and salinity data for the station, samples were then selected for various depths to show the salient features and immediately sealed off in glass ampoules. Originally 100 cc ampoules (commercially available) were used, but we have observed that about 4% of the seals on these thick glass ampoules crack open during

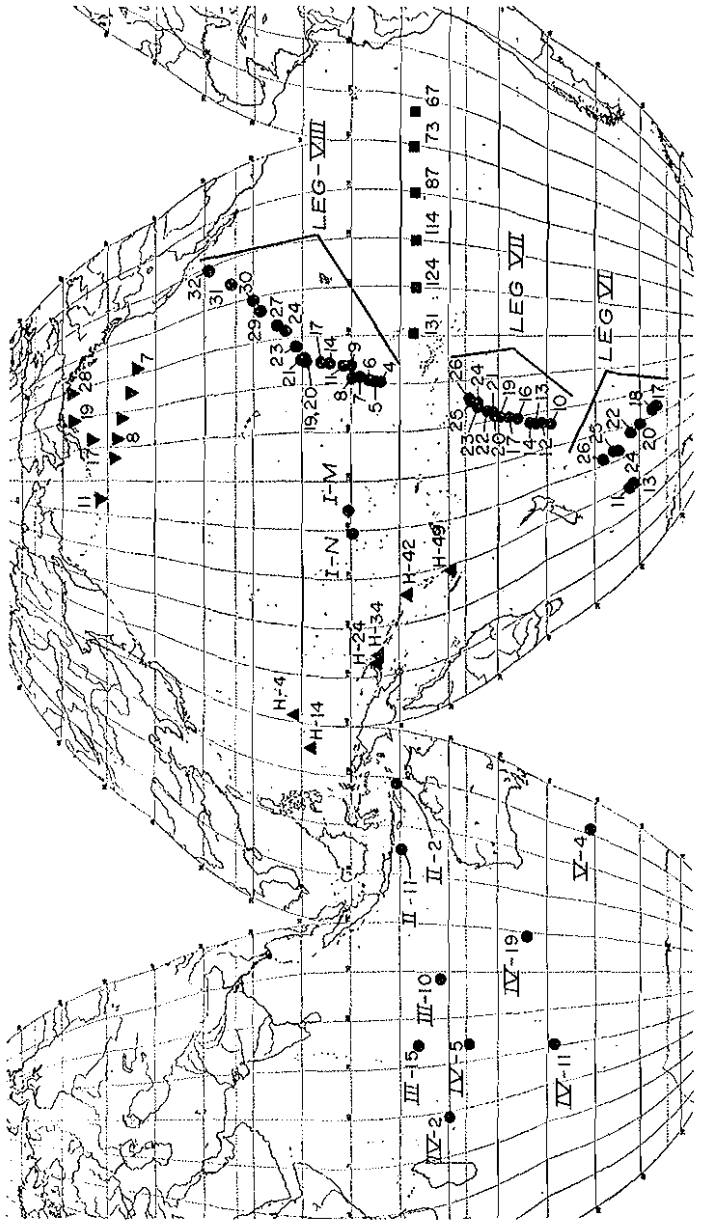

FIGURE 6. — *Sample locations for Pacific and Indian ocean samples discussed in the text. Expedition names shown at bottom.*

storage. We now use the thinner 50 cc ampoules and suffer almost no loss. As long as care is taken to wipe the necks of the ampoules dry before sealing and to exclude moisture from the torch, this is by far the best method of collecting and storing samples for precise measurements. In other cases samples have been held in citrate bottles for long periods during the expedition and brought back in the bottles. In such cases the precision is totally dependent on careful attention to quality of gaskets and prevention of evaporation or contamination (with fresh water or also with sea salt) during handling; we have observed random deviations from all these effects.

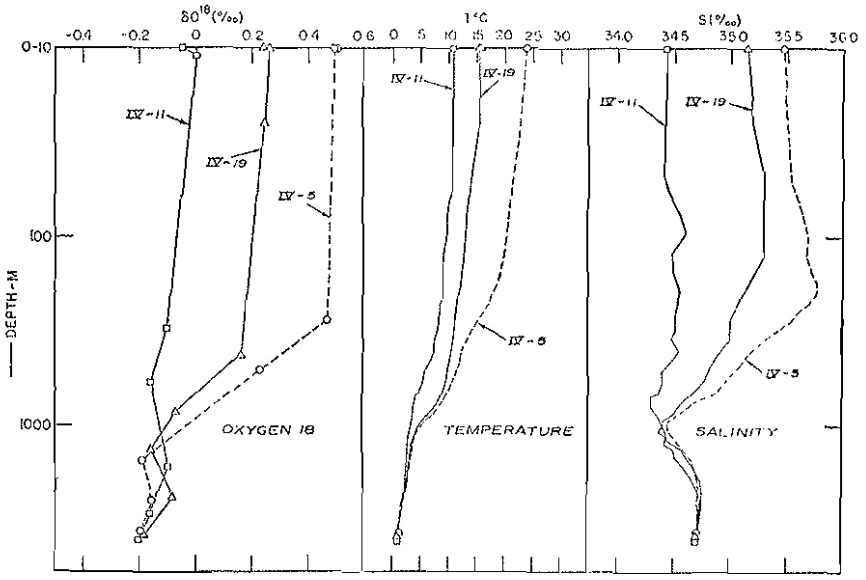

FIGURE 7. — *Isotopic, temperature, and salinity profiles at three stations in the Indian Ocean. Station locations are shown in Figure 6.*

Isotopic, salinity, and temperature profiles vs. depth for three Monsoon stations in the Indian ocean are shown in figure 7 to show the general nature of the oxygen 18 variation with depth. We notice first that the isotopic profiles are very similar to the salinity profiles, as we in general expect. Station IV-5 is located in the center of the large counterclockwise gyre at the surface of the southern Indian ocean (figure 6) in the area of maximum salinity and evaporation. Station IV-11 is approximately at the

Subtropical Convergence and shows minimum variation with depth of all parameters. Each of these isotopic profiles individually resembles a profile of a salinity component, e.g. Cl, in its relation to the salinity profile, but down to 1000 meters the horizontal displacements of the isotopic and salinity profiles are not proportional as they would be for a salinity component. That is, IV-19 is more similar to IV-5 in salinity than in isotopic composition, and more similar to IV-11 in isotopic composition than in salinity.

The isotopic-salinity relations are shown as δO^{18}-salinity plots for the Indian Ocean and the South Pacific in figures 8 and 9

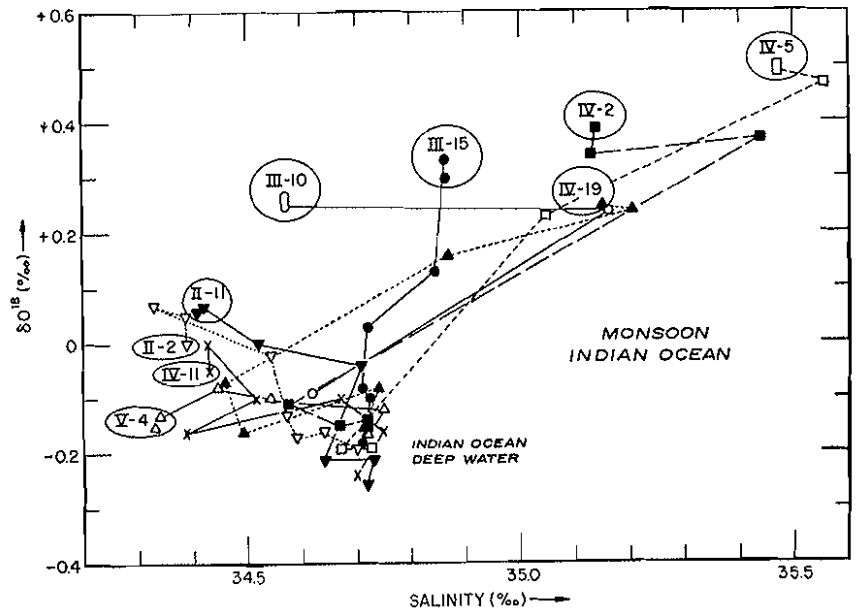

FIGURE 8. — *δ-S diagram for Indian Ocean stations. The circled points are surface samples.*

These plots are similar to T-S diagrams, especially in the way that serial points plot on curves which hook into the composition of the deep water. However, the very large temperature changes for small salinity increments in surface and shallow waters, which force us generally to omit the surface samples in T-S plots, have no analogue in the δ-S plots, on which the surface samples do not

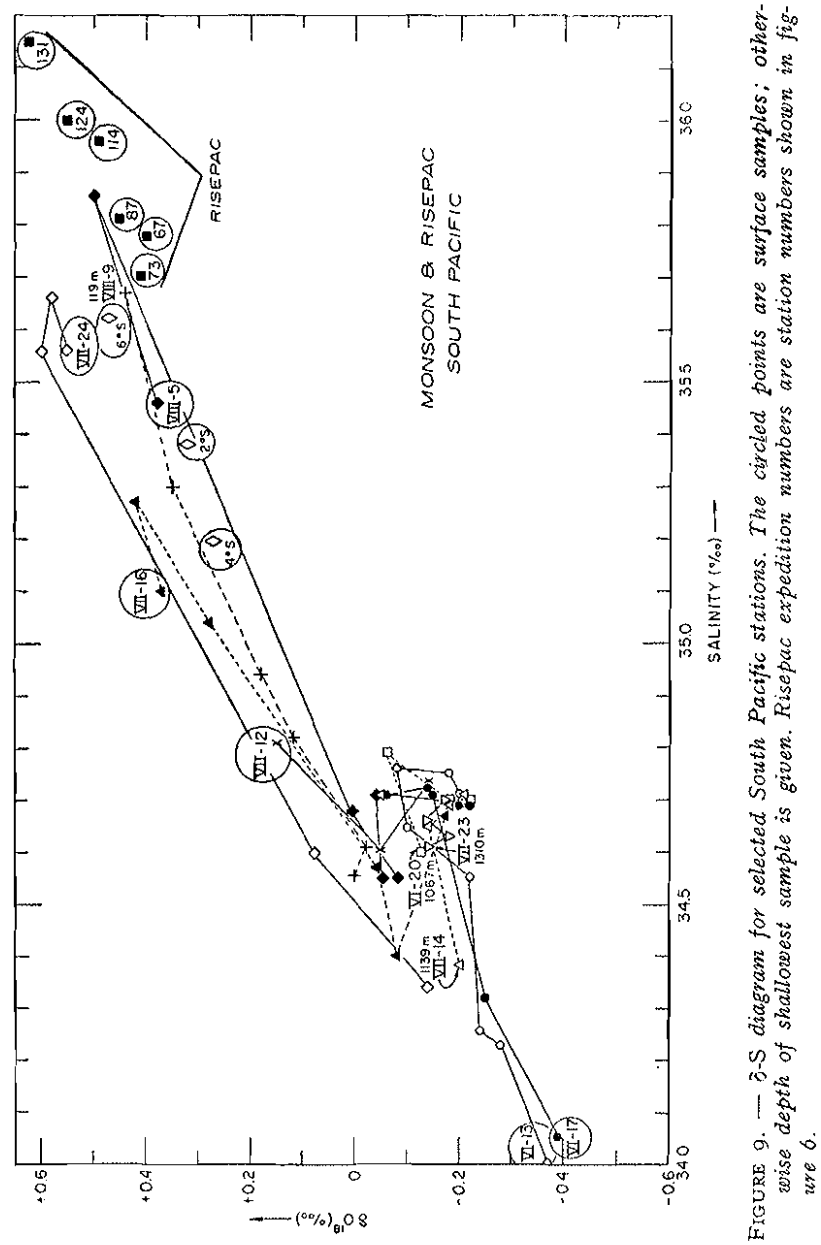

FIGURE 9. — *δ-S diagram for selected South Pacific stations. The circled points are surface samples; otherwise depth of shallowest sample is given. Risepac expedition numbers are station numbers shown in figure 6.*

show large discontinuities. They resemble T-S diagrams on which the temperature axis has been greatly foreshortened in the region of near-surface and surface waters. For this reason the δ-S diagrams are especially useful in studying vertical and lateral mixing in intermediate and high latitudes.

In the present paper we wish to concentrate our discussion on the surface and deep water samples and we shall not discuss the formation and mixing of intermediate waters in any detail. At this stage of the work it is more important to establish the general principles which govern the range and characteristics of the isotopic variations. We mention only a few salient features of these diagrams. (The δ-S diagrams for waters of all depths in the N. Pacific and Atlantic oceans differ only in detail from the S. Pacific and Indian ocean diagrams shown here, and are omitted for brevity).

1. Figures 8 and 9 show a broad band in which δO^{16} generally increases with salinity, in accordance with the preferential evaporation of O^{16} and the depletion of O^{18} in high latitude precipitation. The deviations from a simple linear correlation are due to the differing O^{18}/O^{16} ratios in precipitation in different latitudes. However, the actual envelope of points tends to be fan-shaped in detail, with high-latitude bottom waters at the apex of the fan. That is, the deep oceanic waters do not plot on the general band representing surface waters, but have significantly less O^{18} than surface waters of the same salinity.

2. From the apex of the fan representing high-latitude deep waters, the initial tendency is for an increase in oxygen 18 with approximately constant salinity. This simply reflects the fact that density considerations require that these waters mix with waters of approximately the same salinity.

3. The characteristic occurrence of surface waters from one location lying immediately beneath the surface in other areas shows up on these diagrams in a very marked fashion (e.g. Monsoon stations III-10, IV-2, in figure 8, and VIII-5 in figure 9).

4. The δ-S curves define water types for a given water mass in a manner analagous to, but different from, the T-S curves for the water mass. In a T-S diagram, the intersection of two curves

defining two different water masses defines a pair of isopycnal water types, or *pycnotypes*. (We distinguish these as two types because they may differ in isotopic composition). Similarly, in the δ-S diagram, the intersection of two curves for two different water masses defines a pair of water types similar in salinity and isotopic composition, but differing in temperature and thus density. We call these *isotypes*. Depending on the type of mixing affecting the water mass, a pair of isotypes may or may not be pycnotypes. These considerations are highly informative for the study of mixing effects on water masses.

For example, in figures 7 and 8 (Indian Ocean stations), above 1000 meters the T-S curves for stations IV-5 and IV-19 do not intersect and have no pycnotypes. However, the δ-S curves do intersect in a pair of isotypes at $\delta = +0.24$, $S = 35.1$, per mil, found at 500 meters at the former station and at about 200 meters at the latter, and differing by 2° in temperature. On the other hand station IV-19 and V-4 have water types at $\delta = -0.08$, $S = 34.45$, per mil, which are both isotypes and pycnotypes.

5. The δ-S curves generally pass through a region of approximately 34.55 per mil salinity, at δO^{18} approximately —0.10 per mil, which represents the Pacific and Indian Intermediate Waters. This is generally a salinity minimum (vs. depth) in intermediate and low latitudes and is, of course, well-known on T-S diagrams. In high latitudes the δ-S curves are displaced towards lower δO^{18} values for the same salinity, and in fact all waters of equal or lower salinity, as well as all waters of the same density contain less oxygen 18. The characteristics of these intermediate waters are thus strongly influenced by vertical mixing. This relationship is also present in our N. Pacific data.

Deep and surface waters

Because both the salinity and isotopic composition are conservative quantities altered only at the upper surface of the oceans, it follows that the total envelope of surface water points on the δ-S diagram encloses all points for intermediate, deep, and bottom waters. However, because of the mixing between various water masses it is of course not necessary that sub-surface waters for an

individual ocean lie within the envelope of surface points for that ocean. (Under certain transient conditions between glacial and non-glacial epochs it is also possible to find deep waters not included in the surface envelope for all oceans, as discussed later on, but there is no evidence that this occurs at the present time). Since the deep waters are replenished at the surface we can discuss the deep water data in light of the surface variations with only passing reference to the intermediate waters where necessary.

In a general way we can outline the expected shape of the δ-S relationship for surface ocean waters from a knowledge of the factors affecting the salinity and isotopic composition discussed earlier in this paper. For any surface water point in this diagram, the effects of these factors are represented by vectors with lengths proportional to the relative magnitudes of precipitation, evaporation, or separation of water by freezing, and with inclinations proportional to the isotopic composition of the added or subtracted water. Continuity and a certain amount of smearing are then provided by vertical and horizontal mixing.

Evaporation and Precipitation

As we pass from the equator to the poles on the ocean surface, we encounter an equatorial region where annual precipitation exceeds evaporation, the trade wind region where evaporation exceeds precipitation, and finally the polar regions where precipitation and continental runoff again exceed evaporation. The successive vectors in the δ-S diagram reperesent decreasing, then increasing, and then again decreasing salinity, when taken relative, say, to a point representing a region between the equatorial trough and the trade wind region where precipitation and evaporation are just in balance. Excess evaporation concentrates the less volatile heavy isotopic molecules HDO and H_2O^{18} along with salinity, while the effect of precipitation depends on the isotopic variation in precipitation of different latitudes shown in figure 1. The overall effect can be outlined in a general way as follows.

In the first place the isotopic composition of the vapor evaporating from the sea surface must be equal, in the mean, to the net composition of all precipitation because of the required ma-

terial balance. Since almost all the earth's precipitation falls in the intermediate and low latitudes, the mean isotopic composition of the evaporating water vapor must be similar to the precipitation in these latitudes and not greatly different from the composition of the sea water itself. On the other hand, as shown in figure 1, at high latitudes the precipitation is greatly depleted in the heavy isotopic molecules and the slope of the vector representing the net addition of precipitation and runoff is correspondingly much greater than the slopes for evaporation and precipitation in lower latitudes.

Freezing

As noted earlier the isotopic fractionation between water and ice is very small and for practical purposes can be neglected. The effect of separating fresh water from sea water by freezing essentially corresponds to a zero slope representing salinity variations with almost no change of isotopic composition.

Surface Water Relationships

The above considerations lead to a schematic δ-S diagram for surface waters which may be sketched as follows:

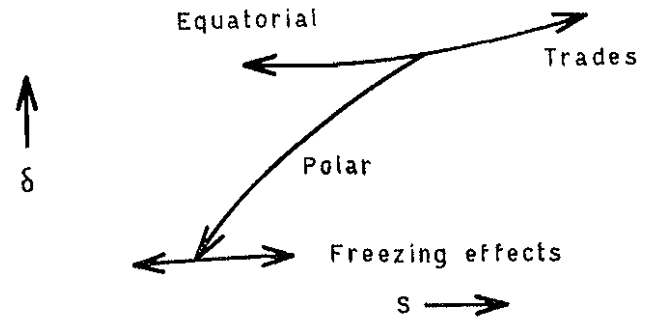

in which the slopes here are purely schematic. (A more quantitative discussion of the slopes is given in the last part of this paper). The branch point which connects the vectors for equatorial, trade wind, and polar regions is here taken as the region of E = P lying between the equatorial trough and the trade wind regions. The

actual diagrams will of course be greatly complicated by mixing and details of the evaporation and precipitation effects; for example passing from the E = P region between the polar and trade wind regions to the evaporation maximum in the trades and thence to the equator would not generally give a single trajectory as indicated above. In a general way, however, the diagram shows us the expected nature of the variations.

Deep Waters

Since the deep waters represent the bulk of the ocean water, their mean position on the δ-S plot simply reflects the average composition of the world oceans. As conditions vary at the surface then, the entire surface water diagram shown above shifts its position relative to the almost fixed position of the deep waters until a steady state condition is reached so that a material balance obtains in the mixing processes which replenish the deep water. For example, if the deep water is replenished entirely by deep convection in a region of a unique salinity and δ of surface water, the deep water would simply plot on the above diagram on one of the lines connecting the surface waters, at the composition of the surface water in the convecting region. The isotopic composition, salinity, and temperature of the surface water in the convecting region are necessarily the same as in the uniform deep water in the steady state, and this serves to « pin » the surface water diagram shown above at this point. The relaxation time for shifts of the surface water diagram will be of the order of decades.

On a longer time scale the composition of the deep water itself varies along a slope similar to that shown in the surface diagram above for polar waters, because of the addition and subtraction of water by continental ice. This variation is of importance for the measurement of paleotemperatures by oxygen isotope variations in shells, and is discussed later on.

At 3500 meters and below the deep waters of the Pacific and Indian Oceans are quite uniform except for slight variations in high southern latitudes (see table 3). The data used here to fix the isotopic composition of these waters are the data from these depths at the stations shown in figure 6. In the Atlantic, however, the Antarctic Bottom Water moving northwards under the Atlantic Deep Water produces significant isotopic variations at great depths even in subtropical northern latitudes, and it is necessary to sample carefully to determine the core values of these two water masses. Table 2 shows the data obtained so far on North Atlantic Deep Water. In addition to our Zephyrus expedition samples, two samples from an Equalant expedition were kindly collected by Dr. R. BADER of the National Science Foundation. The deepest samples with lower salinities are clearly marked by lower oxygen 18 contents. (The individual points are plotted in figure 11 in a following section). From these data the δO^{18} value of North Atlantic Deep Water (core value) has been taken as +0.12, corresponding to a salinity of 34.93. This is probably correct to ±0.02 per mil.

TABLE 2. — *Isotopic composition of North Atlantic Deep Water.*

Expedition	Station No.	Latitude	Longitude	Depth (meters)	T (°C)	Salinity	δO^{18} (‰)
Zephyrus	10	17°28'N	55°27'W	3300	2.51	34.92*	0.14
		»	»	5287	1.88	34.834	0.02
	13	21°05'N	46°34'W	3000	2.75	34.936	0.10
		»	»	3788	2.34	34.893	0.08
	21	24°34'N	37°27'W	5266	2.43	34.886	0.09
	24	26°43'N	21°55'W	2947	2.81	34.96*	0.14
		»	»	4867	2.44	34.898	0.04
	27	35°38'N	9°45'W	4255	2.42	34.899	0.10
Egualant (P-6404)	122	0°20'S	5°E	3760	2.44	34.908	0.06
	114	7°S	5°E	5070	2.42	34.939	0.07

* Interpolated.

The isotopic delta values determined for the principal deep water masses of the oceans are given in table 3. The salinity data listed refer to the mean measured salinities (by conductivity) for the actual samples used for isotopic analysis, rather than to literature values for these water masses. The Antarctic Bottom

Water data refer to samples collected in the Weddell Sea on Eltanin Cruise 12. The Circumpolar Water data refer to the highest latitude bottom water samples from the Indian and S. Pacific stations in figure 6.

TABLE 3. — *Oxygen isotopic composition of the principal deep water masses.*

	Salinity	δO^{18} (‰)
North Atlantic Deep Water	34.93	+0.12
Antarctic Bottom Water	34.65	−0.45
Indian Deep Water	34.71	−0.18
Pacific Deep Water:		
Pacific Antarctic (55-65°S)	34.700	−0.21
South Pacific (22-40°S)	34.707	−0.17
Equatorial Pacific (6°S-30°N)	34.692	−0.17
North Pacific (44-54°N)	34.700	−0.17
Circumpolar Water	34.69	−0.3 to −0.2

Considering the number of samples analyzed, the values in table 6 are believed to be known, relative to each other, to ±0.02 per mil. However, the SMOW standard is defined relative to the NBS-1 standard water which is −7.94 per mil on the SMOW scale. The uncertainty in fixing an experimental working standard relative to SMOW is increased because of the large difference from the NBS standard. Our measured value of the NBS-1 standard is −7.94 ± 0.03 (average error, mean of 12 analyses), so that a systematic error of this order may also exist. Our present value of the NBS-1A substandard is −24.27 ± 0.10 per mil.

In table 3 we show the data for different regions of the Pacific according to latitude; these data represent means of seven or eight samples from different stations for each region except in the North Pacific where only four stations are represented and the data are thus not yet very representative. There is a definite increase in oxygen 18 content in lower latitudes relative to the samples in the high southern latitudes; the lightest sample found at Monsoon station VI-17 (farthest south, see figure 6) has $\delta = -0.26$ with a salinity of 34.69. This is probably close to the value for Circumpolar water in the Pacific Antarctic. A similar slight increase in O^{18} is observed proceeding northwards in the

Indian Deep Water. These very slight variations demand the highest precision possible for study, but should be very useful in studying mixing in the deep waters where temperature is not a conservative property because of the influx of heat from the bottom.

As noted earlier the data on Pacific trenches indicate delta values about 0.02 per mil heavier on the average for deep trench waters relative to the data for Pacific Deep Water in table 3. We do not yet know whether this effect is real, or as discussed earlier, reflects slight evaporation of the trench samples.

PACIFIC OCEAN SURFACE AND DEEP WATERS

The accumulated data on Pacific surface waters are shown in figure 10 together with the values determined for the deep water masses. Although the data are incomplete, several points of interest are clearly shown.

1. No surface waters occur in the Pacific with the isotopic composition and salinity of Pacific Deep Water, indicating, as discussed in the previous section, that the deep Pacific water is not replenished by deep convection from the surface in any region of the Pacific. This is in accord with classical observations based on density considerations.

2. For the same oxygen 18 content, South Pacific waters have a higher salinity than North Pacific surface waters, and the latitudinal variations are quite different in the two hemispheres. The composition of the surface waters in high southern latitudes is essentially fixed by the composition of circumpolar surface waters, which, as shown later, have about this same composition in the S. Atlantic also. Thus the much smaller extent of the surface latitudinal variation in the S. Pacific reflects the influence of the higher salinity and oxygen 18 content of Atlantic waters due to the excessive evaporation in that ocean.

3. The general nature of the observed slopes is in agreement with that outlined in previous section, with larger slopes in high latitudes reflecting the low oxygen 18 content of precipitation, and smaller slopes in subtropical and equatorial latitudes

reflecting the high O^{18} content of precipitation in regions of excess precipitation, and a roughly similar O^{18}/O^{16} ratio in the net vapor removed in evaporation. However, in detail the effects are quite complicated. The South Pacific surface waters are characterized by an *isotopic loop* from about 30°S to the equator, and a transition zone across the equator where the isotopic composition is approximately constant as the salinity decreases from about 35.5 to 34.5. The detailed nature of the connection of this loop with the Risepac samples in the same latitudes farther to the east is still under study with samples from our most recent expedition and is not yet understood.

Origin of Pacific and Indian Ocean Deep Water

The displacement of the Pacific Deep Water from the surface water curves in the δ-S diagram shows clearly that the surface waters do not contribute significantly to deep water formation, independently of the classical density observations. This is also the case with the Indian Deep Water which has a composition essentially the same as the Pacific Deep Water, and as shown in figure 8, also is displaced from the composition of Indian Ocean surface waters. (The Indian Ocean surface waters have a more complicated trajectory in the δ-S diagram because of the enclosed nature of the ocean but the gross effects are similar).

Figure 10 shows also that although the Pacific and Indian Deep Waters must be replenished from the North Atlantic and Antarctic Deep and Bottom Water, they do not correspond to simple mixtures of these two components, as they lie off the line connecting these two source waters. It is necessary to add a small amount of less saline water of approximately similar isotopic composition. As shown previously, the Pacific and Indian Intermediate Waters, with $\delta = -0.10$, $S = 34.45$ (approximate values) have the required composition for such a third component. Bolin and Stommel (1961), using temperature, salinity, and carbon 14 as tracers, also observed that a third component was necessary simply from the T-S diagram (cf. their figure 2 with our figure 10). They assumed *a priori* that the Pacific and Indian Intermediate Waters were in fact this third component. Our isotopic data

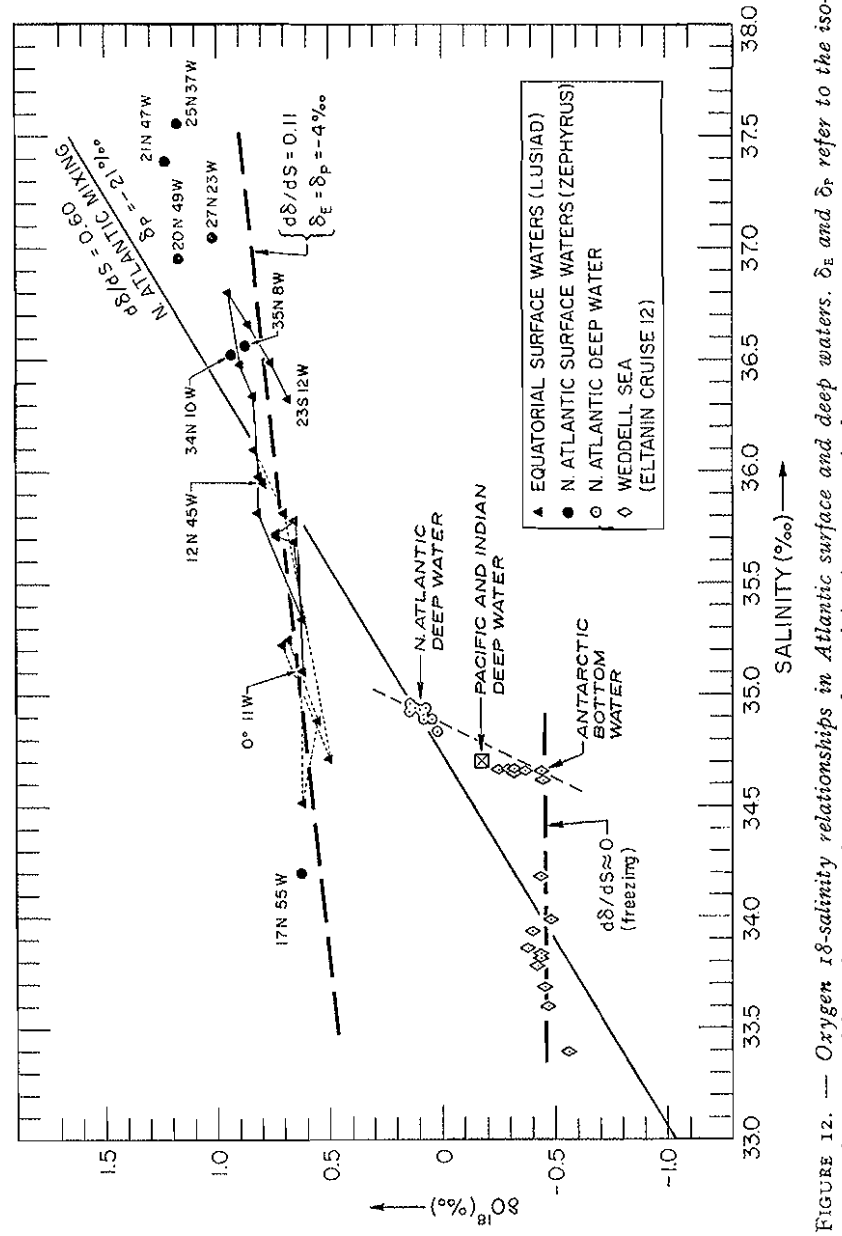

FIGURE 12. — *Oxygen 18-salinity relationships in Atlantic surface and deep waters. δ_E and δ_P refer to the isotopic composition of evaporating vapor and precipitation respectively.*

show that these waters are indeed such a possible component, but do not exclude other waters which may, in fact, be a more probable source.

For example, as noted in table 3 and the discussion thereof, the Circumpolar water in the highest southern latitudes from which we have samples in the Indian and Pacific Oceans is already quite similar to the Pacific and Indian Deep Waters in isotopic composition and salinity. Moreover, as we show in the discussion of Atlantic waters further on (figure 12) water types already exist in the S. Atlantic off the Weddell Sea which are almost identical with the Pacific and Indian Deep Waters. We do not yet have enough detailed data on Antarctic Intermediate Waters in the Atlantic region to make quantitative estimates on the various contributions to the elusive « third component » of Pacific and Indian Deep Water, but the evidence so far seems to favor the view that the Antarctic Intermediate Waters are more important than intermediate waters in the Pacific and Indian Oceans.

North Pacific Surface Waters

The North Pacific waters shown in figure 10 are predominantly from the eastern side of the Pacific; the majority of these are from the area from which EPSTEIN and MAYEDA (1935) obtained most of their Pacific ocean waters. (Waters from this area along the W. coast of North America comprise almost all the samples in Section 2 of their data list, plotted in their figure 2). As we noted earlier, when their data are corrected to SMOW the two sets of data give identical isotopic-salinity relationships. This is of some interest because of the time interval of about a decade between the two studies. EPSTEIN and MAYEDA do not give collection dates for any of their samples, so the time interval may in fact be longer. At any rate the data show that the same isotopic-salinity relationship has been preserved in the N. Pacific current system over at least ten years. In figure 10 we also show data from monthly composites of surface waters collected daily at the SIO pier. The variation in these samples is relatively small compared to the total range of surface waters along the N. Amer-

ican coast, and repetitions of such sampling at intervals of a few years should be of interest for correlation with climatological data.

The slope $d\delta/dS$ of the North Pacific line in figure 10 is 0.54, and if one assumes that the effect is entirely due to addition of fresh water, the slope corresponds to addition of fresh water with $\delta = -18.0$ per mil. (The line extrapolates to —18.5, but there is a 3% correction due to the definition of salinity). EPSTEIN and MAYEDA proposed that the major effect in producing the low salinity of these samples is dilution with melting snow and ice from the N. American continent, and they showed that the Columbia River contains fresh water of the requisite composition.

However, it is also necessary to consider the latitudinal dependence of the isotopic-salinity data. In figure 10, the N. Pacific point marked 53° is a surface sample from the Aleutian Current, just off the Aleutian Islands at about 175° W. longitude (Leapfrog station 11 in figure 6). It has $S = 33.1$, $\delta O^{18} = -0.7$. EPSTEIN and MAYEDA have two samples from the same area with the same salinity, their samples 89 and 92, taken just inside and just outside the Aleutian Islands, which give δ values (corrected to SMOW) of —0.75 and —0.71 respectively.

Thus the Aleutian current waters have already received the major part of their dilution and decrease of oxygen 18 content *before* they are ever subjected to effects of meltwater and runoff from N. America. As shown in Figure 10, the further decrease of salinity in the Alaskan current gyral and the northern part of the California current amounts to only 0.5 per mil, which is to be compared with the total salinity decrease of 2 per mil for Aleutian current waters relative to the equatorial surface waters. The principal effect observed along the N. Pacific surface water line in figure 10 is the *increase* of salinity and oxygen 18 content in the California current due to upwelling and mixing with N. Pacific equatorial water. The Subarctic Water off the Aleutians, composed of mixed waters from the Kuroshio and Oyashio currents, has already received 80% of the total dilution observed in the Gulf of Alaska and in the California current off the northwest U.S.

This difference in interpretation is important because continental runoff cannot have been a major factor in the overall dilution of the Subarctic Water which must be principally due to

the excess of maritime precipitation over evaporation. Our interpretation is extended, in a later section, to a totally different evaluation of the effects of continental ice on the isotopic regime in the oceans.

In figure 10 we do not observe a significant extension of equatorial region points into a region of low salinity and relatively high oxygen 18 content as compared to N. Pacific surface waters of the same salinity, as sketched in the expected diagram shown in a previous section (and as is observed in our surface Atlantic samples). That is, the almost horizontal equatorial region extension toward low salinities shown in the previous schematic δ-S diagram for surface waters is lacking. In a general way, this reflects the much smaller range of salinities found in the equatorial and sub-tropical Pacific waters than found in the Atlantic. Regions of excess precipitation are also strongly affected by upwelling and advective mixing so that the contrasting isotopic-salinity relationships in different regions are not as sharp as seen in the Atlantic.

Atlantic ocean surface and Deep Waters

In order to compare our data on North Atlantic Deep Water (table 2) with surface waters in the North Atlantic, it has been necessary to use the high latitude samples analyzed by Epstein and Mayeda (1953). Only two of our Zephyrus expedition stations were located far enough north to approach the area of North Atlantic Water. These stations, just west of Gibraltar in about 34° of latitude, have salinities of 36.52 and 36.56, and δO^{18} values of +0.93 and 0.87 respectively. We have used all the Epstein-Mayeda samples taken from north of 30° north latitude; these data, corrected to the SMOW standard, are given in Table 4, and plotted in Figure 11 with our data for North Atlantic Deep Water, and the two Zephyrus surface samples.

Figure 11 shows that, in contrast with the Pacific waters, the North Atlantic Deep Water plots directly on the linear relationship observed for the surface waters in the δ-S diagram. As we noted previously in the general discussion of the δ-S diagram, this is expected for deep water renewal by deep convection and mixing with surface waters in a restricted area. This is, of course,

in accord with the classical picture which places the principle source region for North Atlantic Deep Water in the Irminger Sea, off Greenland. (Over the years, estimates vary as to the relative importance of the Irminger Sea, the Norwegian Sea, and the Labrador Sea as source waters, depending on the amount of detailed work done in any given area. The most recent review of all the data is given by Lee (1963). Clearly we do not yet have enough data to discuss the relative importance of these areas as evaluated from isotopic data, but we believe that detailed isotopic studies of these areas may be useful in such studies).

Table 4. — *Oxygen 18 data for North Atlantic surface waters from* Epstein *and* Mayeda *(1953), corrected to the SMOW standard, used in figure 11.*

E-M Sample No.	Location	Salinity	δO^{18} (‰) vs. SMOW
23*	43°04'N, 19°40'W	35.80	+ 0.68
41	« Off Bermuda »	36.3	+ 1.11
42	« Off Bermuda »	36.4	+ 1.00
43	« Off Bermuda »	36.8	+ 1.30
19**	28°05'N, 60°49'W	36.78	+ 1.32
56	« Gulf Stream, off Norway »	35.2	+ 0.26
91	44°09'N, 68°14'W (off Maine)	33.0	— 0.95
90	« Off Greenland »	16.2	—11.33
93	« East coast, Greenland »	29.3	— 3.34

* Albatross station 400. The correction for HCl addition noted in an earlier part of this paper has also been applied.

** Albatross station 373, HCl correction also applied. Salinities used for both the Albatross samples are those given in the Albatross report, rather than the raw data given by Epstein and Mayeda. Note that their sample number 19, when corrected for the HCl addition effect, agrees exactly with the water of the same area given by their sample 43.

Epstein and Mayeda (1953) suggested that effects of freezing in northern waters, with increased salinity accompanied by no isotopic fractionation, could explain the composition of Atlantic deep waters. However, if one plots the data on deep and surface waters as is done in figure 11, the diagram shows that the simple classical picture of deep convection is quite adequate as an explanation of the North Atlantic Deep Water composition. One point of interest is that their sample 91 from the Gulf of Maine, which represents Labrador current water, plots on the line with Nor-

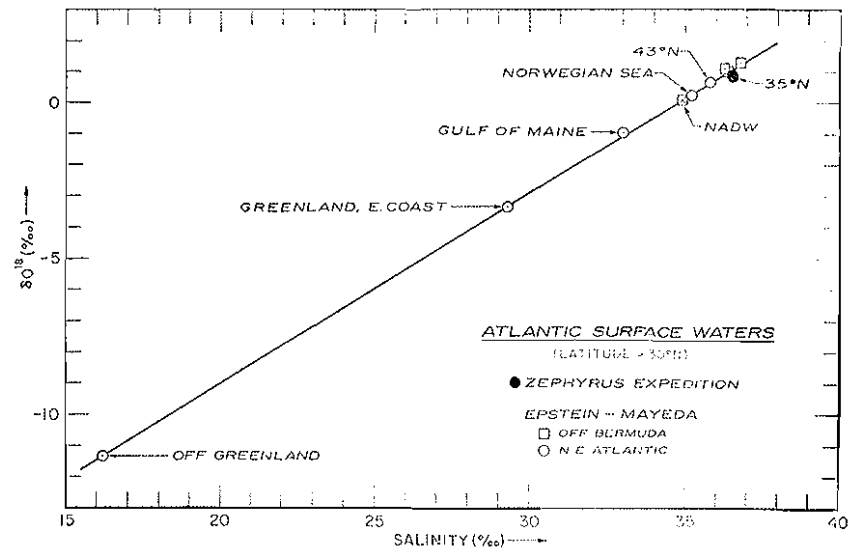

FIGURE 11. — *Oxygen 18-salinity relationship of North Atlantic surface waters and the North Atlantic Deep Water (NADW). Deep water data from the present work; surface waters from* EPSTEIN *and* MAYEDA *(1953) and present work.*

wegian Sea surface water and the waters of Greenland. This indicates that the fresh water diluent has a rather constant isotopic composition in all these areas. The slope of the line in figure 11 is $d\delta/dS = 0.61$, which gives a linear extrapolation to $\delta = -21.2$, for an actual δO^{18} value of —20.6 per mil in the mean fresh water diluent. This is a reasonable value for mean high latitude precipitation. The corresponding deuterium value, from figure 1, is $\delta D = -155$ per mil.

Finally we note that the EPSTEIN-MAYEDA samples 23 and 56 are from areas which should be well representative of North Atlantic water before dilution with the Arctic basin water and formation of the East Greenland current, while their Bermuda samples are representative of the Gulf Stream before extensive dilution at higher latitudes. The actual determination of the source of the fresh water diluent is a more complicated problem which demands a detailed discussion; this is reserved for a later section of this paper dealing with the general problem of the surface water variations.

Subtropical and Equatorial Surface Waters in the Atlantic

In Figure 12 we show the data from Lusiad and Zephyrus expeditions for subtropical and equatorial Atlantic waters, together with the data for deep waters and surface waters from the Weddell Sea. The N. Atlantic mixing line from figure 11 is also shown for comparison. It should be noted that we do not have data for S. Atlantic surface waters between 23°S and the Weddell Sea, so that the diagram is not a complete picture of Atlantic surface waters.

In this figure the striking difference between the δ-S slopes for equatorial and trade wind regions and the high latitude slope is clearly shown. In this case the low salinity branch with relatively high δO^{18} in equatorial regions, lacking in Pacific surface samples, is well shown. It extends out to about 34.2 per mil salinity and $\delta = +0.6$ per mil. The slope is only about 20% of the N. Atlantic slope. This is in accord with the expected picture outlined previously, and is discussed more quantitatively in the final part of this paper.

South Atlantic Surface and Deep Waters

Figure 12 shows also the individual points for the North Atlantic Deep Water samples listed in table 2, and the surface and serial samples from the Weddell Sea collected for us by the Eltanin (Cruise 12, March and April, 1964). These data show three important features on the δ-S diagram.

1. The surface and near-surface waters in the Weddell Sea (collected from 59-65°S. latitude) plot with a slope $d\delta/dS$ approximately equal to zero, as expected for the isotopic-salinity relationships in the freezing of sea ice. (These points in figure 12 are the Weddell Sea points to the left of the arrow connecting the slope legend to the horizontal dashed line.) We note that these surface waters center about a point only slightly less saline than the composition of the Pacific surface water at 65°S latitude, shown in figure 10. This composition, salinity about 34 per mil, δO^{18}

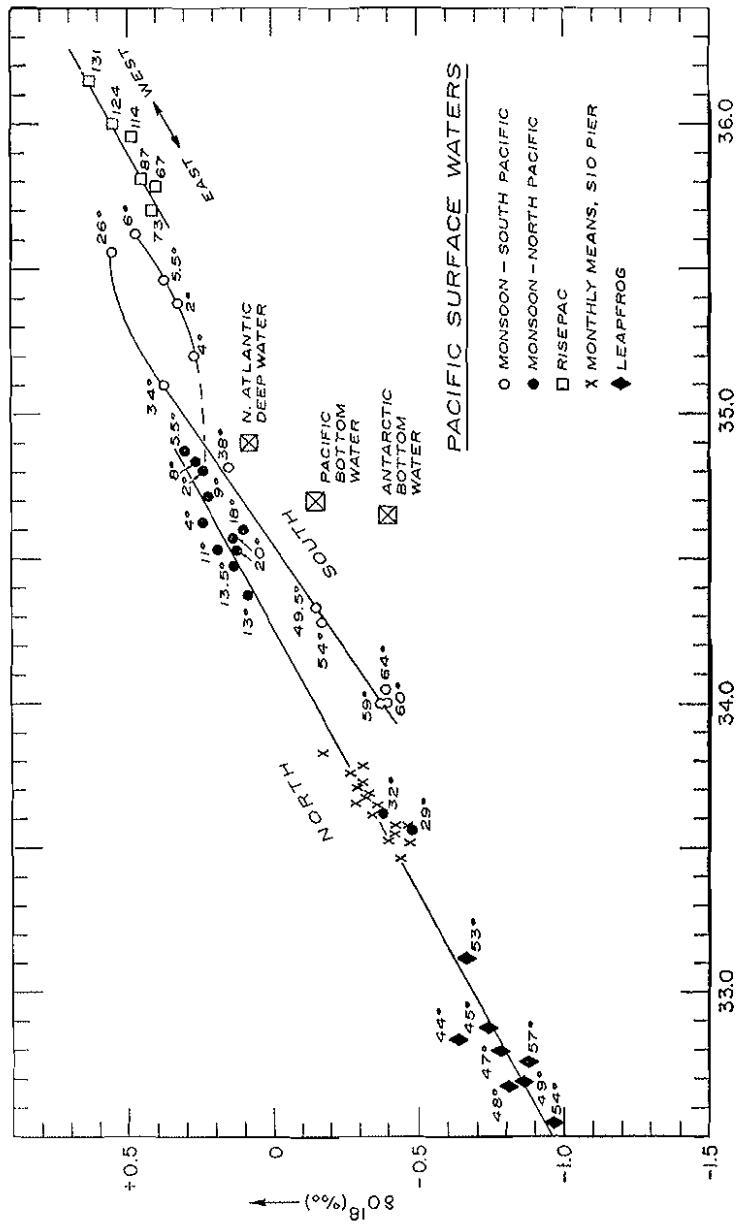

FIGURE 10. — *Oxygen 18-salinity relationships in surface and deep Pacific Ocean samples. Latitudes are shown for Monsoon and Leapfrog samples: the figures on the Risepac expedition points are station numbers shown in figure 6.*

about —0.45 per mil, should be close to the mean composition of the circumpolar surface water. The Weddell Sea surface waters in figure 12 with lower salinities reflect the dilution effect of the summer melting of the sea ice.

We note the curious effect that the equatorial and polar latitude slopes are very similar in the δ-S diagram, although these slopes are produced by the quite different mechanisms of precipitation in the one case, and freezing of sea water in the other.

2. The Antarctic Bottom Water was encountered in two locations, on the bottom; at 64°55'S, 52°10'W (station 3, bottom depth 2935 meters), and in a 600 meter thick layer at 64°00'S, 40°50'W (station 7, bottom depth 4609 meters). These points are plotted in the figure at the observed salinity and δ value of 34.66 and —0.45 per mil. This salinity agrees closely with the well-known minimum value (about 34.62 according to Mosby) required for sea water at freezing temperature to sink to the bottom. The isotopic composition is the same as that of the surface waters plotted along the horizontal line in figure 12, in agreement with the lack of significant isotopic fractionation in the freezing process.

Thus the isotopic values observed in the surface waters and in the Antarctic Bottom Water, when compared with the salinities, corroborate in an entirely independent way the classical process for the formation of bottom water in the Weddell. Sea by freezing, as described by DEACON, FOFONOFF, and others. It is also interesting to note that the « salinity gap » from 34.51 to 34.63 per mil, within which surface waters cannot be found in the open sea in this area because of the contraction effect on mixing with the deeper waters (FOFONOFF, 1956) exists in this set of waters.

Also noteworthy is the pattern of points in figure 12 for the North Atlantic Deep Water samples. Although the isotopic differences are very small (see table 2 for the data), the isotopic-salinity relationship observed is clearly that expected for mixing with the underlying Antarctic Bottom Water, as shown by the excellent fit to the dashed line connecting these water types. These features can only be observed by working at maximum possible precision of the isotopic measurements.

3. The composition of Pacific and Indian Deep Water is also shown in figure 12, and, as noted earlier, it clearly lies off the line connecting the North Atlantic Deep and Antarctic Bottom Waters. This relationship demonstrates very strikingly the need for a « third component », as discussed in the section on the origin of Pacific Deep Water.

Between the Antarctic Bottom Water and Pacific Deep Water points in figure 12 is a series of points representing Weddell Sea samples found at depths from 300 to 3000 meters, in which the isotopic δ value increases markedly at almost constant salinity. These waters at depths of a few hundred meters almost reach the composition of Pacific and Indian Deep Water *. These waters represent the Circumpolar Water, with the compositional range shown in table 3. (A few points representing mixtures of these waters with the surface waters, found at depths down to about 300 meters have been omitted from figure 12 for clarity).

As we noted in the section on Pacific Deep Water, we presently incline to the view that the elusive « third component » is Antarctic Intermediate Water in the S. Atlantic, so that the main part of the Circumpolar water has essentially the composition we observe in our highest latitude Pacific and Indian Deep Water samples by the time it leaves the Atlantic. This implies that Pacific and Indian Intermediate Waters play a minor role as contributors to the « third component ». We are continuing a detailed investigation of this problem with both the hydrogen and oxygen isotopes as samples from these regions become available.

Evaporation - precipitation - salinity relationships in surface ocean waters

We now attempt to formulate a more quantitative discussion of the isotopic and salinity relationships in the surface ocean waters as affected by the water exchange between the atmosphere

* Since preparing figure 12, we have analyzed two samples from Eltanin's station 9A which show a layer of water with salinity 34.693 and δ = —0.20 per mil, from 600 to 1000 meters at 61°59'S, 41°17'W. This is essentially identical with our southernmost samples of Indian and Pacific Deep Water. Temperature of this water ranges from +0.46 to +0.24°C.

and the sea. We shall use here the simplest possible model, corresponding to the one used by Wust to describe the salinity variations in surface waters (see Defant [1961] and Sverdrup, Johnson, and Fleming [1946] for extensive discussions of salinity effects in this model). Wust described the salinity variations in surface waters as a function of the annual evaporation (E) and precipitation (P) over the sea as:

$$S = S_o + k(E—P) \qquad (2)$$

where S is the local surface salinity and S_o is the mean salinity of the oceanic waters which mix and exchange with the surface waters according to the proportionality constant k. Wust correlated the empirical S_o values obtained from estimated (E-P) values for different oceans with the salinity of the underlying intermediate waters and found reasonable agreement. This treatment neglects the effects of horizontal transport and mixing in the surface waters; these effects are discussed by Jacobs (1951) in some detail. Montgomery (1959) has applied this model to the subtropical surface waters, using the modal salinity for the volume of each ocean for S_o. As discussed by Montgomery, the constant k in Wust's model corresponds to $S_o/\emptyset$, where $\emptyset$ is the mean flux of sea water from the surface mixed layer to the body of water of salinity S_o. Thus $\emptyset$, and therefore k, define a residence time relative to mixing in the surface waters, and the Wust model is identical with the two-reservoir oceanic mixing model of Craig (1957b).

Extension of this model to the isotopic data gives an equation analogous to (2) for the isotopic balance for either HDO or H_2O^{18}:

$$\delta \approx \delta_o + \left(\frac{S}{S_o} - 1\right)\left[(\delta_o - \delta_R) + \frac{(\delta_R - \delta_R')}{(1 - E/P)}\right] \qquad (3)$$

in which a small term $(1 - 10^{-3}S)^{-1}$, where S is given in per mil, has been neglected. (The bracketed expression on the right side of the equation should be multiplied by this term, which corrects for the salt content of the water, to make (3) exact.) In this equation, δ_o is the isotopic delta value of the sea water reservoir with sali-

nity $= S_o$, δ_E is the mean delta value of the evaporating water vapor (i.e. the *net* vapor flux removed as a result of the molecular exchange with atmospheric vapor), and δ_P is the mean input of liquid (fresh) water from *both* marine and continental precipitation. The continental precipitation includes two sources we shall wish to distinguish: normal continental runoff from rivers, and the melting of ice from the permanent ice areas. All these sources of fresh water are lumped in the δ_P term. However, the local effects of melting and freezing of sea water, as shown in figure 12 for the S. Atlantic surface waters, are here neglected in equation (3).

The isotopic balance can also be written directly in terms of E, P, and the mixing coefficient, as is done with salinity in (2), giving:

$$\delta \approx \delta_o + [E(\delta_o - \delta_E) - P(\delta_o - \delta_P)]\ (1/\emptyset) \qquad (4)$$

Using two isotopes, D and O^{18}, and salinity, we have three equations for the evaluation of E, P, and $\emptyset$, if the δ_E and δ_P values are known. These δ values will vary seasonally and with location, but these variations can be determined. Knowledge of these will allow direct estimates of E and P for a given area, independently of pan measurements and empirical estimates which are not very reliable. It should be noted that it is easier to determine δ_P than P, as the seasonal variations in δ_P in a given area are probably small enough so that only rough estimates of P variations are required to weight the observed δ values. Furthermore, the next easiest variable to measure directly is P, which allows evaluation of an additional variable. If δ_E can actually be measured, this allows us to add another mixing variable to the model and make it physically more realistic. In the last section of this paper we discuss our present ideas on δ_E.

The isotopic—salinity correlations are complicated because all the parameters E, P, $\emptyset$, S_o, δ_o, δ_P, and δ_E, vary over the oceans. The simplest way to discuss these correlations is in terms of equation (3) applied to local regions where the *ratio* E/P, which appears as a parameter in (3), can be taken as locally constant, together with the subscripted δ values and S_o. Although this is not realistic in detail, it allows us to discuss the isotopic-salinity correlations in a general way in terms of the estimates of E and P,

which is all we wish to do in this paper. With these restrictions, the slope in the δ-S diagram will be:

$$\frac{d\delta}{dS} \approx (1/S_o)\left[(\delta_o - \delta_E) + \frac{(\delta_E - \delta_P)}{(1 - E/P)}\right] \qquad (5)$$

With estimates of δ_E and δ_P, and assumptions of the E/P ratios, we can discuss the expected slopes for different oceanic areas as compared with the diagrams given in the previous sections.

WUST's correlations of (E-P) and S were obtained in the oceanic areas from 40°N to 50°S, which is roughly the same as the subtropical surface water area discussed in MONTGOMERY's (1959) treatment of this model. As noted by MONTGOMERY, the North and South Atlantic and Pacific are characterized in these regions by closure of the surface salinity contours around the high-salinity subtropical maxima reflecting the high evaporation in the regions of the trade winds. At higher latitudes, the model must be quite different, especially in the values of S_o and δ_o which can be taken to represent the mixing with surface waters. In this respect, the salinity models used by WUST and MONTGOMERY are actually equivalent to the « cyclic » or « outcrop » model of the ocean introduced by CRAIG (1958, 1963) for the comparison of radiocarbon and water residence times. We shall not discuss this complication here; we assume that for the general discussion of the δ-S relations, the variations in S_o and δ_o in different regions are not large enough to be significant factors.

From equation (4) we note that although $S = S_o$ when $E = P$ (shown by (2)), the relation between δ and δ_o depends on the δ_E and δ_P values. There are several conditions for which δ and δ_o will be equal:

(*a*) $E = P$, $\delta_E = \delta_P$. Here $S = S_o$.

(*b*) E and $P << \emptyset$. This also gives $S = S_o$.

(*c*) $\delta_P = \delta_o$, $E << \emptyset$. Here S is *not* equal to S_o.

Other cases are also possible. Conditions for which $\delta_E = \delta_o$ are not likely, as shown later. We want here to note case (*b*) above, which is the rapid mixing case. This is the case of deep convection in a specific region, discussed in the previous section on the rela-

tion of surface and deep waters, in which the deep water δ-S values plot on the surface water curve. Otherwise, the occurrence of a surface water with $\delta = \delta_o$ and $S = S_o$ is unlikely as it depends on the coincidence in (a), but is certainly possible.

If δ_P is always less (more negative) than δ_E, the δ-S diagram will show a cusp with infinite slope at the point where $E = P$. (This can be shown from equation (5)). Reference to figures 10 and 12 shows that this has not been observed in the Atlantic and Pacific. We conclude from this that in passing from high latitudes where E is less than P, to the subtropical salinity maxima where E is greater than P, we pass through a region where $\delta_E = \delta_P$ *before* (i.e. at higher latitudes) reaching the latitude where $E = P$. This follows because in high latitudes δ_P is more negative than δ_E as is shown in what follows. Since the regions where $E = P$ occur at latitudes of about 40° N. and S., this gives us some information on the variation of δ_P.

We shall use here only the mean E and P data for the entire oceans as given by WUST (see DEFANT (1961, table 87, p. 226)). The precise values and the differences for individual oceans are not important for the discussion of the general nature of the slopes in the δ-S diagram. The ratio E/P varies from about 0.14 at 60°S to about 2.4 in the trade-winds regions of the average northern oceans, assuming the E and P data to be approximately correct. (The reliability of the E data especially is essentially unknown). The E/P ratio variation is characterized meridionally by two rather sharp peaks in the northern and southern trade winds regions, and a minimum in the equatorial trough region of high rainfall, which looks schematically like this:

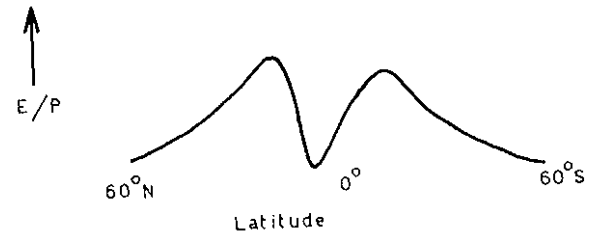

for the regions in which data are available. The mean position of the minimum is in the northern hemisphere (the meteorological equator). The points for $E = P$ occur at approximately 40°N and

S, and at about 0° and 10°N. For general purposes we can discuss three characteristic regions, with very approximate E/P ratios estimated from WUST's data:

(1). The equatorial trough: $E/P = 0.67$

(2). The subtropical maxima (trades): $E/P = 2.0$

(3). The high latitudes (above 40°): $E/P = 0.5$

We emphasize that the E/P values chosen are oceanic means, are arbitrary, and quite approximate. We use these data in equation (5) to discuss the δ-S slopes. First, however, it is necessary to discuss the δ_E and δ_P values to be used.

Isotopic Composition of Evaporating Marine Vapor

The isotopic relationships in evaporation and precipitation have been discussed by EPSTEIN and MAYEDA (1953), DANSGAARD (1954), EPSTEIN (1959), and FRIEDMAN, REDFIELD, SCHOEN, and HARRIS (1964). These authors assumed the value of δ_E, the mean vapor evaporating off the sea, to be the value of water vapor in isotopic equilibrium with surface sea water, i.e. with δO^{18} about 9 per mil, and δD about 70 per mil, less than the δ values for surface water. Figures 2, 3, and 4, show that the observed vapor above the sea does not have such an equilibrium composition for either isotope, and in fact has lower delta values than those corresponding to isotopic equilibrium. However, the data on the vapor over the sea do not give the value of δ_E. (It is important to recall that δ_E refers to the net vapor removal as a result of the molecular exchange between vapor and liquid. If the entire atmospheric cycle took place under equilibrium conditions, δ_E would correspond to equilibrium vapor). There are two ways in which the actual δ_E values can be estimated:

(1) By a detailed treatment of the exchange process at the sea surface, together with a knowledge of the atmospheric vapor delta values.

(2) By material balance with the mean precipitation.

Method (1) is ultimately necessary for application of the isotopic variations to detailed local studies. However, the method depends upon a complete understanding of the processes involved as well as on experimental determination of the isotopic fractionation factors in the exchange process. We discuss the present state of our knowledge of these effects in a later section. For present purposes method (2) gives a much better estimate of δ_E which can be made from very simple considerations.

The material balance depends only on the assumption that the mean value of δ_E must be equal to the mean value of δ_P, i.e. of the net water returned to the sea, in order to maintain the steady state isotopic composition, which is surely closely approximated. In order to use this method, we need only the precipitation δ values given by the authors cited above. Other useful data are given by CRAIG (1961a), CRAIG and LAL (1961), and especially by GONFIANTINI and LONGINELLI (1962) on N. Atlantic precipitation.

The oceanic E—P balance is approximately given by E=100 cm, P=90 cm, and R=10 cm, where R is the continental runoff and P refers here to maritime precipitation, and the units refer to cm over the total oceanic area, for annual mean values. (The runoff figure R is only 10% of the total water return to the sea, so the difference between P and (P+R) is not considered significant for the general discussion in the previous section. However, for use in specific areas, it must be noted that if δ_P refers to the delta value of the mean (P+R), then P in the equations actually refers to (P+R)). The weighting of the latitudinal values of P over the oceans in accordance with the earth's area in each latitudinal belt is shown by JACOBS (1951, figures 39, 40, and 41).

Considering the variation of precipitation rates *and* oceanic area with latitude, and the associated variations in δ, a crude balance sheet for the total world precipitation will be somewhat as follows:

Latitudes	Fraction of total precipitation	δO^{18} of mean latitudinal precipitation (‰)
0 — 20°	0.5	— 2
20 — 40°	0.4	— 5
40 — 90°	0.1	—15

which gives a mean value for δ_P for the entire oceans of —4.5 per mil. Although these estimates are very crude, the δO^{18} value of mean precipitation cannot be much lighter than —4 or —5 per mil. The corresponding δD values for mean precipitation will be —22 to —30 per mil. Since the continental precipitation values are not much lighter, except in very high latitudes where very little precipitation is contributed to the world total, these estimates should be representative of mean world precipitation. CRAIG and LAL (1961) made a detailed estimate of the isotopic water balance for the N. American continent, which gave for average N. American precipitation $\delta D = -30$ per mil, corresponding to $\delta O^{18} = -5$ per mil, in good agreement with the present estimates. The total oceanic range in δO^{18} of precipitation is from zero per mil, to values of about —5 per mil at New Zealand, to values of about —20 per mil at the coast of Antarctica. Even if the mean continental precipitation over the earth were as much as 10 per mil lighter in O^{18} than the mean oceanic precipitation, the effect on the world mean would be only 1 per mil relative to the oceanic mean, and it does not seem possible that the continental and oceanic means, weighted for area, can differ by more than about 5 per mil at most.

We therefore use an approximate value of $\delta_E = -4$ per mil for O^{18}, corresponding to —22 per mil for δD in what follows, and assume these values do not vary greatly over the ocean. (The values for δD corresponding to δO^{18} are taken from the correlation of CRAIG (1961a) shown in figure 1).

The Surface Water Variations

A discussion of the isotopic variations in surface ocean waters has been given by EPSTEIN and MAYEDA (1953) and EPSTEIN (1959), who described the effects of such variations on paleotemperature determinations. It is important for paleotemperature studies that the isotopic variations in the ocean caused by climatic variations be well understood, and the evaluation of the processes proposed by EPSTEIN and MAYEDA is basic for such an understanding. Their ideas can be summarized in four postulates covering the essential steps of their mechanisms:

(1) Evaporation of equilibrium vapor from the sea surface.

(2) Precipitation of rain enriched in O^{18} relative to the vapor in warm areas of the oceans, such that the mean vapor removed from these areas has δ values of the order of —15 to —20 per mil for oxygen 18, corresponding to slopes in the δ-S diagram of the order of 0.43 to 0.55.

(3) Further isotopic fractionation in precipitation in higher latitudes, and precipitation of light water, $\delta O^{18} = -20$ per mil, in the « permanent ice regions » of the world at high latitudes.

(4) Dilution of high latitude ocean surface waters by the melting of this ice, adding melt water of δ about —20 per mil, to give the observed slopes of about 0.55 in the δ-S diagram.

Their discussion is summed up in their statements: « the present vast areas of permanent ice fields keep the surface layers of the present warm oceans enriched in O^{18} by 1 per mil », and « the large areas of permanent snow and ice increase the variation of oxygen 18 by direct mixing of water from melting ice, and by production of water of higher O^{18} content in the warmer ocean surfaces ». This leads them to the conclusion that the « absence of melting glaciers would eliminate a large source of fresh water resulting in greater certainty in measuring paleotemperatures », and that the 1 per mil enrichment in O^{18} in the warm ocean areas, referred to in their first statement above « should disappear in non-glacial times ».

The basic part of this theory is the role played by the permanent ice fields in (*a*) removing water with a mean δO^{18} of —15 to —20 per mil from the warm oceanic areas, causing the enrichment of O^{18} in these waters, and (*b*) adding water with $\delta = -20$ per mil in the form of melting ice in the high latitudes, causing the observed depletion of O^{18} in these waters. We shall attempt a quantitative estimate of the effects of both of these processes.

In the first place however, it should be noted that the mean slopes in the δ-S diagram which they take as characteristic of the « warm areas of the oceans » are considerably higher than those shown in our figures 8, 10, and 12, because in considering the waters in intermediate and low latitudes they plot the surface

waters together with the intermediate waters down to about 1000 meters depth on the same diagram. Since the intermediate waters in the Pacific are offset from the surface waters in the direction of increased salinity for a given isotopic composition, this tends to give somewhat higher mean slopes when all points for all oceans are considered together.

Effect of Permanent Ice Fields on the Isotopic Enrichment in Low Latitudes

Assuming that the approximate 1 per mil enrichment in oxygen 18 of low latitude waters, relative to deep waters, results from precipitation of moisture of $\delta O^{18} = -20$ per mil in the permanent ice fields, we calculate how much precipitation is required in these regions. Equilibrium vapor in the low latitudes would have $\delta = -8$ per mil. If this is split into two fractions of (1) precipitation outside of the permanent ice fields, with $\delta = -4$ per mil, and (2) precipitation in the permanent ice fields, with $\delta = -20$ per mil, then the permanent ice field precipitation must amount to 25 per cent of the total precipitation. Even if the permanent ice field precipitation has $\delta = -32$ per mil, about as light as one can assume as a mean, the ice field fraction must be 14 per cent of total precipitation.

Precipitation in the permanent ice areas, however, is much less than the amounts calculated above. Using a mean annual precipitation rate for Greenland of 40 cm/year (BULL, 1958) and for Antarctica of 10 cm/year (LOEWE, 1960) and the ice cap areas relative to the oceanic area, we find the annual precipitation rates in these areas, expressed as cm/year *over the ocean area*, to be 0.18 cm for the Greenland ice cap and 0.37 cm for Antarctica, for a total of 0.55 cm/year. This is about 0.5 per cent of the total precipitation rate. Even if this permanent ice precipitation differs by as much as 30 per mil from the world mean, the effect on the O^{18} content of the remainder is only 0.15 per mil. Thus the precipitation in the ice regions cannot affect the isotopic composition of the low latitude ocean waters.

About 10 per cent of the total precipitation falls on the continents. If this precipitation differs in O^{18} content by 5 per mil

from mean oceanic precipitation (about the maximum difference which could be assumed), the effect on the oceanic fraction amounts only to 0.5 per mil. The actual effect is probably about half of this, so that even the total continental precipitation does not have a very important effect on the oceanic variations.

Effect of Permanent Ice Fields on the Isotopic Depletion in High Latitudes

We now discuss the possibility that the large slopes in the δ-S diagram observed for high latitude surface ocean waters are primarily due to dilution with meltwater from permanent ice regions. As shown by EPSTEIN and MAYEDA, and by the data in this paper, the slopes for these waters indicate a net addition of water with a mean δO^{18} of about −20 per mil, a value which is indeed characteristic of the ice in the outer regions of the permanent ice sheets in Greenland and the Antarctica. (Mean values of the δ-S slopes for high latitude surface waters in different oceans are given in the next section). The question, then, is whether quantitatively the melting of the ice sheets, which is the principal process by which they return their moisture to the water cycle, is an important contribution to the observed δ-S slope. It should be noted here that the δ-S relation is in general governed by the *net* resultant effect from marine precipitation, continental runoff, ice melting, and evaporation via equation (5); we are here examining the case in which the term P in equation (5) is assumed to represent *primarily* melting from permanent ice regions, and further, is assumed to be much greater than E. When the latter is true, the ratio E/P goes to zero, and it will be seen in equations (3) and (5) that the δ_E term vanishes, and the delta values and δ-S slopes are simply governed by δ_P, in this case the −20 per mil value assumed for the ice cap meltwater.

We discuss Antarctica first, the only permanent ice source for the southern oceans. The annual accumulation rate on the ice cap can be taken as 10 cm/year as noted in the previous section. Observations show that the ice cap is very close to a balance between accumulation and depletion, but that a slight net accumula-

tion rate is probable (LOEWE, 1960); we shall take the estimated rate of meltwater production as 9 cm/yr (over the ice cap), which cannot be far wrong. (LOEWE shows that melting is the only important process in the depletion of the ice cap). The area of Antarctica, including ice shelves, is 13.5×10^6 km^2.

The area of the Southern Ocean (water only) from 45°S to the Antarctic coast is 61.5×10^6 km^2, with an annual precipitation rate of about 90 cm. Thus the *marine precipitation* over the Southern Ocean thus defined is 46 times greater than the contribution from melting Antarctic ice. The melting ice contribution is then 2 percent of the total fresh water dilution (continental runoff from the other continents is negligible in this area), so that if the Antarctic ice is as much as 15 per mil lower in O^{18} than marine precipitation in this area (an upper limit estimate, probably a factor of two in excess), the net effect on the isotopic composition of the surface ocean water is only 0.3 per mil decrease in δO^{18} beyond the decrease produced by marine precipitation.

Alternatively, taking the Southern Ocean as comprising the water from 60°S to the Antarctic coast (a water area of 17.0×10^6 km^2) and repeating the calculation, marine precipitation is 12.6 times the meltwater contribution to the ocean water. If the meltwater is as much as 10 per mil lighter than the precipitation in this area, the total effect on the surface ocean water is to lower the δO^{18} value by 0.7 per mil over the dilution effect of the marine precipitation, again an insignificant amount.

For the entire S. hemispheric ocean, the Antarctic meltwater supplies an annual increment equivalent to 0.6 cm measured over this oceanic area, which is unnoticeable in comparison with the approximately 100 cm supplied by marine precipitation and continental runoff. As seen in figure 10, the δ-S slope corresponding to the approximately −20 per mil net addition effect, is seen in the S. Pacific from latitude 34° on south, at least in the central Pacific. As these calculations show, the Antarctic meltwater makes no significant contribution to this slope, which must reflect primarily the direct coupling between the sea and the atmosphere.

We now turn to the Greenland ice cap and its contribution to the North Atlantic. The water balance of the Arctic and N. Atlantic oceans is discussed by SVERDRUP, JOHNSON, and FLEMING (1946, p. 652-657), ZUBENOK (1956), and LEE (1963). The only

important exchange of Arctic ocean water is with the North Atlantic, from which water of about 35 per mil salinity enters the Arctic east of Iceland. The outflow to the N. Atlantic occurs in the Denmark Strait between Iceland and the E. Greenland coast, the emerging water having a salinity of about 31 per mil on the surface. The fresh water dilution in the Arctic ocean consists of an annual precipitation of 24 cm, and runoff from Siberian rivers amounting to 23 cm, for a total of 47 cm measured over the Arctic area (ZUBENOK, 1956). SVERDRUP *et al* find a total of about 53 cm, distributed the same way between the two sources.

The annual precipitation over Greenland amounts to about 29 cm (BULL, 1958). Assuming a steady state for the size of the ice cap, the meltwater contribution to the oceans, measured over the 8.8 times larger area of the Arctic ocean, is 3,3 cm, or about 6 percent of the total of Arctic ocean plus Greenland freshwater contribution to the Atlantic. If we include marine precipitation in the North Atlantic oceanic area immediately south of Greenland and Iceland, over say an area about four times as large as Greenland (extending to about 45°N) with more than twice as high an annual precipitation rate, then marine precipitation in the N. Atlantic alone contributes more than 8 times as much fresh water as Greenland meltwater.

Except close to the Greenland coast and in the Labrador Sea, the Greenland icecap contribution to the N. Atlantic is thus neglible in comparison with the Arctic Ocean contribution and small in comparison with precipitation in the N. Atlantic. In figure 11, we showed a δ-S plot for some N. Atlantic surface ocean waters. The Greenland E. coast sample has a salinity only about 2 per mil lower than the surface water flowing out from the Arctic through the Denmark Strait, so that more than two-thirds of the dilution of this water took place in the Arctic. The other Greenland sample with a salinity of 16 per mil must be representative of waters very close to the coast. If most of the dilution takes place in the Arctic and in the adjacent N. Atlantic, it is not surprising that a linear relation is observed, as the precipitation and Siberian runoff in the Arctic may be expected to have about the same isotopic composition as in Greenland and the evaporation rate in the Arctic is believed to be only about one-fourth of the precipitation and runoff.

In the North Pacific, there is no contribution of meltwater from permanent ice regions, except near the N. American coast. We have shown previously in our discussion of the data on these waters that almost all the dilution of N. Pacific surface water takes place *before* the Aleutian current reaches this area. However, as shown in figure 10, the high latitude waters show almost the same δ-S slopes as in the other oceans. This is another indication that marine precipitation and evaporation are the predominating factors in fixing the high latitude δ-S slopes, and that the effects of meltwater from permanent ice caps are unimportant except in areas immediately adjacent to Antarctica, Greenland, and the Alaskan coasts.

Isotopic-Salinity Relationships in High Latitude Surface Ocean Waters

We now discuss the δ-S relations in the context of equations (3) (4) and (5), for the three general oceanic areas for which mean E/P ratios were listed in the first section of this chapter. In discussing the slopes given by equation (5) it is useful to note that $(d\delta/dS)(S_o)$ gives the δ value in per mil of fresh water to which the straight line extrapolates at zero salinity, i.e. the net water added or removed as a resultant of all processes. (As noted in the discussion of (5) this delta value is about 3 percent higher than the actual value, due to the approximation in which the salt content of the seawater was neglected). Thus a δ-S slope may be characterized by its numerical value, or by the $S_o(d\delta/dS)$ product as a fresh water delta value in per mil, obtained by extrapolating the observed slope. The observed slopes in the high latitude surface ocean waters shown in figures 10, 11, and 12, and the equivalent water deltas (per mil) are:

Area	Slope ($d\delta/dS$)	Extrapolated δ	Actual δ
N. Atlantic	0.61	— 21.2	— 20.6
N. Pacific	0.54	— 18.5	— 18.0
S. Pacific	0.68	— 23.5	— 22.8

We shall not discuss these areas individually here. Rather we shall only compare the mean ratio E/P indicated by these data with the estimates given by WUST. The E/P ratio is given from the slope, according to (5) by:

$$E/P = \frac{[(d\delta/dS)S_o - \delta_o + \delta_P]}{[(d\delta/dS)S_o - \delta_o + \delta_E]} \qquad (6)$$

Note that the $(d\delta/dS)S_o$ terms are actually *positive* in sign, in contrast to the deltas for corresponding fresh water given in the above table. We may take δ_o as zero as it is small relative to the other terms. We assume $\delta_E = -4$ permil as discussed earlier in the section on evaluation of this term, and we take a mean value for the high latitude $(d\delta/dS)S_o$ of 21 per mil. Considering all the precipitation data available, a lower limit for δ_P is about —8.5 per mil; an upper limit may be placed at about —15 per mil. These values give E/P values of 0.73 and 0.35 respectively, in good agreement with the value of 0.5 estimated from WUST's data earlier in this chapter. WUST's value actually corresponds to a δ_P of —12.5 per mil.

Thus the high latitude slopes are in a general way understood when interpreted in terms of the marine precipitation and evaporation rates. However, the persistence of these slopes over large stretches of latitude in each ocean is more difficult to explain. We shall not pursue this topic here, except to point out that both horizontal and vertical mixing are certainly important; *cf.* our earlier discussion of the N. Pacific surface water data in which upwelling effects play an important part in increasing the salinity in the California current.

The Equatorial Trough and Subtropical Highs

In figure 12 we show an approximate mean slope drawn through the points for the Atlantic equatorial trough, with a value of about 0.11, corresponding to a net fresh water addition or depletion with δ of —4 per mil. The track location was described earlier. If $\delta_P = \delta_E = -4$ per mil, the E/P ratio is indeterminate, and this is probably close to being the case in this region. The

precipitation in this region is influenced by moisture brought in from the trade winds which may have undergone slight fractionation. If we assume the mean E/P value of 0.67 given earlier in the discussion of WUST's data, and $\delta_E = -4$, then as δ_P varies from 0 to —5, the value of $(d\delta/dS)S_o$ varies from —8 to +7 per mil (negative to positive δ-S slopes). The various segments connecting the actual equatorial trough points lie within this range, but we shall not attempt a detailed discussion here.

The solid points in figure 12 between the dashed equatorial trough slope and the solid high latitude slope are surface waters in the subtropical N. Atlantic surface waters. In particular, the four points marked with latitudes from 20-27 N represent a section directly through the high evaporation, maximum salinity region of the North Atlantic. A mean slope connecting these points with the other Zephyrus points has a slope of about 0.22, corresponding to a delta of 8 per mil. If δ_P ranges from 0 to —2 per mil, the E/P ratios calculated are 2 and 1.5, in good agreement with the average estimate from WUST's data of 2.0 for all oceans. As noted above, the precipitation in this region may in fact be somewhat heavier than equatorial precipitation, but there are not enough data to determine this. We do not yet understand the exact relationships between these points in figure 12 for the N. Atlantic trade winds belt, and a more detailed study is necessary.

Figure 12 also includes data in the S. Atlantic area of maximum evaporation in the southern trades. The four Lusiad point beginning at latitude 23°S, and which plot approximately in a straight line represent a section from the high latitude side to the peak of the E/P maximum in the S. Atlantic, according to WUST's values. The fourth point is at 14°S, and the track is along the 12°W meridian, it continues to the equator, though the slope changes abruptly at the fourth point as shown in the figure. The slope of the line through these four points is 0.55, corresponding to a delta value of 19.2 per mil. We have used $S_o = 34.5$, $\delta_o = -0.2$ per mil in this region. It should be noted that all four points have salinities equal to the mean S. Atlantic values at the corresponding latitudes.

Using $\delta_E = -4$ permil as in the above calculations, and assuming $\delta_P = -2$ permil we have calculated E/P ratios from the general slope of all four points, according to equation (5), and

also from the observed δ and S values for the individual points at 23° and 14°S, using equation (3). The three E/P ratios thus calculated are 1.13 from the slope equation, and 1.15, 1.15, identical values from the two points. Thus both methods of calculation agree well.

However, the E/P values given by WUST for this area of the S. Atlantic are markedly different, namely 3.1 at 23°S and 7.2 at 14°S (his maximum value), with a general mean value of about 5 for the area included by the points. If we assume an E/P ratio of 3 is correct, and reverse the calculation to give δ_P, we find that the required value is $\delta_P = +14$ per mil, which is impossible.

On the other hand, if we treat δ_E as the unknown parameter, then from WUST's mean $E/P = 5$ and the slope equation (5) we obtain $\delta_E = -16$ per mil. At 23°S using WUST's $E/P = 3$ and the δ-S equation (3), we obtain $\delta_E = -12$ per mil. And with this equation at 14°S using WUST's E/P ratio of 7, we find $\delta_E = -15$ per mil. These values of δ_E also appear impossible, for reasons pointed out in the evaluation of this parameter. Moreover, if we assume a δ_E value as low as —12 in the N. Atlantic trades region discussed above, we obtain $\delta_P = -16$ per mil for an assumed $E/P = 2$, which is impossible. Using a δ_E value of —13 in the high latitude regions gives a calculated E/P ratio of 1.65, which is also impossible.

In summary it is not possible to vary the δ_P and δ_E values assumed by any reasonable amount to agree with WUST's E/P ratios, which appear to be far too high. On the other hand, the E/P value of about 1.15 calculated for this region from the isotopic data is probably somewhat too low. ZUBENOK (1956) gives a mean E/P for all oceans at this latitude (south) of 1.7, considerably lower than WUST's and higher than ours.

It is also curious that the δ-S curve through this area shows a sharp break and reversal of slope at 14°S where WUST finds only a very gradual decrease of E/P ratio from his maximum of 7.2 (at 10°S he finds 6.5). It appears that the isotopic-salinity data, which agree quite reasonably in a general way in other areas with the E/P estimates, are markedly discordant here for reasons not understood.

Applications to Paleotemperature Studies

Our discussion leads us to conclude that the isotopic variations in surface ocean waters may well be about the same in both glacial and non-glacial periods. (Of course the absolute oceanic values for δ and S shift along a slope somewhat similar to the high latitude surface water δ-S slope with the addition and removal of water from the oceans by the continental glaciers. Also there are transients during the growth and decay periods because of the mixing time between surface and deep waters. We speak here of the variations in the surface ocean waters at any given time).

Our calculations indicate that the permanent ice fields now present on the earth have a negligible effect on the magnitude of the variations. This is seen especially in the North and South Pacific, but also in the other oceans. The surface water variations are controlled principally by the processes of evaporation, precipitation, and mixing in the ocean itself, with minor effects from the continental precipitation. The isotopic fractionation effects depend on the humidity and the temperature variations in the atmosphere controlling the precipitation over the sea, and the relative humidity and turbulent mixing from wind stress over the sea surface which control the evaporation. Moreover, if the continents drift around, such movements may have profound effects on the variations, as may be seen in the large variations which occur in the relatively enclosed North Atlantic. We do not wish to discuss the effects of glaciation on oceanic mixing and precipitation and evaporation here, as these effects are very complicated. But for applications to paleotemperatures, it is probably most reasonable to assume that variations fairly similar to those seen today have generally been present in the surface ocean waters.

EVAPORATION AND MOLECULAR EXCHANGE IN AN ATMOSPHERE OF FIXED HUMIDITY AND ISOTOPIC COMPOSITION

In order to understand the molecular exchange of water between the atmosphere and the sea and the factors governing the isotopic composition of atmospheric water vapor, we must first

discuss the much simpler case of an isolated water body evaporating into an atmosphere of fixed humidity and isotopic composition. This is the case, for example, of a small lake with no drainage in or out, evaporating into an atmosphere with properties fixed by a much larger body of water, i.e. the ocean. It was shown by CRAIG (1961a) that natural bodies of water which have undergone excessive evaporation relative to their water supply do not fall on the δD-δO^{18} line given in figure 1 with a slope of 8, but plot on straight lines extending off to the right of this line with a slope of about 5. These lines originate from points on the normal meteoric water line representing the mean precipitation supplied to the water bodies in question. One system of such points, representing the lakes and rivers of East Africa, is shown in the upper part of figure 1, plotting along the dashed line extending from a point on the line just above the point representing SMOW. Other such water bodies are plotted in the elliptical dashed area marked « closed basins » in figure 1; the lines extending from the precipitation in these areas are not shown but they have similar slopes of about 5 except in cases of high salinity lakes, where the isotopic relationships are strongly affected by the differences in isotopic activity coefficients.

CRAIG, GORDON, and HORIBE (1963) showed that the evaporation of an isolated body of water is characterized by a rapid molecular exchange with the atmosphere, so that the water body comes to an *isotopic stationary state* long before the total mass of liquid has evaporated away. However, when the atmosphere is completely dry there is no steady state and the liquid continually increases in heavy isotope concentration with an enrichment at any stage proportional to the logarithm of the fraction of initial liquid still present. The dry atmosphere process thus corresponds to a simple « batch distillation » process governed by equation (1), applied to one phase (i.e. the ratio of the two phases in eqn. (1) is to be taken as zero, since the present system is all liquid phase). However, it was shown by CRAIG, GORDON, and HORIBE that in this case the fractionation factors observed did not correspond to the α^+ values in eqn. (1), i.e. to the ratio of the equilibrium isotopic vapor pressures, so that evaporation into a dry atmosphere is *not* characterized by simple loss of vapor in isotopic equilibrium with liquid. It is of course obvious that the evaporation into normal « wet » atmospheres is also not a simple loss of equilibrium vapor, as such a process would also obey the batch distillation law and would never lead to an isotopic stationary state. In both cases the molecular kinetic effects associated with the net loss of vapor in the exchange dominate the isotopic fractionation. The theory of this process has been worked out by CRAIG (1965) for fresh waters, and experimental work, data on natural samples, and the theory, for saline waters have been studied by GONFIANTINI and CRAIG in papers to be published. The salt effect is not important for open ocean waters and is much more complicated, so that the present discussion is limited to the case in which salinity has essentially no effect on the evaporation process. In the following discussion we omit the mathematical derivations (CRAIG, 1965) and set down only the equations necessary for understanding the processes affecting the isotopic composition of the vapor evaporating from the sea and the vapor found in the marine atmosphere.

The Model for an Isolated Water Body

The isotopic composition of an evaporating isolated water body reflects the differences in the isotopic transfer rates in the processes of (*a*) condensation on, and escape from, the liquid surface, (*b*) molecular diffusion, and (*c*) eddy diffusion or turbulent transport. Classically it is difficult to write the eddy diffusivity as a continuous function varying with altitude because of the uncertainty in the mechanism of transition from a region of pure molecular transport to a region of pure turbulent transport. The continuous representation is even more difficult for the comparison of isotopic transport rates because one has a free parameter which essentially governs the rate at which the flux differences due to differing molecular diffusion coefficients are wiped out with increasing altitude by the increasing dominance of non-fractionating turbulence. The eddy diffusion coefficient itself is often written as a function of the molecular diffusion coefficient raised to some power between zero and one, the molecular coefficient having been inserted as part of a dimensionless group of properties. Such a representation implies that turbulent transport is fractionating with

respect to different components. This is possible if the overall transport by turbulence is dependent upon exchange by molecular transport between adjacent eddies. At present there is no experimental evidence for fractionation of components by turbulent flow, so that the validity of such a representation is unknown. In most studies of turbulent transport there are always enough free parameters to be adjusted so that the transport of *one* component can be adequately represented by the experimental data, and it is necessary to study the transport of several components from a source in order to resolve this question.

Nevertheless, it can be shown that inclusion of the molecular diffusion coefficient as a parameter in the functional representation of the eddy diffusion coefficient does not alter the conclusions reached below on the importance of the transport rates across the two-phase interface and the lack of equilibrium at this interface (CRAIG, 1965). We can, therefore, use the much simpler model in which we consider discrete layers within which one or the other transport mechanisms is totally dominant, and the fluxes through the layers are approximately linearly proportional to the boundary concentrations of the layers. Such a model corresponds to the « resistance » model of RIDEAL and LANGMUIR for liquid-vapor exchange, in which the fluxes are related to the concentrations at the layer boundaries by the « resistance » to transport across the layer, in simple analogy to Ohm's Law. It is well-known that, with certain assumptions, both molecular and turbulent transport can be so represented.

The first simple model is shown in figure 13. The liquid-vapor interface is bounded on either side by a laminar layer in each phase in which the principal transport is by molecular diffusion. Beyond the laminar layer in each phase is the section in which turbulent or eddy diffusion is dominant. The vapor phase profile shown (heavy curve) represents the atmospheric concentration of H_2O^{16} or the δ value of either heavy isotopic species. In the liquid phase, the profile represents the δ value of HDO or H_2O^{18}; the very slight concentration change of H_2O^{16} is not shown. (It can be shown that the « water » transport can always be taken as pure H_2O^{16}, and similarly, the slight diffusion gradient of H_2O^{16} in the liquid phase can always be neglected. This will be assumed in what follows). The atmospheric gradients vanish

at a certain point where the humidity and δ value of the vapor become constant with values h and δ_A characteristic of the « free air », unaffected by the evaporation process.

The transport « potentials » for water (H_2O^{16}) are taken as the relative humidity values, designated by a subscripted h on the left ordinate for the various layer boundaries. These relative humidity values are defined as the ratio of the specific humidity or mixing ratio at any altitude, z, to that of saturated air at the *pressure and temperature of the interface*. That is, h_z is a normalized relative humidity calculated relative to the P,T conditions of the interface. The transport resistances for water are shown on the left ordinate, denoted by a subscripted ρ for each layer. Thus the flux E_M of water vapor through the molecular diffusion layer of the vapor phase is simply given by:

$$E_M = (h_V - h_M)/\rho_M$$

where E_M is the upward flux of H_2O^{16}. In this case $\rho_M = Z_M/DC^*$, where Z_M is the thickness of the molecular diffusion layer, D is the molecular diffusion coefficient for water (H_2O^{16}) in air, and C^* is the absolute water vapor concentration (moles/cc). This approximation neglects the slight contribution to the flux by mass transport which is not important at ordinary temperatures; an exact expression necessary for high temperature transport is given by CRAIG (1965).

We shall use the subscript i to designate either isotopic species HDO or H_2O^{18}. The upward isotopic flux $E_{i,M}$ through the same molecular diffusion layer is then given by:

$$E_{i,M} = (h_V R_V - h_M R_M)/\rho_{i,M}$$

where R is the isotope ratio HDO/H_2O^{16} or H_2O^{18}/H_2O^{16}, and the isotopic resistance is the same as for H_2O^{16} except that it contains the isotopic molecular diffusion coefficient D_i. The isotopic delta values corresponding to the humidity values at each point are shown on the right hand ordinate in figure 13. The values h_V and δ_V refer to the vapor at the liquid-vapor interface. δ_S is the isotopic delta value at the liquid surface, and δ_L is the value in the mixed liquid below the laminar layer. The corresponding potential values for H_2O^{16} are simply one because of the formulation in terms of relative humidities and the neglect of liquid diffusion

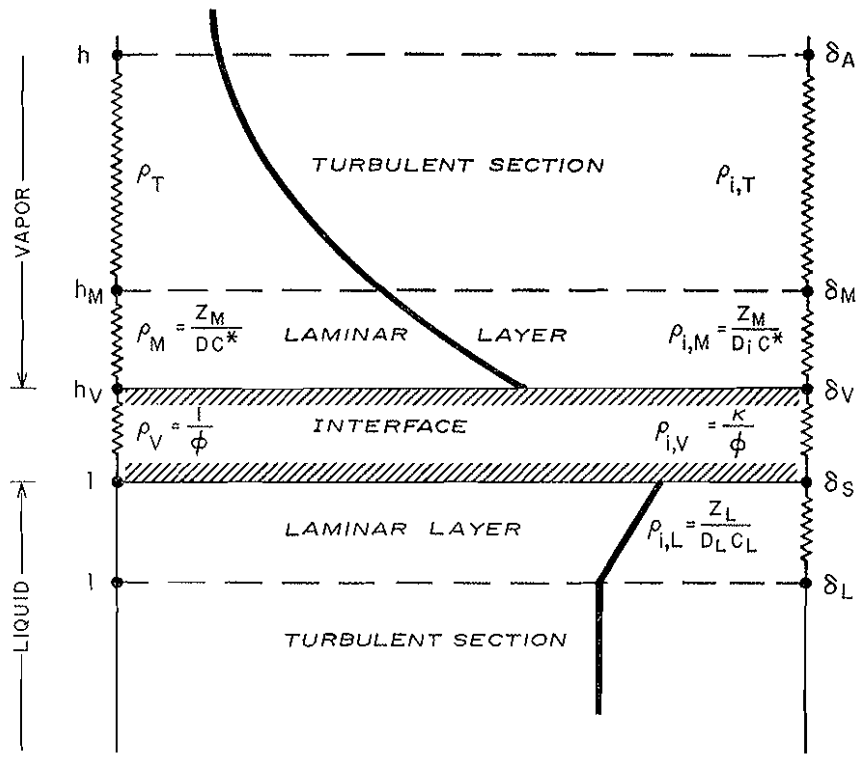

FIGURE 13. — *A laminar layer model for an isolated liquid. The heavy curve in the vapor phase represents water vapor concentration or isotopic delta value of the vapor. The heavy profile in the liquid represents the isotopic delta value of the liquid. The various* ρ *and* ρ_i *expressions are the transport resistances for* H_2O^{16} *and for the heavy isotopic species. The other symbols are defined in the text.*

of this species. In the liquid phase Z_L is the thickness of the surface layer of molecular transport, D_L is the « tracer » diffusion coefficient of either heavy isotope in the liquid, and C_L is the absolute concentration of water molecules in the liquid (moles/cc).

If liquid-vapor equilibrium exists at the two-phase interface we have $h_V = 1$, and $R_V = \alpha^* R_L$, where α^* is the equilibrium fractionation factor given by the ratio of the saturation vapor pressure of the heavy isotopic species to the saturation vapor pressure of H_2O^{16}. This fractionation factor is less than unity and is the reciprocal of the α^+ factor used in the discussion of the pre-

cipitation process preceding equation (1); the α^* factor is much more convenient for discussion of the liquid phase fractionation by vapor removal. Defining $\alpha^* = 1 - \varepsilon^*$, where ε^* is a small positive quantity (9.1 per mil for H_2O^{18} and 69 per mil for HDO at 25°C) the equilibrium isotopic condition at the interface is:

$$\delta_V = \alpha^* \delta_L - \varepsilon^* \tag{7}$$

in terms of isotopic δ values (we are here assuming $\delta_S = \delta_L$).

The transport rates for the different species through the interface, i.e. the relative evaporation rates, are given by:

$$E = \Phi(1 - h_V) = -dN/dt \tag{8}$$

$$E_i = (\Phi/K)(\alpha^* R_S - h_V R_V) = -dN_i/dt \tag{9}$$

where N and N_i refer to the number of moles of H_2O^{16} and of the isotopic species, per unit area in the liquid. Here Φ is the vaporization rate for H_2O^{16} (the concentration of which can be taken as constant), equal to $p^* \chi (2\pi MkT)^{-1/2}$, where p^* is the saturation vapor pressure at the same temperature, M is the molecular weight, an χ is the « condensation coefficient », namely the fraction of molecules impinging on the liquid surface which actually condense. The expression for E is readily understood by noting that $h_V\Phi$ is the condensation rate or flux of molecules from vapor to liquid, equal to Φ when h_V goes to unity. The fractionation factor K is equal to the ratio of the condensation rate of H_2O^{16} to the rate for the pure isotopic species, given by:

$$K = (M_i/M)^{1/2}(\chi/\chi_i) \tag{10}$$

where the subscript i is used for the isotopic species H_2O^{18} or HDO. The interfacial resistances are simply $1/\Phi$ for H_2O^{16} and K/Φ for the isotopic species.

The expressions (8) and (9) give the instantaneous evaporation rates from the liquid surface. However, if a molecular diffusion gradient exists in a surficial laminar layer of the liquid, as shown in figure 13, the R_S is not equal to R_L and it is necessary to evaluate the transport rate for the heavy isotopic species through this layer. The flux of H_2O^{16} through this layer can be taken

simply as E, the evaporation rate of the liquid. The flux of the heavy isotopic species through this layer, due to molecular diffusion and mass flow is then given by:

$$E_{i,L} = [(1 + E\rho_{i,L})R_L - R_S]/\rho_{i,L} \qquad (11)$$

where $\rho_{i,L}$ is given by the expression in figure 13. The mass flow contribution is required because the thickness of the laminar layer, Z_L, in the liquid is assumed to be constant during the evaporation process. The resistance to H_2O^{16} transport is zero. As we show below, the isotopic gradient in the liquid vanishes when the stationary isotopic state is reached. The isotopic resistance in the liquid affects the time constant for attainment of the stationary state, but does not influence the final isotopic composition of the evaporating liquid.

We shall not discuss the turbulent resistance in any detail, as we assume here that this resistance is the same for all molecular species, and is thus non-fractionating. Many specific models can be discussed based on combinations of the representations shown in figure 13 with various types of gradients. We shall not discuss these variations here, but only the transient and steady-state characteristics common to all models. Later on we describe a « rough surface » model in which the turbulent section extends to the interface, and which is probably more correct in detail than the model used in figure 13.

The Transient Isotopic Variation

It is evident that when the evaporation rate is steady, the flux E of H_2O^{16} is constant through any cross-section in the « one-dimensional » model shown in figure 13. Summation of the equations such as (8) for transport through the sections up to any level then gives:

$$E = (1 - h_z)/\rho_z = (1 - h_A)/\rho \qquad (12)$$

where h_z is the normalized humidity at any altitude z, ρ_z is the sum of the various resistances from the surface to the level z, and in particular h_A is the normalized relative humidity in a layer

we may term the « free air » whose properties are independent of the evaporation process. In the case of an isolated water body this layer is provided by the increase of wind speed and advective transport with altitude. The transport resistance ρ corresponding to the « free air » humidity h_A is the total resistance up to this layer:

$$\rho = 1/\emptyset + \rho_M + \rho_T \qquad (13)$$

for the specific model in figure 13. This is the fresh water case; in the case of a solution the activity of the water must be substituted for the value of unity in (12).

From equations (9) and (11) it is further evident that, when h_V is constant due to steady evaporation conditions, R_L and R_V will change until R_V reaches a value such that the flux ratio E_i/E of molecules leaving the liquid will become equal to R_L. At this point the liquid has reached the isotopic stationary state, so that δ_L and all δ values along the atmospheric gradient are constant. It should be noted that E_i and E in any section are the *net* transport rates upward as a result of the two-way exchange processes. In the stationary isotopic state the E_i values are constant and equal in all sections, so that E_i will factor in the summation of equations such as (9) for the isotopic flux in each section, and an equation analogous to (12) can be written for the isotopic flux.

In the transient condition before the isotopic steady state is reached, δ_L, and thus δ_V and all δ values along the atmospheric gradient, are time-dependent and the isotopic flux is not exactly the same in all sections. Nevertheless, we can still write an equation analogous to (12) for the instantaneous isotopic flux. To do this we note that the water concentration in the liquid phase (moles/cc) is 5×10^4 times larger than that in saturated air at room temperature, so that the isotopic ratio in the vapor phase has a very much faster response time than the ratio in the liquid. That is, the vapor phase can be assumed to be in an « instantaneous steady state » with the liquid phase isotopic composition, so that although the isotopic composition of the net flux from the liquid is changing with time as the liquid composition changes, at any instant of time the upward flux of O^{18} or D is approximately the same in all atmospheric cross-sections. This approximation a-

mounts to neglecting the rate of change of the number of isotopic molecules in any layer as small relative to the isotopic rate of evaporation. For example an evaporation rate of 1 meter/year of water corresponds to about 2 mm/year of H_2O^{18} ($R_L = 2 \times 10^{-3}$), an amount contained in 100 meters of saturated air. If the evaporation of one meter of water changes the O^{18} content of the liquid by 20 per mil, assume the vapor phase below the « free air » layer changes by 10 per mil in mean δO^{18} (its composition being pinned at one end of the gradient). Then in order for the rate of change of the vapor phase isotopic composition to be comparable to the evaporation rate of O^{18}, the height to the « free air » layer would have to be equivalent to 10 kilometers of saturated air. For HDO a comparable change in δ of the liquid would be 100 per mil (as shown by experiments) and R_L is about 3.2×10^{-4}, so that the « free air » height corresponds to 320 meters of saturated air. These are actually considerable under-estimates, as most of the transient isotopic variation in the vapor phase occurs in the immediate vicinity of the interface in a section which contains only a small amount of vapor, while in the rest of the vapor phase the change in isotopic composition is very small. In any case, for any realistic depth of original liquid and height to the « free air », we can neglect the rate of change of vapor phase composition, and similar considerations will apply to the laminar liquid layer when liquid diffusion is included in the model.

With this assumption, we sum the E_i expressions for the various layers, factor E_i, and obtain:

$$E_i = [\alpha^* R_L(1 + E\rho_{i,L}) - hR_A]/[\rho_i + \alpha^*\rho_{i,L}] \qquad (14)$$

where by analogy with (13) we have written:

$$\rho_i = K/\emptyset + \rho_{i,M} + \rho_{i,T} \qquad (15)$$

That is, ρ_i is defined as the total *atmospheric resistance*, exclusive of the molecular diffusion resistance in the liquid phase.

Equations (12) and (14) give the net removal rates of H_2O^{16} and of the isotopic species from the liquid, in terms of the transport resistances and the humidity and isotopic composition of the « free air » layer. The ratio E_i/E of these rates is $(dN_i/dN)_L$, the derivative of the number of moles of isotopic species in the liquid

with respect to H_2O^{16}. In general the progress variable most convenient is the fraction of liquid remaining, rather than time. From a theorem of the calculus, we have the relationship:

$$\left(\frac{d \ln R}{d \ln N}\right)_L = \frac{(dN_i/dN)_L}{R_L} - 1 \qquad (16)$$

in which the term $(dN_i/dN)_L/R_L$ is the instantaneous single-stage isotopic fractionation factor, which in this case varies during the process until it becomes unity in the steady state. Let the fraction of original liquid left at any time be $f = N/N^\circ$, where N° is the initial amount. Then evaluating (16) from (12) and (14), and changing from R to δ nomenclature, we have:

$$\left(\frac{d\lambda}{d \ln f}\right)_L = \frac{[h(\delta_L - \delta_A)/(1 + \delta_L)] - \varepsilon^* - \Delta\varepsilon}{(1-h) + \Delta\varepsilon + \alpha^* E\rho_{i,L}} \qquad (17)$$

where:

$$\lambda = \ln (1 + \delta)$$
$$\Delta\varepsilon = E(\rho_i - \rho) = E(\Delta\rho) = (1-h)[(\rho_i/\rho) - 1] \qquad (18)$$

and ε^* is the equilibrium vapor-pressure enrichment, defined in (7). We note that both ε^* and (as it turns out) $\Delta\varepsilon$ are positive in sign; moreover the sign of $\rho_{i,L}$ is taken as positive by convention (i.e. Z_L is defined as positive). Since the epsilon factors are always additive, it is convenient to define a total effective enrichment:

$$\varepsilon = \varepsilon^* + \Delta\varepsilon \qquad (19)$$

which is a function of the evaporation rate (or humidity) and the transport resistances of the isotopic species, as given by (18) for a given temperature. It should be noted that the liquid phase isotopic resistance is *not* included in the term ρ_i, which refers only to the vapor phase, as defined in (15) for the specific model in figure 13.

Equation (17) is the differential equation for the transient approach of the liquid to the stationary isotopic state. In the stationary state $d\lambda/d(\ln f)$ is zero, and the liquid phase has the composition:

$$(\delta^s_L - \delta_A)/(1 + \delta^s_L) = \varepsilon/h \qquad (20)$$

where the superscript S denotes the stationary liquid delta value. For example, in the experiments of CRAIG, GORDON, and HORIBE (1963) it was observed that with a humidity of about 75%, ε was of the order of 14 per mil ($\Delta\varepsilon$ about 5 per mil) for H_2O^{18}, so that the stationary liquid composition was about 18.5 per mil heavier than the incident atmospheric water vapor.

Using (20) we can write (17) in the simpler form:

$$\frac{d \ln (\delta - \delta^s)_L}{d \ln f_L} = \frac{h - \varepsilon}{(1-h) + \Delta\varepsilon + \alpha^* E \rho_{i,L}} \approx h/(1-h) \qquad (21)$$

which gives the slope when $\ln(\delta - \delta^s)$ is plotted against $\ln f$ for the liquid. This slope is essentially determined by the relative humidity of the free air as the other factors are normally small in comparison with h and $(1-h)$; equation (21) correctly gives the slopes observed in the CGH experiments which shows that the model is basically correct (CRAIG, 1965). We note that whereas the isotopic resistance in the liquid does not influence the steady state liquid composition, as shown by (20), the slope, or « fraction constant » is affected by diffusional holdup in the liquid. The time constant for the rate of approach to the isotopic steady state can be shown to be $(N_L/\alpha^*)(\rho_i + \alpha^* \rho_{i,L})$ for the case of pure isotopic exchange with no evaporation, that is with h equal to 100%. In the stationary isotopic state the isotopic gradient in the liquid vanishes. This can be seen by applying the steady-state condition $E_{i,L} = ER_L$ to equation (11), which gives $R_L = R_S$. In this state the transport through the liquid layer is entirely by the convective mass flow required to maintain the assumed constancy of the laminar layer thickness Z_L.

Although we are in general more interested in the steady-state phenomena, the transient equations are important for three reasons: they provide (1) a test of the validity of the model for experiments, (2) the « fraction » or time constant for the exchange, and (3) a method of calculating δ_E, the isotopic composition of the net water flux evaporating from the liquid. For example, we see from (21) that the log-log plot of $(\delta - \delta^s)$ vs. f for the liquid is linear when E,h, and the resistances are constant, with a slope which, with normal humidities, is essentially controlled only by the relative humidity and is thus approximately the same for all

isotopic species. This was observed in the CGH experiments. Furthermore, the stationary isotopic state vanishes, not at $h = 0$, but at $h = \varepsilon$, as shown by (21); that is at a relative humidity of about 1.4% for H_2O^{18} and about 9.0% for HDO, using the CGH epsilon factors. Thus there are low humidity values for which a stationary state composition can be attained for one isotope and not the other.

The mean isotopic composition of the evaporating moisture, R_E or δ_E, can be obtained from $R_E = E_i/E$, using (12) and (14), or directly from the transient equation (17), using the δ formulation of (16):

$$\frac{d\delta_L}{d \ln f_L} = \delta_E - \delta_L \qquad (22)$$

remembering $\lambda = \ln(1+\delta)$. In delta nomenclature we obtain:

$$\delta_E = \frac{\alpha^* \delta_L (1 + E\rho_{i,L}) - h\delta_A - \varepsilon}{(1-h) + \Delta\varepsilon + \alpha^* E \rho_{i,L}} \qquad (23)$$

As an example of the oxygen 18 values to be expected for the case of an isolated liquid, we give in table 5 the values of δ_E for four humidity values, for evaporation into an atmosphere of $\delta_A = -12$ per mil (characteristic of marine vapor and continental vapor near seacoasts), and also for $\delta_A = -20$ per mil, such as might be found at higher altitudes and in high continental latitudes. The values are calculated for a water with $\delta_L = 0$ per mil, for example sea water in the initial stage of evaporation. Also, the liquid diffusional resistance term in the denominator of (22) has been assumed to be negligible relative to $(1-h)$.

The value used for $\Delta\varepsilon$ is +5 per mil, the mean value observed in the CGH experiments (range 4-6 per mil); the corresponding $\Delta\varepsilon$ for HDO would be +20 per mil, so that the ε values are respectively 14 and 89 per mil (CRAIG, 1965). With a normal humidity of 75% and $\delta_A = -12$ per mil, the first vapor evaporating from an isolated body of sea water would have $\delta O^{16}/ = -20$ per mil, as shown in table 5, much lighter than equilibrium vapor which would have $\delta = -9$ per mil. Hower, if δ_A is as light as —20 per mil, the net evaporating vapor is actually heavier than equilibrium vapor, $\delta_E = +4$ per mil. With $\delta_A = -20$, we also see that

if $h = 70\%$, than $\delta_E = 0$ per mil, and since we have taken $\delta_L = 0$, this is the steady-state liquid composition for this humidity. The stationary-state liquid isotopic composition, δ^s_L, is shown in the last column of table 5 for each case.

TABLE 5. — *Calculated oxygen isotopic composition of the net water flux evaporating from a liquid phase with* $\delta_L = 0$ *per mil,* $\Delta\varepsilon = +5$ *per mil, and of the steady-state liquid.*

δ_A (‰)	h (%)	δ_E (‰)	δ^s_L(‰)
−12	75	−20	+ 6.8
	50	−16	+16.5
	25	−15	+46.6
	0	−14	+ ∞
−20	75	+ 4	− 1.4
	50	− 8	+ 8.2
	25	−12	+38.1
	0	−14	+ ∞

The deuterium delta value for marine and seacoast vapor is δ_A about −86 per mil (figure 4), so that with $\delta_L = 0$ per mil, $\Delta\varepsilon = +20$, and $h = 75\%$, we have $\delta_E(HDO) = -91$ per mil compared with equilibrium vapor of −69 per mil. Relative to equilibrium vapor, the deviation from equilibrium vapor is much less for deuterium than for oxygen 18 because of the much larger value of ε^* for HDO.

The sign of the diffusional gradient in the liquid (if one exists), shown in figure 13, is that of $(\delta_L - \delta_E)$; that is, if $\delta_L > \delta_E$, then $\delta_S > \delta_L$, and vice versa. In table 5, the surface layer is enriched in the heavy isotope, if a diffusional gradient exists, in all cases except that of $\delta_A = -20$ per mil, $h = 75\%$, in which case the surface layer is lighter than the main liquid, and the liquid is becoming lighter as the evaporation proceeds. It is obvious that the liquid can become lighter or heavier during evaporation, depending on the humidity and isotopic composition of the moisture in the « free air ».

The Isotopic Stationary State

The stationary isotopic composition of an isolated water body (no liquid input) is given by equation (20); as shown in (22) the composition of the net evaporate is the same as that of the liquid at steady state, so that we have:

$$\delta^s_E = \delta^s_L = (h\delta_A + \varepsilon)/(h - \varepsilon) \approx \delta_A + (\varepsilon/h) \qquad (24)$$

For the isolated water body there is no effect of liquid diffusion, as discussed below (21). The stationary liquid composition δ^s_L is always more positive than δ_A, the difference decreasing as h increases, until at $h = 1$, (where $\Delta\varepsilon = 0$), the difference has decreased to the equilibrium value. Typical steady-state values for several values of δ_A and h are given in table 5.

In the stationary state E_i and E are the same in all horizontal sections, and the isotopic composition of the vapor at any altitude, z, is fixed by the value of h at the same altitude. From (24) we have:

$$\delta_z \approx \delta^s_L - (\varepsilon_z/h_z) \qquad (25)$$

where δ_z is the vapor composition at height z. The parameter ε will be a function of z, because $\Delta\varepsilon = E(\Delta\rho_z)$, until a height is reached at which ρ and ρ_i begin to differ by a constant amount; i.e. at a point where the transport resistances through all sections above this point are the same. This point is more than likely reached just above the laminar atmospheric layer, assuming the turbulent resistances to be the same, though there are as yet no experimental data to show that this is the case. In any case, once the point is reached where $\Delta\rho$ is constant, the value of ε_z in (25) can be replaced by the constant value of ε (which can be obtained from (20)), and (25) fixes the relation between δ_z and h_z. As we shall see, this consideration is important for fixing the isotopic gradient over the sea. Moreover, it is important to note that once it is determined at what altitude the value of $\Delta\varepsilon$ becomes constant, then *any* values of δ_z and h_z measured at any altitude above this point can be used in (20) and (24) to calculate the actual value of $\Delta\varepsilon$, without having to sample the « free air » layer values δ_A and h. This again is important over the oceans.

Differentiating (25) we have:

$$d\delta_z/dh_z = \varepsilon/h^2_z \tag{26}$$

and:

$$d \ln (\delta_z - \delta^s_L) = - d \ln h_z \tag{27}$$

in which we are assuming ε has become constant with altitude. (27) shows that the fractional change in $(\delta_z - \delta^s_L)$ is the same as the fractional change in the (normalized) humidity with increasing altitude. For a normal humidity of 75%, using ε for $H_2O^{18} = 14$ per mil (from the CGH experiments), (26) shows that δ_z is decreasing 0.25 per mil per one per cent decrease in humidity with altitude. Since we can measure δ to probably 0.05 per mil, we can measure differences which correspond to h differences which are too small to measure, except for the necessity of sampling for a time long enough for turbulence to wipe out these small differences.

Conditions at the Liquid-Vapor Interface

The isolated water body experiments are particularly important because the effect of any laminar layer in the liquid surface vanishes in the steady state, so that the observed values of $\Delta\varepsilon$ provide information about the interfacial and vapor phase transport effects without the complicating effects of isotopic fractionation in liquid diffusion. Since these experiments have an important bearing on our understanding of the thermodynamic state at the interface and the condition of the laminar vapor layer, we shall briefly discuss our present interpretation of the data.

The kinetic contribution to the isotopic fractionation effect is given by the magnitude of the parameter $\Delta\varepsilon = E(\rho_i - \rho)$. Writing this out for the model in figure 13, we have:

$$\Delta\varepsilon = \frac{E}{\emptyset}(K - 1) + E\rho_M \left(\frac{D}{D_i} - 1\right) + E\rho_i \left(\frac{\rho_{i,T}}{\rho_T} - 1\right) \tag{28}$$

Of course all stages in which $\rho = \rho_i$ are non-fractionating and do not contribute to $\Delta\varepsilon$. We shall assume here that this is true for the turbulent transport, so that the last term in (28) is zero (this is

discussed in the following section). The contributions to $\Delta\varepsilon$ of the various stages are of course proportional to transport resistances of the stages.

The factor K is the ratio of the isotope ratio in the vapor at the interface to the isotope ratio in the molecules actually condensing on the liquid. It is also equal to the isotope ratio of vapor in equilibrium with the liquid surface divided by the isotope ratio in the molecules leaving the liquid surface, and as shown in equation (10) it depends on the molecular weights and condensation coefficients of the molecular species. The ratio of the condensation coefficients is not known experimentally at present, but there is no reason to think they are the same. The condensation coefficient is a measure of the « sticking probability » for a molecule striking the surface, or it may be considered as a measure of the escape probability for leaving the liquid.

The ratio of the isotopic molecular diffusion coefficients is readily calculated from kinetic theory for a gas, such as water vapor, in low concentration in another gas; it is simply the ratio of the binary diffusion coefficients for each isotopic species, given by the square root of the reduced masses (CRAIG, 1954, p. 122):

$$\frac{D}{D_i} = \left[\frac{M_i(M + 29)}{M(M_i + 29)}\right]^{1/2} \tag{29}$$

where M_i is the isotopic mass and M is the mass of H_2O^{16}. Equation (29) gives the diffusion coefficient ratio in air, which has a molecular weight of 29; the dependence of this ratio on the molecular weight of the « carrier gas » provides a good method for determining the contribution of molecular diffusion to the transport effects, by performing experiments in e.g. helium as well as in air.

The values of ε^* and the contributions to $\Delta\varepsilon$ from the interfacial effects and diffusion coefficient ratios are given in table 6. The interfacial fractionation ratio represents *only* the effect from the molecular weights in equation (10), that is assuming the ratio of condensation coefficients, (χ/χ_i), to be unity.

TABLE 6. — *Isotopic fractionation terms for HDO and H_2O^{18}, expressed in per mil. Values for (K — 1) represent only the mass effect, assuming the condensation coefficient ratio to be unity.*

	ε^* (25°C)	(K—1) (for $\chi = \chi_i$)	$[(D/D_i) - 1]$
HDO	69	27.4	17.3
H_2O^{18}	9.1	54.1	32.0

The ratio of the kinetic terms for HDO to H_2O^{18} in table 6 is 0.506 for the interfacial term and 0.541 for the diffusion term. Thus the ratio $\Delta\varepsilon(HDO)/\Delta\varepsilon(H_2O^{18})$ must be approximately 0.5 if *either* of the following conditions obtains:

(1) $\chi = \chi_i$ for *both* isotopic species HDO and H_2O^{18}.

(2) The vapor pressure at the interface is the saturation vapor pressure. In this case $h_v = 1$, and in the first $\Delta\varepsilon$ term in (28) $E/\emptyset$ goes to zero, so that the (K—1) term vanishes regardless of the condensation coefficient ratio. (It should be noted that the vanishing of this term does not require $E = 0$, but only that E becomes insignificantly small relative to $\emptyset$, the escape rate from the surface, so that h_v does not differ significantly from unity).

The CGH experiments showed clearly that in no case was the $\Delta\varepsilon$ ratio for HDO and H_2O^{18} equal to 0.5. The observed values ranged from 2.7 to 4.2 for experiments in which the humidity of the « free air » ranged from 0 to 80 per cent and E varied from about 0.4 to 2.0 meters/year (CRAIG, 1965). The observed values of the $\Delta\varepsilon$ ratio are all greater than unity. This indicates that neither of the conditions (1) and (2) above were obeyed. Since these $\Delta\varepsilon$ values provide slopes in the δD—δO^{18} plot such as are observed for evaporation of natural waters (as shown in the section on the Open System Model, below), it seems that these conditions are also violated in all cases of natural evaporation.

It should be noted that it is certainly possible experimentally to obtain a $\Delta\varepsilon$ ratio of 0.5 for HDO and H_2O^{18}. We have only to design experiments in which vapor phase molecular diffusion is made rate controlling, and the interface has the equilibrium vapor

pressure; this can be done by the use of long narrow tubes for the diffusion path, and numerous experiments have been made under such conditions for the measurement of diffusion coefficients or vapor pressures. However, it seems that, in natural evaporation, while molecular diffusion may constitute a significant part of the transport resistance, it never completely dominates the interfacial resistance due to slow escape from the liquid surface.

The PASQUILL-SUTTON *Turbulence Model*

As we noted previously the molecular diffusion coefficient for water vapor in air is often included in the formulation of the eddy diffusion coefficient as D raised to some power between 0 and 1. The most detailed example of such a theory is PASQUILL's (1943) modification of the turbulent diffusion theory of O. G. SUTTON (1934). (See also the detailed theoretical treatment by W. G. L. SUTTON (1943)). SUTTON's theory is two-dimensional in that the down-stream variation of the advective « free air » layer above a strip is considered; it is based on the statistical theory of turbulent diffusion developed by G. I. TAYLOR combined with the mass transfer problem solved by JEFFREYS for the case of a wind speed and diffusion coefficient independent of height. In SUTTON's theory there is no discrete laminar layer above the interface; the momentum transfer coefficient and wind speed increase continuously with height according to power laws governed by a parameter *n*, which is a measure of the extent to which turbulence is developed at any given time. We shall not discuss the theory itself; reference is made to the papers cited above, and to the excellent review of evaporation theory in general by ANDERSON, ANDERSON, and MARCIANO (1950). The SUTTON theory gives, with one exception, the best agreement with the detailed observations made in the Lake Hefner evaporation study (MARCIANO and HARBECK, 1952). (The only other theory, of the many proposed, which gave good results in this study is that of SVERDRUP (1937). The SVERDRUP model, which gave results as good as the SUTTON theory, is a two-layer model as shown in figure 13, which assumes that turbulent transport is non-fractionating, i.e. not a function of D).

PASQUILL's modification of the SUTTON theory is based on the belief that the molecular diffusion coefficient must be included in the eddy diffusion coefficient because the ultimate microscopic transfer process between eddies must be molecular. On the basis of a similarity argument with momentum and heat transfer, he replaces the kinematic viscosity of air in the momentum transfer coefficient by the molecular diffusion coefficient of water vapor, and takes the result as the eddy diffusion coefficient. The result is that the ratio of the eddy coefficients is given by $(D/D_i)^n$, where n is the turbulence parameter mentioned above. In the actual flux equations the eddy coefficients go in with a more complicated power of n; the end result is that in the third term of equation (28) above, the ratio of the turbulent resistances for the two molecular species, $\rho_{i,T}/\rho_T$, is given by (D/D_i) raised to the power $(2n)/(2+n)$.

The range of n is 0 to 1, with a value of 0.25 representing smooth flow and neutral equilibrium. Expanding the diffusion coefficient ratio in the last term of (28), we obtain the turbulent contribution to $\Delta\varepsilon$ in the theory:

$$(\Delta\varepsilon)_T = E\rho_T \left(\frac{2n}{2+n}\right)\left(\frac{D}{D_i} - 1\right) \qquad (30)$$

which is always a valid approximation. In the PASQUILL-SUTTON theory *per se*, this is the total $\Delta\varepsilon$, as the interface is assumed to be saturated. On the other hand the term in (30) can be taken as the third term in (28). In either case, if the conditions (1) and (2) listed in the previous section are obeyed, we see that the $\Delta\varepsilon$ ratio in (28) for HDO to H_2O^{18} will be about 0.5, just as in the case in which turbulence is non-fractionating. Thus the inclusion, in the turbulent coefficient, of the molecular diffusion coefficient raised to a power, does not alter the conclusions of the previous section.

It can be shown (CRAIG, 1965) that the values of the turbulence parameter n derived from (30) applied to the oxygen 18 data in the CGH experiments are quite reasonable (n = about 0.2), whereas those derived from the deuterium data (values of 2 to 3) are impossible, as the upper limit of n for fully developed

turbulence is 1. Although PASQUILL has shown that his formulation of the SUTTON theory can be reconciled quite well with experimental data on the evaporation rates of various pure liquids, it is evident that in detail the theory does not reproduce the evaporation rates of different molecular species.

The Rough-Surface « Micro-eddy » Model

Another way to model the turbulent transport is to assume that the laminar layer is periodically invaded or swept away by mass mixing, such as might occur with a hydrodynamically rough surface (CRAIG, 1965). This can be represented by a turbulent resistance placed in *parallel* with the diffusional resistance, rather than in series as is done in figure 13. The molecules in the laminar layer have probabilities, inversely proportional to these resistances, to be transported upwards by diffusion or by mass flow. In such a model, it is easy to show that the contributions to $\Delta\varepsilon$ for HDO and H_2O^{18} remain in the ratio 0.5, and this model leads to the same conclusions.

In the extreme case of such « parallel resistances » at the boundary, the laminar layer no longer has a real meaning and the turbulence extends down to the boundary itself. Such a model has been described by SVERDRUP (1937, 1951) in an attempt to construct a physical picture of the boundary layer over a hydrodynamically *rough* surface. SVERDRUP assumed that over a smooth surface the laminar layer has a fixed thickness for a given wind speed, and that the thickness varies inversely with wind speed. This is the model shown in figure 13 which we have discussed in the preceding pages. Over a rough surface, however, he proposed that the laminar layer of fixed thickness disappears, and that the turbulent eddies actually reach the sea surface as small air masses which immediately exchange momentum with the sea. The vapor flux into such an eddy is, however, controlled by molecular diffusion, so that the net vapor flux from the surface will then be controlled by the diffusion rate *plus* the exchange rate of eddies at the boundary. As an analog for such a process SVERDRUP introduced a boundary layer with a mean thickness, the value of which is a statistical quantity representing the average exchange

conditions over a rough surface. An implicit aspect of this model is the concept of a critical wind speed, introduced by MUNK, below which the surface is smooth and above which the surface is hydrodynamically rough. If such a critical wind speed exists, then we may expect that the model shown in figure 13 applies below the critical velocity, but that a different model describes the exchange process at higher wind speeds when the surface is rough, the transition between these models being discontinuous. We now describe briefly the model for the rough surface.

In calculating the isotopic fractionation in this statistical model for a rough surface, we cannot use the diffusional resistances shown in figure 13 for smooth surfaces because the diffusion process is not, in the microscopic process visualized, a steady-state process with a fixed vapor gradient. The details of the calculation have been treated elsewhere in terms of the diffusional flux into the small « micro-eddies » which contact the rough surface (CRAIG, 1965). In the simplest case, the unsteady-state diffusion causes a vapor flux into the micro-eddy over a mean residence time τ of a micro-eddy on the rough surface, and it is assumed that there is no reflection of the vapor gradient at the upper « boundary » of the eddy. Over the time τ the integrated flux into the micro-eddy is proportional to the square root of the diffusion coefficient, so that the ratio ρ/ρ_i, in this model is given by $(D/D_i)^{1/2}$ rather than to the power unity, and ρ_M becomes a function of the mean residence time τ, which replaces SVERDRUP's statistical thickness in our formulation as the critical parameter controlling the flux between the interface and the turbulent mixing zone above. The contribution to $\Delta\varepsilon$ from this process is given as in (30) above by expanding the diffusion coefficient ratio to a power which is now 1/2 so that the diffusional contributions to $\Delta\varepsilon$ are approximately one half those shown in the last column of table 6, i.e. about 8.6 and 16 permil for HDO and H_2O^{18} respectively. These contributions may be termed $\Delta\varepsilon_M$ for the rough surface model. As the micro-eddies rise from the surface, they blend with the overlying air in the turbulenn mixing zone where the truly turbulent resistance is encountered along a vapor gradient as shown in the turbulent section of figure 13, and, if PASQUILL's formulation of the turbulent diffusion coefficient is correct, an additional turbulent contribution to $\Delta\varepsilon$ would be given by equation (30).

In the CGH experiments in enclosed systems, the emerging air has a normalized relative humidity h_T, the humidity at the top of the turbulent mixing zone within the enclosure, so that in (12) if h_z is taken as h_T, the resistance ρ_z corresponding to this humidity is $(\rho_V+\rho_M+\rho_T)$. (The *total* resistance includes an additional exchange resistance, denoted ρ_X, which is inversely proportional to the flow-rate of air through the enclosed system. The proportionality in (12) between E and the humidity h of the *entering* air is governed by this total resistance, including ρ_X). Now it may be expected that in an enclosed system of small dimensions ρ_T may be small compared to the total ρ because of the short path length between the interface and the advective stream. In addition, if ρ_V is small compared to ρ_M, and if $(K-1)\rho_V$ is also small compared to $[(D/D_i)-1]\rho_M/2$, then we can easily show that $\Delta\varepsilon$ will be given by $(1-h_T)\varepsilon_M$, where ε_M is the diffusional fractionation term. That is, ε_M will be given by the diffusional terms in the last column of table 6 if the smooth flow model with a laminar layer of fixed dimension and fixed gradient applies to the process, or, if the statistical model for rough flow outlined above applies, ε_M will be given by one-half these values for each isotope. (It is assumed here that $\Delta\varepsilon_T$, the purely turbulent contribution to $\Delta\varepsilon$, is zero). Therefore we see that if the turbulent resistance can be made small enough, it is possible (*a*) to determine if the interfacial resistance ρ_V is comparable in magnitude to ρ_M, (*b*) to determine if $(K-1)$ is comparable to the diffusional fractionation for each isotope independently, and (*c*) if for either isotope $(K-1)$ is not significant, then we can distinguish between the laminar layer model for smooth flow and the statistical « micro-eddy » model for rough flow.

In figure 14, we show a plot of the observed $\Delta\varepsilon$ values for H_2O^{18} as a function of the humidity of the *emerging* air from the enclosure, for the CGH exeriments with dry N_2 and for data given by DANSGAARD (1961) for similar experiments. The detailed calculations are given by CRAIG (1965). The calculated line in the figure corresponds to the model for a *rough* surface described above, so that ε_M is taken as 16 permil, one-half the value shown in table 6. It is seen that the fit of the observed $\Delta\varepsilon$ values is quite good over a broad temperature range, considering the uncertainties involved in measurements of h and $\Delta\varepsilon$ in all these rather crude experiments.

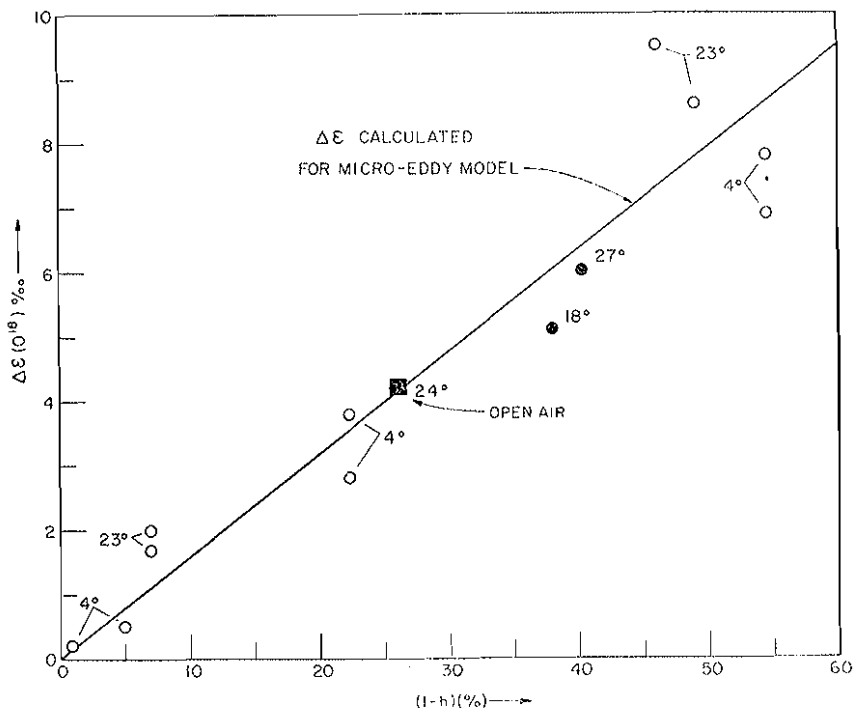

FIGURE 14. — *Observed values of* $\Delta\varepsilon$ *for* H_2O^{18} *from experiments compared with values calculated for a hydrodynamically rough surface, as a function of the humidity of the air emerging from the apparatus. Solid points from CGH experiments (and one later experiment not given in that paper); open circles calculated from data of* DANSGAARD *(1961). Temperatures refer to the liquid during the experiment. The point marked « open air » is plotted relative to the humidity of the ambient « free air ». The line represents the values calculated from the model, which differs from that shown in Figure 13 by having no fixed laminar layer over the rough surface.*

(If the model applies, the fit to this curve is independent of temperature, except that at higher temperatures the fractionation factor for diffusion, which is concentration dependent, changes as the concentration of vapor in the air increases. No correction for concentration has been made in this plot.) The open air point shown from the CGH experiments represents the actual humidity of the advective air used in an unenclosed experiment; in such an experiment there is no exchange resistance ρ_x, and the proper humidity to use to calculate $\Delta\varepsilon$ is this free-air humidity if the turbu-

lent resistance is small so that ρ_m is approximately the total resistance. In all of the CGH experiments plotted, the $\Delta\varepsilon$ values for HDO do *not* fit the calculated relationship for this isotope, and they are always greater than the values calculated from the above assumptions.

These considerations indicate that the interfacial fractionation factor K may be very close to unity for H_2O^{18} but significantly different for HDO, an effect which is plausible because of the presumably large steric factor introduced by the asymmetric character of the HDO molecule and the large vibrational effect on substituting D for H. The data further indicate that that the statistical model introduced by SVERDRUP for rough surfaces correctly describes the exchange process, at least in these experiments. If this can be shown to be generally true, then from the equations given here it will be possible to use isotopic data on oxygen-18 to calculate the actual molecular and turbulent resistances independently for the evaporation and exchange process, and thus to have individual values for these exchange coefficients which can be relatied to actual physical conditions. Further, if the interfacial fractionation factor for HDO can be determined, it will then be possible from the corresponding HDO isotopic data to determine the degree of interfacial undersaturation of water vapor and thus the extent of the thermodynamic disequilibrium at the interface. However, it is necessary to be cautious, because as noted above, we have neglected the possible contribution of turbulence to the fractionation via the effects discussed by PASQUILL and calculated in equation (30) above. For example, if we take a value of the turbulence parameter $n = 0.67$, then the coefficient in (30) becomes 1/2, and the relationship in figure 14 could be calculated just as well from assumptions that the molecular fractionation at the boundary is small and the principal effect is due to a PASQUILL-type fractionation in the actual turbulent transport above the boundary. A value of $n = 0.67$, intermediate between the expected values of 0.25 for smooth flow and 1.0 for fully developed turbulence, is certainly not excluded in the experiments done to date, and it is necessary to do experiments in which the turbulence spectrum is drastically changed so that different values of n *must* be expected, before the conclusions given above on the applicability of the statistical rough-surface model to H_2O^{18} fractionation under all conditions

can be considered established. However, with either molecular or turbulent fractionation models, we can see that the relationships of $\Delta\varepsilon$ for the two isotopic species always indicate that there must be some degree of undersaturation at the surface of the liquid, so that the expected ratio of 1/2 is not observed.

All these considerations lead to the conclusion (from conditions (1) and (2) in the previous section) that: (1) the condensation coefficient ratio, χ/χ_i, differs from unity *for at least one* isotopic species, HDO or H_2O^{18}, and (2) the liquid-vapor interface *deviates significantly from saturation equilibrium* during normal evaporation. Both these conditions are necessary to explain the data.

In this context « significantly » means to the extent that the first term in (28) is the dominant contribution to $\Delta\varepsilon$ for at least one isotope. Without a knowledge of the isotopic condensation coefficient ratios it is not possible to know at present the degree of interfacial disequilibrium. From the discussion of the data shown in figure 14, it seems likely that the condensation coefficient of HDO differs significantly from that of H_2O^{16} while that for H_2O^{18} does not, and this is plausible. However, as we noted, the turbulent contribution to the fractionation as given by (30) must be evaluated before this relationship can be considered firmly established.

It should be noted that in the empirical evaporation equations used for lakes and the ocean, it is assumed that the surface is at the saturation vapor pressure. If the relative humidity at the height used for wind speed measurements is, say, 80%, then an undersaturation at the interface of 10% means that the calculated evaporation rate is in error by a factor of two. Moreover, if the undersaturation depends on the evaporation rate, it is clear that the use of evaporation pans, especially at sea, is of very doubtful validity, as the interfacial conditions may be quite different from those of large water bodies.

The theory of interphase mass transfer has been treated with great thoroughness by SCHRAGE (1953) from the viewpoint of kinetic theory; he also reviews the experimental data on condensation coefficients, including the classical work of Alty and later workers which indicated a coefficient for water of about 0.04. For various reasons SCHRAGE doubts the validity of the experiments on which this value is based, and he also concludes that there is

no very conclusive evidence for interfacial disequilibrium of any significance in evaporation at normal pressures. It is apparent, however, that if only about 4 per cent of the water molecules colliding with a liquid surface can condense under even the best surface conditions, it is very reasonable that the isotopic condensation coefficients should differ significantly, more so than if essentially all colliding molecules could easily condense. The isotopic data therefore indicate that it would be worthwhile to pursue the work on the magnitude of the condensation coefficient, to establish the validity of Alty's work.

The Open System Model

It is evident that for the study of natural water bodies we have to consider a system open to exchange with liquid water. We shall here consider only the case where (*a*) this exchange is limited to input (I) of liquid, and (*b*) the steady mass state, $I = E$, has been attained. In this case the progress variable is time, and the isotopic equation is:

$$\frac{d\delta_L}{dt} = \frac{E}{N_L}(\delta_I - \delta_L) \tag{31}$$

where N_L is the mass of water, and δ_E is given, as before, by equation (23). The stationary isotopic state is simply: $\delta^s_E = \delta_I$. The stationary isotopic composition of the liquid, obtained from (23) is then given by:

$$\left[\frac{(\delta^s_L - \delta_l)}{(1+\delta_l)}\right]\alpha^*(1 + E\rho_{l,L}) = \varepsilon + h\left[\frac{(\delta_A - \delta_l)}{(1+\delta_l)}\right] \tag{32}$$

$$\delta^s_L \approx \delta_l(1-h) + h\delta_A + \varepsilon$$

We note that, in contrast to the isolated liquid, the liquid diffusional term $E\rho_{l,L}$ appears in the steady-state liquid equation. This has been neglected in the approximate formulation given below the exact expression). When there is a liquid input the diffusion gradient in the surface of the liquid can be maintained at steady state because the requirement is $\delta_E = \delta_I$ rather than δ_L.

At constant humidity, the derivative of δ^s_L with respect to δ_I is $(1-h)$, while with respect to δ_A it is simply h. The effect of the isotopic composition of the « free air » on the stationary isotopic composition of the liquid is thus $h/(1-h)$ times that of the input water, or about a factor of 3 to 4 at normal humidities, when the evaporation is balanced by input.

It is important to note that in equation (32) if $\Delta\varepsilon$ goes to zero so that there are no kinetic effects, the steady-state liquid composition still depends on *both* δ_I and δ_A via the humidity terms, and the atmospheric effect does not vanish unless h goes to zero. This is also true when the model which includes outflow of liquid is considered. The effect of the humidity is *independent* of considerations of the state of vapor equilibrium at the interface and the relative importance of molecular and turbulent transport in the vapor phase. FRIEDMAN, REDFIELD, SCHOEN, and HARRIS (1964) have made calculations, based on deuterium data, of the water balance of many lakes, neglecting the humidity effect. For example their model for lakes with no outflow is equation (32) above, for the case $h = 0$, which cannot be correct. Redoing their calculation (p. 186) on Pyramid Lake, assuming $h = 0.50$, $\varepsilon^* = 80$ per mil, and that δ_A is the equilibrium value of vapor relative to the unevaporated inflow water, we calculate $\Delta\varepsilon$ from equation (32) to be 17 per mil, almost exactly the mean value of 19 per mil obtained in the CGH experiments. Using an equation such as (32) which also includes outflow in the model, and takes account of the humidity, we have also recalculated their water balance for Lake Tahoe (*op. cit.* p. 187), assuming $\Delta\varepsilon = 20$ per mil. Whereas their calculation, assuming $h = 0$, gives the fraction of inflow removed by outflow as 38 per cent, our calculation indicates this fraction to be 90 percent. FRIEDMAN *et al* note that the very low salinity of Lake Tahoe and other lakes is surprising in view of the high evaporation rates they calculate, but the inclusion of the humidity term in the material balance calculation shows that in fact the evaporation rate is very much lower. Similar considerations apply to the deuterium balance calculations of BONNER *et al* (1961) which gave a fractional outflow for Lake Tahoe as low as 10 percent.

We now show that the open system model conforming to (32) explains the fact that the $\delta D - \delta O^{18}$ plot of evaporating natu-

ral water bodies, relative to their input waters, shows slopes ranging from 4 to 6, rather than the equilibrium slope of about 8 (CRAIG, 1961a; CRAIG, GORDON and HORIBE, 1963). We assume the incident vapor over such bodies to be that in isotopic equilibrium with the original precipitation in the region, i.e.:

$$\delta_A \approx \delta_I - \varepsilon^*$$

as given by (7). Using this value of δ_A in (32), we have, approximately:

$$\delta^s_L - \delta_I \approx \varepsilon^*(1-h) + \Delta\varepsilon \qquad (33)$$

The slope in the $\delta D - \delta O^{18}$ plot is simply the ratio of (33) for HDO and H_2O^{18}. The epsilon terms for HDO and H_2O^{18} respectively are taken as $\varepsilon^* = 69$ and 9 per mil (25°C), and $\Delta\varepsilon = 19$ and 5 per mil (the mean of the CGH values, which do not vary significantly over the wide range of their humidities and evaporation rates). The result is that over the humidity range from 0 to 100 per cent, the calculated D/O^{18} slope varies from 6.3 to 3.8. At humidities of 75 and 50 per cent respectively, the slopes are 5.0 and 5.6; these values are found for most of the highly evaporated water bodies studied. For an *isolated* water body (no input), application of the same considerations to equation (24) shows that the same slopes are obtained as a function of humidity.

It is seen that the model and the observed $\Delta\varepsilon$ values explain the non-equilibrium isotopic slopes observed for natural waters quite well. It is shown by CRAIG (1965) that the D/O^{18} slope in evaporation is very close to linear, as observed in nature.

The variation of the atmospheric vapor composition at any height z with h_z is formulated in this model in an entirely similar way to equations (26) and (27) for the isolated system. We obtain for the model with inflow:

$$d\delta_z/dh_z = (\delta_I - \delta^s_L + \varepsilon)/h^2_z \qquad (34)$$

and:

$$d \ln (\delta_z - \delta_I) = -d \ln h_z \qquad (35)$$

in which we note that δ_I occurs in the logarithmic differential, rather than δ^s_L as in (27) for the isolated water body. These equations fix the isotopic composition of the vapor relative to the humidity, when ε has become constant with altitude, in the steady state.

The ocean - atmosphere moisture exchange

Up to this point we have been considering the exchange of water between a liquid and an atmosphere not strongly influenced by the water body itself, but approximately fixed in its properties by the large-scale processes of the ocean and the atmosphere. When we come to consider the sea, the situation is quite different; there is no independent « free air » and the atmospheric properties are adjusted to a self-determined, more-or-less steady state fixed by the cyclical return of precipitation and by the zonal, meridional, and vertical mixing rates. We now wish to ask how, in general, this comes about, and how the system works for our particular terrestrial ocean.

We have shown in equation (23) and table 5 that sea water ($\delta O^{18} = 0$) evaporating from an isolated container into normal marine air with a relative humidity of about 75 percent, will lose a net water flux with $\delta O^{18} = -20$ permil. Equilibrium vapor would have a δ value of -9 permil. (The value of -20 permil matches the δ-S slope observed for high-latitude surface waters, but this is simply a coincidence; the ocean as a whole does not exchange with the atmosphere like a pan of sea water). We pointed out earlier that the material balance with the mean atmospheric precipitation shows that the mean composition of the net evaporate from the sea corresponds to δ values of about -4 and -22 permil for O^{18} and D. The actual vapor found over the sea surface is much lighter, and is even lighter than equilibrium vapor, ranging up to -14 permil for δO^{18} (figures 2, 3, and 4). In order to understand these relationships between the equilibrium vapor, the evaporating vapor, and the actual vapor in the atmosphere, it is necessary to discuss the steady state of a very simple and schematic model before attempting to treat the ocean more realistically.

The Isotopic Steady State over the Ocean

When the vertical fluxes through a given column are constant, δ^s_E, the steady composition of the net flux is given by equation (23), in which we can write h_z and δ_z for the humidity and isotopic composition of atmospheric vapor instead of the h and δ_A in (23). This is discussed in connection with equations (25-27). The δ-h gradient for the open system with input is given by equations (34) and (35) in the previous section. We shall use δ_P rather than δ_I in discussing the input of liquid water into the ocean. From equation (23) we have in general:

$$h_z(\delta_P - \delta_z) - \Delta\varepsilon_z(1 + \delta_P) = \text{constant} \qquad (36)$$

and, in particular, when an altitude is reached at which the rate of increase of transport resistance with altitude becomes identical for all molecular species, so that $(d\rho/dz) = (d\rho_i/dz)$, and thus $\Delta\rho = (\rho_i - \rho)$ is constant, then $\Delta\varepsilon$ becomes constant regardless of the fact that the transport resistances continue to increase with altitude and δ_z and h_z may continue to change. Because of the rapid increase of eddy diffusivity with altitude this non-fractionating level almost certainly occurs very close to the sea surface. Above this level we have:

$$h_z(\delta_P - \delta_z) = \text{constant} \qquad (37)$$

which is exact, and relates the normalized humidity and δ value of atmospheric vapor at any level z. This is simply the integrated form of (34).

Equation (37) shows that, as we would expect, the processes which fix the humidity at any point are those which fix the isotopic composition, and that the vapor composition is not fixed relative to the δ value of precipitation as long as the humidity is a variable. In order to see how the composition of the vapor is determined, the instructive question to ask is why, after all, the marine atmosphere is not saturated with water vapor. The undersaturation of the atmosphere as a whole is simply due to the localized nature of the vertical circulation, which restricts the

upward motion of air to a small fraction of the total area of the sea. In these localized areas the rising air is wrung out by adiabatic cooling and fed to wide-spread areas of descent where it warms adiabatically and returns to the surface as dry or undersaturated air.

A picture of this type applies to both the regional and local circulation. We can think of the area between the subtropical high pressure zones which bound the tropics as having an adiabatic funnel over the equatorial trough, where the air rises, precipitates its moisture, and descends as warm dry air at the high latitude boundaries to pick up moisture from the sea in the trade winds flowing back to the equator. This is a steady-flow system in which the isotopic variations and the humidity will reflect the transport and mixing rates. Alternatively, in any local region the convective processes responsible for the vertical motion restrict the rising air to local jet-like vertical currents which produce saturated clouds surrounded by large areas of descending drier air. For example, in the areas of the trade cumuli where the mean cloud cover is about 50 percent, the actively ascending air in cumuli may occupy about one percent of the entire area and 2 percent of the cloud area, if it is assumed that the velocities of descending air inside and outside of clouds are equal (RIEHL, 1954). Even in the high precipitation area of the equatorial trough only about one percent of the area has active rain at any given time (MALKUS, 1962). Thus in either a regional or a local model, we are never dealing with a continuous layer of saturated air at the condensation altitude, but with local condensation in the upper air at convection sites, surrounded with descending air whose humidity and isotopic vapor composition are fixed by such factors as the heights to which cumuli can grow, the fraction of moisture wrung out in the ascent, the degree of entrainment of dry air, etc. The general mean motion is downwards over most of the area, with a net upward transport of moisture due to turbulent diffusion against the mean motion. Grossly speaking, it is this phenomenon of limited precipitation areas and general descent of drier air which provides the equivalent of a « free air » layer over the sea. Once the cloud base is reached the moisture exchange at higher altitudes is rather simply treated as an exchange between rather well-defined layers.

We now discuss a simple case in which δ_A and h are taken as the values characteristic of this rather uniform descending air over a general area in which horizontal gradients are neglected. We are interested in the deviation of the vapor from isotopic equilibrium with the surface sea water. Using the open system equation (32) for a general model in which $E = P$, and designating the surface water steady composition as δ^s_L and the input as δ_P in (32), we compare δ_A with the value δ^*_A characteristic of isotopic equilibrium with the water where we have by (7) $\delta_A = \alpha^* \delta^s_L - \varepsilon^*$, and obtain:

$$(\delta_A - \delta^*_A) = \frac{(1-h)}{h}(\alpha^* \delta^s_L - \delta_P - \varepsilon^*) - \frac{\Delta\varepsilon(1+\delta_P)}{h} \qquad (38)$$

in which we see that of the two terms on the RHS the first is a humidity effect and only the second is due to the kinetic isotope effect. Thus even if there is no kinetic effect ($\Delta\varepsilon = 0$), *the vapor over the sea surface will never be at single stage isotopic equilibrium with the water unless the air is completely saturated.* With $h = 0.75$, the first term is about —1.3 permil for O^{18} and —12 permil for HDO. The magnitude of the second term depends on $\Delta\varepsilon$ as well as h, and thus reflects the mean evaporation conditions. We shall attempt to evaluate the mean values for D and O^{18}, but before doing this it is worthwhile discussing a special case of this general model.

The Single-Stage Precipitation Model

We continue to discuss the very general model of the previous section, assuming a homogenous vapor phase over the ocean with steady-flow values. However, we now assume that the upward flux of moisture in the precipitation sites is very large compared to the mean precipitation (or evaporation) rate, so that only a very small part of the moisture carried up is actually precipitated, and the rest is cycled by mixing. In such a case, the isotopic composition of the precipitation will differ by one equilibrium fractionation stage from that of the atmospheric vapor, i.e.:

$$\delta_A = \alpha^*_P \delta_P - \varepsilon^*_P \qquad (39)$$

where we designate by the subscript P the fractionation factors *at the temperature at which precipitation occurs*, which will be somewhat lower than the evaporation temperature so that ε^* will be larger. In this case δ_A and *h refer* to the vapor *in equilibrium with the precipitation*, and cannot be replaced by h_z and δ_z, but since the moisture flux is large compared with precipitation there will not be much of a gradient. As we show in the next section, this model actually is surprisingly good despite the restriction on the precipitation process.

We now wish to characterize four vectors in the $\delta D - \delta O^{18}$ diagram (e.g. figures 1 and 4) which fix the steady relationships of all components of interest; these are the lines connecting δ^s_L, δ_P, δ_A, and δ^*_A the equilibrium vapor relative to the surface water. We note that δ_P and δ_E are required to be equal by the material balance. These are all obtainable from (23) or (32) putting in the above precipitation restriction and from (38). (In (23) and (32) we are neglecting the effects of liquid diffusion; our present justification for this that the kinetic effects at the sea surface are quite similar to those observed in the CGH experiments where liquid diffusion could not have contributed to the observed $\Delta\varepsilon$ values obtained on systems without liquid input. However, this needs further study).

In this model equation (38) for the vapor deviation from equilibrium becomes:

$$\frac{(\delta^*_A - \delta_A)}{(1 + \delta_A)} = [\varepsilon^*_P(1 - h) + \Delta\varepsilon] / \alpha^*_P \qquad (40)$$

so that for a precipitation temperature of about 20°C, and $h = 0.75$, the vapor deviation from equilibrium with the surface, even with $\Delta\varepsilon = 0$, is about 20 permil for deuterium and 2.5 permil for oxygen-18, and is of course larger when $\Delta\varepsilon$ is not zero. Of course if $\Delta\varepsilon = 0$, the slope ratio in (40) for D to O^{18} will be 8, and all four components will plot on the meteoric water line. However, we see that δ_A *is always lighter* (lower in D or O^{18}) than equilibrium vapor, as long as $\Delta\varepsilon$ is positive which is the case in all experiments to date, as well as for the oceanic values.

The second relationship, between surface water and precipitation, is given by:

$$\frac{(\delta^s_L - \delta_P)}{(1 + \delta_P)} = [\varepsilon^* - h\varepsilon^*_P + \Delta\varepsilon] / \alpha^* \qquad (41)$$

or:

$$(\delta^s_L - \delta_P) \approx \varepsilon^*(1 - h) + \Delta\varepsilon \qquad (42)$$

in which the slight difference in ε^* and ε^*_P has been neglected. This equation fixes the precipitation relative to the surface water, for the mean values of all parameters. Finally the values of δ_P relative to δ_A and of δ^s_L relative to δ^*_A are fixed by (39) and the equation in the sentence before (38).

The ratios of the left sides of these equations for HDO to H_2O^{18} define the vectors in $D - O^{18}$ space. The vector $[\delta^s_L - \delta_P]$ is seen from (42) to depend on the ratio of $[\varepsilon^* + (\Delta\varepsilon)/(1 - h)]$ for the two isotopes, just as in the case of the evaporation of lakes with input, as given by (33); this slope will be about 5.5. Also, (40) shows that the vector $[\delta^*_A - \delta_A]$ depends on the same terms and has very close to the same slope of the order of 5.5. The slopes of the other two vectors, $[\delta^s_L - \delta^*_A]$ and $[\delta_P - \delta_A]$, are fixed by the ε^* ratio only, and will be about 8, the slope of the meteoric water line. The end result is a D-O^{18} diagram which can be sketched as follows:

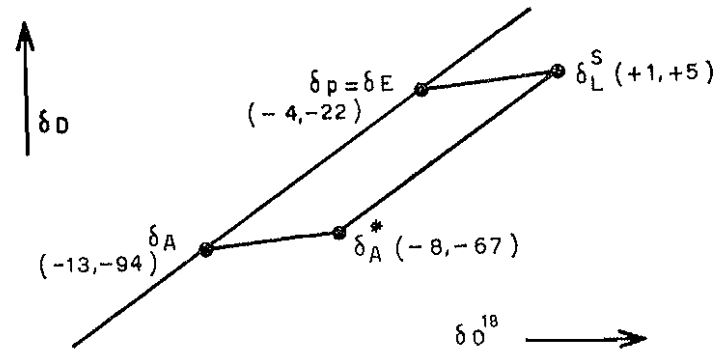

as a parallelogram with slopes of about 5.5 and 8.0 on the sides. The long side of slope 8 is the meteoric water line shown in figure 1. The approximate delta values in permil, for world averages of the components, are shown in parentheses as δO^{18}, δD.

Of course the values are estimated mean values, but they should be approximately correct over most of the oceanic areas.

The two diagonals are also of interest. For the surface water relative to the vapor we have:

$$\frac{(\delta^s{}_L - \delta_A)}{(1 + \delta_A)} = [\varepsilon^*(2 - h - \varepsilon^*{}_P) + (\varepsilon^*{}_P - \varepsilon^*)(1 - h) + \Delta\varepsilon] / \alpha^*{}_P\, \alpha^* \qquad (43)$$

or:

$$(\delta^s{}_L - \delta_A) \approx \varepsilon^*(2 - h) + \Delta\varepsilon \qquad (44)$$

so that this vector depends on the ratio $[\varepsilon^* + (\Delta\varepsilon)/(2 - h)]$, and normally has a slope of the order of 6.5, closer to the equilibrium value. This vector has the same slope for lakes with input. For isolated water bodies, the slope of this vector depends only on the ratio of the ε values for D and O^{18}, and this normally has about the same numerical value.

Finally the other diagonal is simply given by:

$$(\delta^s{}_E - \delta^*{}_A) \approx [h\varepsilon^* - \Delta\varepsilon] \qquad (45)$$

where $\delta^s{}_E = \delta_P$. This relates the composition of the actual net flux of water or evaporating vapor to the equilibrium vapor. We see that if there is no kinetic effect, *the evaporating vapor is always heavier than equilibrium vapor.* However if $\Delta\varepsilon$ is not zero, and the humidity is low enough or $\Delta\varepsilon$ large enough, the relationship may be reversed. The normal situation is that the evaporating vapor is heavier than equilibrium vapor, for the values we have observed for $\Delta\varepsilon$ (1).

(1) Since this was written we have seen a paper by W. DANSGAARD (1946)*, in which he discusses kinetic effects in the evaporation of vapor from the ocean. DANSGAARD states (p. 449) that, relative to the vapor in isotopic equilibrium with the surface sea water, the « fastly evaporated vapor must have lower δD and δO^{18}, because H_2O^{16} is the fastest reacting component ». In general this will not be true for a system like the ocean which is not undergoing a continuous net loss of mass. As we state following equation (31), the equation for the evaporating vapor in such a system is $\delta_E = \delta_I$. For the ocean as a whole δ_I is the mean value of δ_P; for any region of the sea, δ_I is the weighted mean composition of the precipitation and the net oceanic mixing flux, which together keep the local sea level constant. Since the precipitation over most of the sea is *higher* in δ value than equilibrium vapor, the evaporating vapor, no matter how fast it evaporates, will generally be *higher* in δ values than equilibrium vapor. The condition for DANSGAARD's statement to apply is , in fact: $\delta_I < (\delta^s{}_L - \varepsilon^*)$, so that the mean *input* of liquid water must be isotopically lighter than equilibrium vapor. This can happen only at very high latitudes and will certainly not be true over most of the ocean. (DANSGAARD's paper adds a great deal of valuable data to the literature, so that even better weighted means for oceanic precipitation can now be made).

* W. DANSGAARD: Stable isotopes in precipitation. Tellus 16, 436 (1964).

For the case $\Delta\varepsilon$ goes to O, and there are no kinetic effects, the parallelogram shown above condenses to a single line, the meteoric water line, with slope 8.0. However, as shown by the above equations, *the points for the four components remain discrete*, unless h becomes unity. But if $\Delta\varepsilon$ is O, then the surface ocean waters lie on the meteoric water line, and this is not observed. Thus we conclude that the mean oceanic $\Delta\varepsilon$ values are not zero, and are, in fact, comparable with the CHG data.

The delta values at the corners of the parallelogram are estimated mean values for the oceans, taking into account the area factors as was done for weighting the precipitation values earlier in this paper. None of these data are known to better than one permil for oxygen or 5 permil for deuterium, so no great attempt at accuracy has been made.

The $\Delta\varepsilon$ values for this model of single-stage precipitation equilibrium have been calculated from equation (40) assuming a precipitation temperature of about 20°C, and $h = 0.75$. (This is the best equation because the α^* and $(1+\delta_A)$ terms cancel). We obtain $\Delta\varepsilon$ values of 14.2 permil for HDO and 2.6 permil for oxygen. These values could each be zero within the present accuracy of the data. We emphasize that the present calculation is based on a restrictive model for a relationship between δ_A and δ_P which, as shown later is an oversimplification and probably not correct. The best evidence that the $\Delta\varepsilon$ values are, in fact, not zero is that the surface ocean waters do not lie on the meteoric water line, as shown in the above sketch.

The variations of δ_P with h and $\Delta\varepsilon$ are: $(\partial\delta_P/\partial h) = \varepsilon^+$; $(\partial\delta_P/\partial\Delta\varepsilon) = -\alpha^+$ (where $\alpha^+ = 1/\alpha^*$). The partial derivatives of δ_A are the same. Thus for fixed $\Delta\varepsilon$ values, humidity variations

cause the points to move back and forth along the meteoric water line with a slope of 8.0. For a fixed h, if we assume the ratio $\Delta\varepsilon_D/\Delta\varepsilon_O$ to be constant, δ_P and δ_A will vary along slopes given by $(\alpha^+\Delta\varepsilon)_D/(\alpha^+/\Delta\varepsilon_O) = 3.4$ for the present data. For a fixed δ^s_L, the h and $\Delta\varepsilon$ variations outline ranges for δ_P and δ_A which are small parallelograms centered on the points shown in the sketch, with sides represented by slopes of 8 and 3.4 and lengths proportional to the h and $\Delta\varepsilon$ variations.

If we take the present $\Delta\varepsilon$ values at face value, then of the mean δ_A value 5 per mil less than the equilibrium value, half the deviation is due to the mean humidity being 75 percent, and half is due to the $\Delta\varepsilon$ value, as shown in (40). If $\Delta\varepsilon$ were zero, the O^{18} value for δ_A would be —10.5, for δ_P would be —1.5, and both points would plot on the right side of the parallelogram above, on the line connecting δ^s_L and δ^*_A. The separation of these two lines is thus a measure, albeit not a very useful one, of the kinetic effects in the exchange process. For example, for a fixed O^{18} value, the deuterium difference between δD, on the meteoric water line, and δD^*, on the lower line, is:

$$\delta_D - \delta^*_D = 8(\alpha^+\Delta\varepsilon)_O - (\alpha^+\Delta\varepsilon)_D \qquad (46)$$

The intercept value of 10 permil on the meteoric water line (figure 1) is clearly determined by the $\Delta\varepsilon$ values and the mean δ of surface sea water. We emphasize that a decrease of $\Delta\varepsilon$ would cause points on this line to become enriched in D and O^{18} along slopes which are *not* about 5.5 as in evaporation of a water body and as the line connecting δ_P and δ^s_L in the above sketch, but along slopes given by the $\Delta\varepsilon$ ratio, here estimated to be of the order of 3.5 for this model. As noted earlier, this ratio is about the same as that found in the CGH experiments, which gives some reason for thinking the ratio may be approximately constant. It is clear that it may be possible to find meteoric waters on the enriched side of the meteoric water line which have not become enriched by evaporation of the water itself, but only represent derivation from moisture which originated over the sea with smaller than usual $\Delta\varepsilon$ values. However, this effect should be small, of the order of 1 or 2 permil for O^{18} for example.

Kinetic Effects at the Sea Surface

A much more accurate value of $\Delta\varepsilon$ is obtained from equation (23) which is general, and not restricted to a special assumption about precipitation and vapor as in the previous section. From here on we shall deal with the general model without this assumption. Equation (23) can be written as:

$$\Delta\varepsilon \approx \delta^s_L - \delta_P(1-h) - h\delta_A - \varepsilon^* \qquad (47)$$

In the exact form, the entire right side should be divided by $(1+\delta_P)$ and the ε^* term should be multiplied by $(1+\delta^s_L)$, but these two effects cancel each other, and the above approximation is quite accurate. We use the mean values for the terms on the RHS given in the last section; the fractionation factors are taken at 27°C. We note that an error of 2 permil in the O^{18} value of δ_P causes an uncertainty in $\Delta\varepsilon$ of only 0.5 permil. Moreover, in order to make $\Delta\varepsilon$ as calculated from (47) equal to zero, δ_A has to be as heavy as —9.3 permil for O^{18}, and this is clearly impossible for a mean value of δ_A according to the present limited data (figures 2 and 3).

The $\Delta\varepsilon$ values calculated from (47) are 14 and 3 permil for D and O^{18} respectively, not significantly different from those of the last section, but much more reliable. They are each about 2/3 of the experimental values observed in the laboratory in the CGH experiments (CRAIG, 1965). Of course the reason the present values compare so closely with those obtained in the restricted model calculation in the last section is the fact that the values used for δ_P and δ_A are in fact quite close to single-stage isotopic equilibrium (representing temperature of 26°C for O^{18} and 20° for D; these temperatures are too high to be realistic, so the model does not work in detail). However, our weighting estimates for δ_P were made quite independently of our measurements on marine vapor without the present calculations in mind, indicating that the restricted model has some element of correctness. As we show in the next section, the actual case is more complicated.

We now compare the $\Delta\varepsilon$ values with those which can be obtained from molecular diffusion in the vapor phase. From (18) we have for the contribution to $\Delta\varepsilon$ from diffusion in the laminar layer:

$$(\Delta\varepsilon)_M = (h_v - h_M)[(D/D_i) - 1] \qquad (48)$$

The diffusional fractionation factor is given in table 6. We are using the laminar layer model for *smooth* surfaces, shown in figure 13, for this calculation, rather than the more probable statistical «micro-eddy» model used for figure 14, because we want to calculate the *maximum* contribution from molecular diffusion, and although the micro-eddy model seems to work for the laboratory experiments, it has not been established that this is the correct model for the oceans. In order to get a maximum contribution, let h_V at the interface be 1, and h_M at the top of the laminar layer be 0.75, about the mean value of h over the oceans. Then the maximum diffusional contributions to $\Delta\varepsilon$ are 4.3 permil for HDO and 8.0 permil for O^{18}, to be compared with the total $\Delta\varepsilon$ values of 14 and 3 permil respectively estimated above. The diffusional contributions we list here are almost certainly a factor of two larger than the most probable maximum contributions. If the mean values of E and h are 1m/y and 0.75 over the sea, the *total* transport resistance for evaporation is 0.25 y/m.. The *diffusional* resistance is given by:

$$\rho_M = 0.6\,[Z_M(\text{cm})]\ \text{y/m}$$

where Z_M is the thickness of the laminar layer in cm. The gradient we used in (48) corresponds to the total resistance being diffusional, which requires $Z_M = 0.4$ cm, almost certainly too large as a mean value.

In any case, we see that while diffusional resistance can possibly account for the oxygen value of $\Delta\varepsilon$, there is an excess deuterium resistance amounting to at least 10 permil in $\Delta\varepsilon$ which cannot be accounted for by diffusion.

At the interface, we have from (8) $E = (1 - h_v)\Phi$, where Φ is the vaporization rate, equal to $(8 \times 10^4 \chi)$ meters/year, and χ is the condensation coefficient. Since the mean E is 1m/y, a

mean value of h_v allows us to estimate the mean condensation coefficient, χ_{sea}, over the ocean surface. χ_{sea} is the mean probability for a water molecule to surmount the energy barrier to be absorbed into the sea from just above the interface, or, it is the probability to surmount the energy barrier to escape from the sea surface.

The most detailed humidity profiles close to the sea are those of MONTGOMERY (1940). Extrapolating his profiles to the 1 meter level above the sea, we find values of h ranging from about 63 to 92 percent at this level. These values are directly correlated with his measurements of ΔT_4, the sea surface temperature minus the temperature at 4 meters, the humidity increasing as ΔT_4 decreases. All of MONTGOMERY's h values at one meter, greater than 90 percent, occur with ΔT_4 negative by about 0.4°C, so that the profile is stabilized by the temperature inversion. For the normal situation of ΔT_1 positive by 0.4 to 1°, about the oceanic mean value, the h values at 1m range from 0.67 to 0.89. There are not many data and we do not know how representative they are. But with such values at the 1m level, it seems to us that h_v cannot possibly be less than 0.85 as a mean oceanic value for the interfacial humidity. Using this as a lower limit for h_v, then from the value of Φ given above, we obtain a *lower limit* for χ_{sea} of 8×10^{-5} If χ_{sea} is not at least equal to this, the interfacial resistance is too large to allow the observed evaporation rate.

We now want to calculate an upper limit for χ_{sea} from the isotopic data. We can do this from the deuterium $\Delta\varepsilon$ value, because as we have shown there is demonstrably an excess transport resistance for this isotope which cannot be due to vapor-phase molecular diffusion. (We are here assuming that this excess resistance is not due to liquid-phase diffusion, on the grounds that quite similar excess values were observed in the CGH experiments on isolated liquids in which a diffusional gradient could not exist at the isotopic steady state).

We assume that there is no turbulent contribution to $\Delta\varepsilon$, so that only the first two terms of (28) are involved. Then using the numerical value of Φ given above, we have:

$$\chi_{sea} = \frac{1.25 \times 10^{-5}(K - 1)}{\Delta\varepsilon - (\Delta\varepsilon)_M} \qquad (49)$$

where $(\Delta\varepsilon)_M$ is the molecular diffusion contribution given by (48); we take this as the maximum estimate of 4.3 permil, and we take $\Delta\varepsilon$ itself as 14 permil as given by (47). Then the upper limit for χ_{sea} is simply $1.25 \times 10^{-6}(K-1)$.

Since χ must be positive, we learn from the experimental data that K_D is greater than 1, so that if the theory is correct we have $\chi > \chi_i$, showing that H_2O condenses and escapes faster than HDO, which is reasonable. An absolute upper limit on K can be obtained by equating it with the maximum ratio of the rates of O-H to O-D bond breaking at 25°C; this can be calculated to be 10.6 (WIBERG, 1955). Then the upper limit for χ_{sea} is 1.2×10^{-2}. Thus the absolute limits are approximately:

$$10^{-4} < \chi_{sea} < 10^{-2}$$

The maximum upper limit is thus of the same order of magnitude as ALTY's value for clean water of 0.04, referred to previously. If ALTY's value is indeed the correct one for sea water, then Ø is 3200 meters/year and the interfacial resistance is negligible for H_2O^{16} transport. However, it is very unlikely that K is as large as 10, but more likely that a realistic upper limit is about 2. $K\alpha^+$ is the ratio of the vaporization rate of pure H_2O^{16} to that of the hypothetical liquid HDO, and this is unlikely to be greater than about 2. If this is correct the upper limit for χ_{sea} is reduced to 10^{-3}, and the mean estimate will be of the order of 3×10^{-4}, about one percent of ALTY's value. This reduction of ALTY's value is in turn only one percent of the reduction produced by certain monolayers with which coefficients of 10^{-4} of ALTY's values have been obtained, so that it is possible that film resistance due to organic substances is important in determining the interfacial resistance of sea water. It is clear that if the isotopic condensation coefficients can be determined relative to that for H_2O^{16} a great deal may be learned about the surface effects on the sea.

The Atmosphere - Sea Exchange Model

The difficulties of treating the oceans as a whole are compounded by the varying regimes under which evaporation and exchange of moisture take place. Although in the early part of

this paper we have spoken rather loosely of a generalized meridional profile of the E/P ratio, in reality as JACOBS (1951) has shown, there are two quite different types of oceanic regions where maximum evaporation rates occur. One type is represented by the western boundary regions of the oceans, where the poleward flowing currents transport the surface waters into areas subject to the winter invasion of cold dry continental air. In the Atlantic this process is responsible for the high evaporation rate in the Gulf Stream in latitudes of about 35-40°N; a similar evaporation maximum is found in the winter in the Kuroshio off Japan, in latitudes of about 25-40°N.

The second type region is the tropical trade wind belt in each ocean between the equatorial trough and the subtropical high pressure zones, in which the dry descending air picks up the large mass of moisture carried down to the equatorial regions for precipitation. The trade wind regions are quantitatively the most important oceanic areas for moisture exchange because of the seasonal nature and relatively small areas of the western boundary processes. Within the 50 percent of the earth's surface from 30°N to 30°S, more than three-quarters of the total evaporation and precipitation take place. Therefore, in constructing a model for the isotopic balance in the atmosphere-sea exchange, we shall restrict ourselves to the physical characteristics of this region.

The structure of the tropical marine atmosphere has been studied and described by BUNKER, HAURWITZ, MALKUS, and STOMMEL (1949), RIEHL (1954), and MALKUS (1962). The general features of the region of the trade winds, between the equatorial trough and the subtropical highs, are shown in figure 15, using the terminology of BUNKER *et al.* The structure is shown up to the 2 km level which is roughly the extent of the moist, stable convective section in the outer trades. The top of the diagram is the trade-wind inversion which caps this section and separates it from the very dry upper troposphere above; the inversion altitude varies from about 2 km in the outer trades to almost 4 km near the equatorial trough, where it finally vanishes. Within the section shown the easterly trade winds pick up the moisture evaporating from the sea, precipitate about 27 percent of it locally, and transport about 60 percent of it down to the equatorial trough (MALKUS, 1962).

The most important characteristic of this region is the permanent presence within the section of a lower « homogeneous layer » which is exceedingly well mixed by turbulent stirring. In this layer the specific humidity decreases very rapidly in the first 10-20 meters above the sea and is then essentially constant up to about 600 m, where a thin stable layer just below cloud base is encountered. The stable layer marks the onset of the convective regime which transports moisture up to the overlying cloud layer where the trade cumuli are produced over the actively rising air; the thickness of this stable layer varies from 100-300 m, and within the layer the specific humidity drops off approximately linearly until the base of the cloud layer is reached. Above this layer is the « cloud layer » which is a second rather well-stirred layer of almost uniform humidity outside of the actual cumuli. In this layer convective mixing is dominant, and the mean motion is a large-scale subsidence, with local jets of rising air in the cumuli. The vertical extent of the cumuli is limited by the entrainment of drier air from outside the cloud which finally produces undersaturation in the rising jet and destroys the buoyancy by mixing.

The whole section consists of two well-mixed reservoirs of essentially uniform but different moisture content, separated by a thin layer of transition. Within the homogeneous layer the eddy diffusivity increases rapidly from the sea surface up to the base of the cloud layer, so that, in the terminology used in figure 13, the specific transport resistance per unit of altitude decreases very rapidly above the laminar layer and becomes vanishingly small above about 50 meters. Thus the total transport resistance for this layer is essentially determined when this height is reached.

The vertical humidity gradient between the sea surface and about 20 m is not well known. Measurements above deck level were made only by plane; these extend down to 8 m, but of course no fine structure was obtained. The only data at such low levels known to us are those of MONTGOMERY (1940), taken at much higher latitudes, and the earlier data of WUST which MONTGOMERY reviews. These data show a rapid decrease of specific humidity between the surface and 40 m; the variation is linear with the logarithm of altitude. In the trades the « altitude constant » is probably less than in the latitudes where MONTGOMERY

worked, so that the humidity decreases much more rapidly to the mean value for the homogeneous layer.

The variation of the isotopic composition of the vapor with humidity is given by equation (34). Let $\delta_I(O^{18})$ be —4 permil, equal to the mean value of δ_P for the earth, and assume the mean humidity near the surface to be 0.85. Then the gradient $(d\delta_z/dh_z)$ is 0.1 permil in δ per 1 percent in h. This is about half the value for an isolated water body as calculated following equation (27). In the present case the gradient varies as the square of the humidity, and of course varies with δ_I which locally is not equal to δ_P because E and P are not equal.

In table 7 we show data we have measured at five stations scattered over the world on the variation of the vapor isotopic composition with altitude. Vapor was collected as close to the sea surface as possible and high up on the mast. The collection height of the near surface samples was determined by the sea state and the pitch of the ship when the ship was held into the wind and maintained steerage at about 1-2 knots; the samples were collected 3-5 meters in front of the stem in order to avoid hull effects. Vapor is pumped through specially designed collection traps held at about —80°C which collect all the water. (The design of these glass traps which depend on shape variations and a fine filter to trap ice particles, and the development of the most efficient form, are due to the work of Dr. Y. HORIBE in our laboratory). The vapor is collected over a two to three hour period in order to get a representative sample and have enough water for the isotopic analysis. The analyses are made in replicate on 1 ml aliquots of the water collected. The reproducibility of the analyses is about 0.03 permil. All of the samples were analyzed at least in duplicate, and the first two sets were analyzed three to four times in order to be sure of the slight differences. The differences shown are all real except for the second Red Sea set, although collection errors are of course not precluded.

In any case, as shown in the table the differences, if truly representative of the air being sampled, are extremely small. In only one case, the Gulf of Aden, is the gradient in the direction expected for a decrease of humidity with altitude, i.e. a decrease of δ with altitude. Even this difference is only 0.1 permil. The humidity measurements are very difficult to make with high pre-

TABLE 7. — *Oxygen isotopic variations in marine vapor as a function of altitude (Z) above the sea surface. Altitudes are in meters; δ (O^{18}) in permil vs. SMOW.*

Area	Z (surface)	δO^{18} (surface)	Z (mast)	δO^{18} (mast)
W. Mediterranean	3	—11.21	13	—11.14
Red Sea	2.5	— 9.86	13	— 9.76
Red Sea	2.5	— 9.90	13	— 9.93
Gulf of Aden	1	— 9.61	13	— 9.73
N. Pacific (28°N)	1	—14.10	15	—14.00

Surface water = + 1°/₀₀ in Mediterranean and Red Sea; + 0.6°/₀₀ in the Gulf of Aden; about 0 °/₀₀ in N. Pacific.

cision. Spot readings are made in sequence and the variations are several percent due to instrumental inaccuracy and real fluctuations due to turbulence. For example in the N. Pacific set in table 7, the spot readings indicated that the specific humidity in the upper air was 1.8 percent higher than in the air at surface sample height, although the dry bulb temperature was 1 degree lower. Of course the samples are also collected sequentially rather than simultaneously, and since the sampling time is at least two hours and the ship's position as well as the wind can change, precise humidity data are not obtained. However, the close agreement of the isotopic data in table 7 indicates that the average specific humidity, averaged over an hour or so, did not differ by more than one percent between the two levels sampled. The measurements near the sea surface can be made only in very calm weather, so the data may not be indicative of mean conditions although we would not expect the gradient to increase with more turbulence.

As we mentioned earlier, the model in figure 15 can be taken to represent a local area in the trade wind region, or the entire equatorial region of the trades and the equatorial trough, or even the total ocean — atmosphere system. Since we are here discussing the general system in which P and E balance we take the model to represent the mean parameters for the total ocean. However the trades and the equatorial trough together constitute a system

which is essentially closed for moisture transfer, since only minor losses of atmospheric water (about 10 percent of the amount evaporated) leave the system. Therefore if the E and P rates of 1 m/y shown in figure 15 are taken to represent unit precipita-

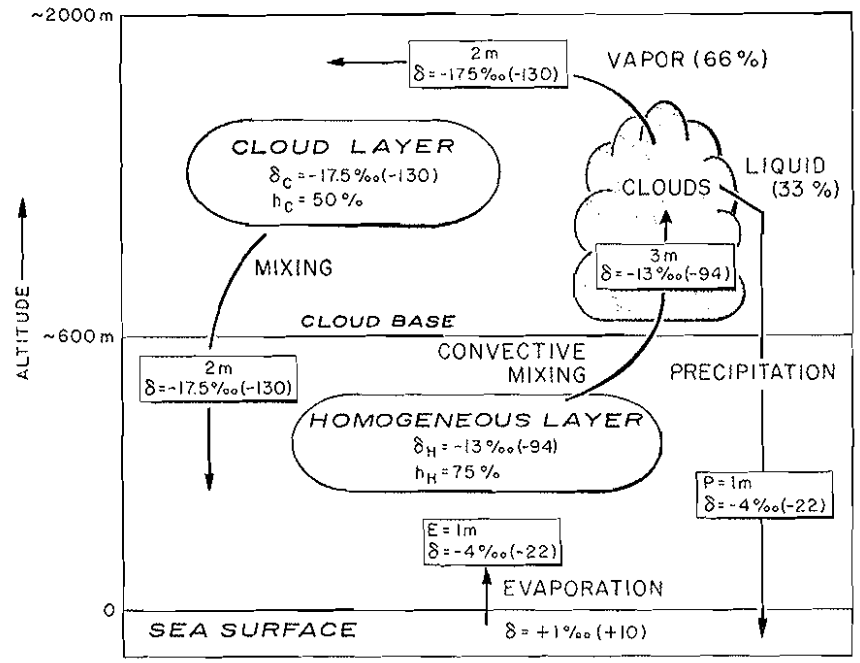

FIGURE 15. — *A model of the evaporation, mixing, and precipitation conditions over the sea, based on the atmospheric structure in the trade winds regions. The water transport values shown on the arrows, e.g. 2 m, represent meters/year of liquid water. The isotopic delta values give first* δO^{18}, *then in parentheses the corresponding value of* δD. *Data within the ovals marked « Cloud Layer » and « Homogeneous Layer » show the assumed values of relative humidity* (h), *normalized to sea surface temperature, and the assumed or calculated delta values for these atmospheric regions. The terminology is that of* BUNKER et al. (1949).

tion and evaporation rates, rather than actual amounts, the isotopic balance to be drawn up will apply approximately to the tropical regions as well as to the entire earth. We emphasize that no attempt has been made to use precise mean values of humidity, etc., since we are only discussing how the system works in the steady state.

The classical parameters assumed for the homogeneous layer and cloud layer (subscripts « h » and « c ») are the two humidity values, 75 and 50 percent, the mean annual E and P rates of 1 m/y (actual or unit values), and the heights of the sections, all as shown in figure 15. We recall that the « humidities » are the specific humidities or mixing ratios, normalized to the sea surface temperature.

The isotopic data assumed to be known are the delta values of the vapor in the homogeneous layer, δ_H, of the mean precipitation, δ_P, and of the surface water, δ^s_L. The data on marine vapor are not extensive; they consist of the data in figures 2, 3, and 4, and table 7. From the measurements shown in table 7, we can assume that at least the data in the N. Pacific (figure 2 and table 7) are representative of the homogeneous layer. (All the data in figures 2 and 3 refer to vapor collected at the mast heights shown in table 7). In any case, the δ-h correlation we have discussed above, which as calculated is in reasonable agreement with the data in figures 2 and 3, indicates that we can have some guidance from humidity data in choosing representative isotopic data. We have taken the assumed values for δ_H from the N-S profile data in figure 2, since the profile in figure 3 is very restricted in latitude. The mean values of δ_H taken are —13 and —94 permil for O^{18} and D; the surface water values taken are respectively +1 and +10 permil. All these data are shown in figure 15 with the O^{18} value listed first, followed by δD in parentheses. The δD surface water value has been taken from FRIEDMAN *et al* (1964); it differs slightly from the value of +5 permil (estimated from our own less extensive data) which we used to estimate the mean $\Delta\varepsilon$ in the previous section. None of the values used in the present discussion are very critical. The δ_P values have been given earlier in this paper, estimated from weighting the precipitation data.

As we have shown in our earlier discussion of the isotopic steady state and the restricted model which assumed that δ_P represents single-stage isotopic equilibrium with δ_H (i.e. the parameter which is δ_H in this physical model), the isotopic more-or-less steady state is fixed by the transport processes which fix the humidity. Specifically, this is fixed by the dependence of δ_E, the composition of the evaporating moisture, on δ_H, the composition of the vapor, as stated in equation (23). The liquid composition is

essentially constant because of the small amount of moisture in the atmosphere. When the vapor reaches the steady state composition, the evaporating flux has the composition of the liquid input. In the present model, however, we are placing no *a priori* restrictions on the precipitation mechanism or the isotopic equilibrium with any particular vapor.

The model is determined by three basic equations. The first is the simple mass balance for the system:

$$P = J(h_H - h_c) \tag{50}$$

where J is an exchange constant (equal to the moisture flux between the two layers if the air were saturated). This gives the fluxes of 3 m and 2 m water equivalent between the two layers, as shown in figure 15 on the arrows leading from each layer into the other.

The second equation is the steady-state correlation of isotopic composition and humidity given in equation (37), which becomes:

$$h_H(\delta_P - \delta_H) = h_c(\delta_P - \delta_c) \tag{51}$$

which gives the value of δ_c when the other parameters are known. The calculated values of δ_c are —17.5 and —130 permil for O^{18} and D. We note that the $\Delta\varepsilon$ equation is not an independent isotopic equation because of the isotopic balance requirement. Also the meteoric water relationship between D and O^{18} (CRAIG, 1961a) is not an extra relationship if all precipitation and vapor fall on this line. The calculated $\Delta\varepsilon$ values for the present model are 2.85 permil for O^{18} and 19 permil for D; the O^{18} value is the same as obtained earlier; the D value is larger simply because FRIEDMAN's higher value for δD of surface water has been used. The present value is just the average value of the CGH experiments, but we feel that the lower value given earlier is the more realistic.

The third equation is the isotopic relationship between precipitation and the water vapor values. Several precipitation models could be made, and it is noteworthy that the choice is restricted by the measured parameters. For example we could imagine that the precipitation originates from condensation of the homogeneous vapor *within the cloud layer*; that is, that the mixing process between the two layers is a simple exchange of air, and

that farther up in the cloud layer a convective process initiates precipitation from the mean vapor characteristic of the cloud layer itself. But the isotopic composition of the vapor in the cloud layer is fixed by (51), which, we note, is also an isotopic mass balance which can be derived quite independently of equation (37) for this two-layer model. In order to derive precipitation of composition δ_P from vapor of composition δ_c, using the values already fixed for these variables, we require fractionation factors of 1.0135 and 1.124 (α^+ values) for O^{18} and D, and from the vapor pressure data we find that the initial precipitation temperature must be less than —10 to —20°C. These temperatures are far lower than cloud layer temperatures which vary from about 22° at the base to about 12° at cloud tops.

Thus the isotopic data independently show that the precipitation takes place from ascending moisture from the homogeneous layer, as a part of the exchange process between the two layers. This conclusion is fixed as soon as the humidities of the two layers, and the δ values of precipitation and of the vapor in the lower layer are established. The same temperature requirement shows that the ascending vapor from the H layer is not simply stripped out in an « equilibrium box » in which uniform isotopic concentrations occur throughout the stripping region. It is necessary to strip the vapor by an inverse « batch distillation » process as was first pointed out by KIRSHENBAUM (1951) for the case of isotopic variations in continental precipitation.

The differential equation for this process is equation (1), which in integrated form applicable to the present case may be written:

$$\lambda_c - \lambda_H = \left[\frac{\varepsilon^+}{1 + \alpha^+(N_L/N_V)}\right] \ln [h_c/h_H] \qquad (52)$$

where λ is ln $(1+\delta)$, and for simplicity we have here taken α and the ratio of liquid to vapor phase in the cloud to be constant over the small integration range. These will be the mean values for the process. Then the mean value of ε^*, the single-stage enrichment, is fixed by the isotopic and humidity values and by the value assumed for the mean liquid water content of the cumulus. For example if ε^* (O^{18}) is 12 permil, the mean liquid water content is 8 percent. The minimum fractionation factor required in this

process for oxygen-18 is 1.011, which also corresponds to too low a temperature (about 4°C), but this is because we have over-determined the system by choosing the humidity value of the H layer and the flux P, together with δ_P,δ_H, so that (50) and (51) completely determine the system. Grossly, one can see that the system works, and we do not want to pursue the details in this paper, these must be worked out in applications to specific areas.

At the actual cloud base temperature the first precipitation to fall out will have δ values of about —3.5 and —22.5 permil for O^{18} and D, so that we see that the stripping process is possible, as the values are heavier than δ_P. The humidity values indicate that about 1/3 of the moisture is stripped out by precipitation, the remainder mixing into the cloud layer, as shown in figure 15. The entire cycle involving the exchange between vapor in the H layer with the sea, the stripping process in the cumuli, and the injection of the stripped H vapor into the C layer with consequent downward mixing from this layer, constitutes a feedback system which maintains the approximate steady state. As we have shown earlier, the deviation of the surface waters from the D-O^{18} plot of the precipitation and vapors is due to the $\Delta\varepsilon$ values reflecting the kinetic effects in the cycle. (The relationship for precipitation shown in figure 1 seems to represent equilibrium between liquid and vapor in the precipitation process, so that we assume all the fractionating kinetic processes occur in the evaporation process).

Moisture Exchange with the Continents

FRIEDMAN, REDFIELD, SCHOEN, and HARRIS (1964) have discussed the deuterium balance over the oceans in some detail. They present an entirely different model for the isotopic balance, based on the effects of interaction with the continents. We wish to mention briefly several points which disagree most with our interpretation.

In the first place they assume the immediate evaporate from the oceans is equilibrium vapor, and thus quite light relative to surface water. Regardless of any further mechanism in the atmosphere of the sea or the land, we have pointed out here that this requires that mean precipitation have this composition, and this

cannot be the case. The model we have presented shows how the experimentally observed kinetic isotope effects and the steady-state exchange act to produce an evaporate as heavy as the observed mean precipitation.

Secondly, they strip the evaporating vapor from the central Atlantic by local precipitation to account for the fact that the δ-S relation in surface sea water in this area shows that the slope corresponds to net loss of moisture of about —100 permil relative to the water. They equate this value of —100 permil with the net vapor *lost from the sea*, which they state has to be equal to the δD value of the average continental runoff, in order that the deuterium balance of the ocean and the continents be maintained. In order to get the vapor this light they have to raise it to an altitude of 2200 meters (to remove enough precipitation over the sea), and then transfer this vapor to the continents. They state that « the exchange of moisture between the ocean and land thus appears to take place in the main at relatively high altitudes, that is, above the cloud layers from which the local precipitation occurs ». However, they find that they cannot demonstrate from their data that continental precipitation averages —100 permil, so that they conclude that the information is far too scanty to make a quantitative balance.

In the first place it can be shown at once that the moisture exchange with the continents does not take place at altitudes such as 2 km, above the clouds. The water vapor transfer into the N. American continent has been studied in detail by BENTON and ESTOQUE (1954) and the transport as a function of altitude is well known. The maximum fluxes of vapor into the continent occur in winter at pressure levels of 800 mb on the west coast and 850 mb on the Gulf coast; in summer the maximum flux in through the Gulf coast is at 925 mb, and on the west coast the net flux is out of the continent at 700 mb. Except for the outward flux at 700 mb, the other fluxes, all inward, are well down in the upper part of the homogeneous layer and the lower part of the cloud layer; especially the S. Atlantic flux into the continent is within the homogeneous layer. This is well shown in the various plots given by BENTON and ESTOQUE.

Secondly, however, it is not this moisture which must balance with the continental runoff, but only the small fraction of the

moisture flux into the continents which actually runs off instead of passing out to sea again as vapor. The data of BENTON and ESTOQUE show that only 17 percent of this vapor flux into the continents remains on the continents in liquid form long enough to run off into the sea; the remaining 83 percent is transferred out in the vapor phase*. Put in terms of meters of water over the sea surface, as we have been using the fluxes, the vapor flux into the N. American continent is 0.6 meters of water; of this, 0.5 meters are exchanged back into the marine atmosphere as vapor, and 0.1 meters is the net precipitate over the land which runs off to the sea. Thus it is clear why the mean continental precipitation is much heavier than the actual moisture which is carried into the continent in the vapor phase: only a small fraction, enriched relative to the large vapor flux by the precipitation process, is taken out of the vapor as it moves across the land.

In our model (figure 15) this exchange can be indicated by arrows out from the H layer to the continents, showing an exchange flux with the values given in the last paragraph, with a net loss by vapor exchange of 0.1 m, which is returned by runoff. The vapor phase entering the continent, as shown in figure 15, already has a composition of —94 to —130 permil for δD, depending on the proportions of vapor withdrawn from the two layers. This composition is established by the oceanic processes outlined in the last section.

Where does the missing vapor go in the FRSH model? It goes to the equatorial trough for precipitation, as we have outlined. The principal balance for moisture over the ocean is simply the evaporation in the trades and precipitation in the trough, as is well established by the work of the WHOI group referred to in the last section. To first order, in considering the oceanic processes involving water, the continents simply do not exist, because of the insignificant amount of net precipitation on the land relative to the marine precipitation. The marine atmosphere is *almost* a closed system in itself.

---

* The BENTON and ESTOQUE data are summarized in metric equivalents and discussed in some detail by CRAIG and LAL (1961).

Applications to Local E-P-Salinity Relations in the Sea

In our earlier discussion of the isotopic — salinity relationships in surface waters, we noted in the discussion following equation (4) that δ_E varies over the ocean, and, since we could calculate only a mean value from the balance with mean precipitation, we found it necessary to assume that δ_E did not vary greatly. We now have an explicit equation for δ_E in any local area, which is obtained by setting δ^s_E, the steady flux composition, equal to δ_1 in equation (32) remembering that δ_1 is the mean composition of the liquid water input. We have:

$$\delta^s_E \approx \frac{(\delta^s_L - h\delta_A - \varepsilon)}{(1-h)} \tag{53}$$

where δ^s_L is the surface water composition, and h and δ_A are correlated as we have seen, so that they refer to measurements on the same vapor. Equation (53) is the isotopic balance for any local area of the sea. In addition to (53) we have three other equations in the simplified surface water model we discussed: (1) the mass balance, (2) the isotopic balance in terms of δ_E, δ_P, δ_o, and E,P, and two mixing fluxes with the larger reservoir of composition δ_o and S_o, and (3) the salt balance.

Assume we can measure the δ values for surface water in the area, for precipitation, vapor, and δ_o for the mixing water, and the values of h, S, and S_o, (salinities). Then we are left with five variables as follows: two mixing fluxes, and E, all three of these taken as *ratios* to the precipitation rate P, δ_E, and finally $\Delta\varepsilon$. If $\Delta\varepsilon$ can be determined the other four variables can be determined.

Additionally we have two isotopes to work with, so that potentially we can free more parameters to become unknowns. However, we do not yet know enough about the $\delta D - \delta O^{18}$ relationships in the sea to know if the equations are independent or simple linear transforms. This needs to be determined by very careful work on both isotopes in the same samples, and we are now engaged in such a study. Finally, of course, it has to be established that the $\Delta\varepsilon$ values can indeed be known in some independent manner, and this is at present the main limitation.

We shall not attempt to discuss the local variations in any detail using a variable δ_E over the ocean. Even assuming $\Delta\varepsilon$ to be constant with the mean values we have estimated, we do not have enough data on the isotopic composition of the marine vapor in different areas to be able to compute a meaningful δ_E. The partial derivatives of δ_E are: $(1-h)^{-1}$ with respect to δ^s_L; $[(-h)/(1-h)]$ with respect to δ_A; $-(1-h)^{-1}$ with respect to $\Delta\varepsilon$; all of the values being of about the same numerical magnitude, being respectively 4, —3, and —4, for $h = 0.75$. Relative to humidity we have:

$$\left(\frac{\partial\delta_E}{\partial h}\right) = \frac{(\delta^s_L - \delta_A - \varepsilon)}{(1-h)^2} \tag{54}$$

which has a value of about 0.32 permil per 1 percent variation of h, at normal humidity. From these relations it is clear that δ_E probably varies by several permil over the oceans so that it is a real variable in the set of parameters listed above. Therefore it is very necessary to study the problem of $\Delta\varepsilon$ and the isotopic condensation coefficients before a real application to local variations in the oceans can be made.

We have not discussed the problems of spray in the ocean and exchange of raindrops from the upper air with the lower air; these problems are still minor in relation to our present problems. Dr. Y. HORIBE has made some measurements recently on vapor collected seaward and landward of the surf zone at La Jolla and has found no detectable effect of the spray, but of course the problem must be studied in detail.

Tritium Exchange Rates Between the Atmosphere and the Sea

It was pointed out by CRAIG (1957) that the original estimates of the natural tritium production rate, calculated from the known transfer of tritium into the sea by marine precipitation, were far lower than rates calculated from oceanic mixing rates and also from the continental balance. This was attributed to the fact that most of the tritium must actually enter the sea by direct molecular exchange. CRAIG and LAL (1961) later showed, by normalizing

the tritium data with deuterium measurements on the same samples, that many of the early samples had actually been contaminated with tritium from pre-Castle nuclear devices, so that, in fact, the higher production rates, calculated by geochemical methods which did not depend on knowing the molecular flux, were reduced again to rough agreement with the cosmic ray data. This, however, did not invalidate the original argument, which is still correct. We shall show briefly how the molecular exchange rate can be estimated from the isotopic equations given earlier.

The molecular exchange flux (E_i) is given by (14); we assume here that there is no isotopic resistance in the liquid. The direct tritium flux into the sea by precipitation (F_P) is ($\alpha^+ PR_A$) where R_A is the T/H ratio in atmospheric vapor. We take the ratio of these fluxes, substituting for the isotopic resistance from (18) and for the transport resistance of H_2O^{16} from (12), obtaining:

$$\frac{E_i}{F_P} = -\left(\frac{E}{P}\right)\frac{[\alpha^*(R_L/R_A) - h]}{\alpha^+[1 - h + \Delta\varepsilon]} \tag{55}$$

(The precipitation flux is by definition negative in the sense of the equations). Neglecting the α terms which are close to unity, and the $\Delta\varepsilon$ term as small for the normal value of (1-h), then for a mean oceanic humidity of 0.75, we have:

$$[E_i/F_P] = -(E/P)[4(R_L/R_A) - 3] \tag{56}$$

where R_L is the ratio in the water. For the present day nuclear era, with R_L about 2 tritium units, and R_A from several hundred to a thousand tritium units, and taking E/P as 0.9 (treating continental runoff separately), we have a flux ratio of +2.7, (positive as *both* fluxes are into the sea). From the D-T normalization of CRAIG and LAL we take the pre-nuclear value of R_A for the marine atmosphere as 2.3 T units. The early ocean data are very erratic; let us use a value of 0.2 T units from the measurements of BUTTLAR and LIBBY. These values give a flux ratio of 2.4. So it is clear that as long as the tritium content of the liquid is small, the molecular exchange flux will be of the order of 2.5 times that carried in by precipitation. This can result in quite a different input distribution into the sea from what would be expected if the transport were all by precipitation.

SUMMARY AND CONCLUSIONS

In attempting to set down what we have learned about the variations in the isotopic composition of water in the marine environment, it has been necessary to range over many fields from physical oceanography through meteorology to chemical kinetics. It will be obvious to the reader that we are not experts in any of these fields; we have, moreover, attempted to cover as many aspects of the existing data and the possible applications to the marine sciences as possible, and this has necessarily resulted in a good deal of oversimplification of rather complicated problems. As in all new areas of research it has been necessary to treat very simple models, using the results of the classical studies in these fields to explain how the variations in the multicomponent system H_2O are produced. Only when the general nature of the processes involved in the isotopic fractionation of water in the atmosphere and sea are well understood, will it be possible to use the techniques outlined here for detailed studies of the real physical problems in specific areas.

We summarize here a few of the principal points we have tried to develop in this paper. In the first place, the isotopic variations in the ocean proper are extremely small, even on the scale of isotopic geochemistry. The principal deep water masses of the sea differ by only about 0.3 permil in oxygen 18 content and about 3 permil in deuterium content. It has therefore been necessary to expend a great deal of effort to improve existing methods to the point where we can work reproducibly over long times with a precision of about 10 percent of these deep water variations, i.e. to $\pm$ 0.02 permil in O^{18} and $\pm$ 0.2 permil in D variations.

When this is done, however, the deep water relationships in the sea are remarkably displayed on the isotopic-salinity charts (figure 12). The classical theories of the origin of deep water masses are in many cases graphically confirmed: the North Atlantic Deep Water is shown to have a purely convective origin; the Pacific and Indian Ocean Deep Water have compositions which do not match any surface waters in these oceans and clearly do not form by deep convection in these basins, and the effects of freezing

in forming bottom water in the Weddell Sea, well-known to oceanographers, are very clearly demonstrated by the isotopic data.

We show in figure 12 that there is a real problem of what we call the « third component » in the origin of Pacific and Indian Deep Water; the isotopic composition and salinity of these waters cannot be explained by simple two-component mixtures of characteristic water masses, e.g. the Antarctic Bottom Water and the North Atlantic Deep Water. Detailed isotopic studies in the southern oceans should be very helpful in working out the exact details of the processes by which the deep waters are renewed in these regions.

The isotopic variations in the surface waters are produced by the processes of precipitation, evaporation, mixing, and in some cases freezing, just as the salinity variations are so produced. The differing properties of the isotopic species, such as melting point, vapor pressure, and the differing rates of transport through the path of the water cycle, insure that the isotopic composition is not a simple, fixed function of salinity, and result in markedly different types of correlations of isotopic composition with salinity in different regions and water masses of the sea. In other instances very similar types of correlations occur in different regions of the sea, produced by different processes. A striking case of this is the similarity of slopes in the δ-S plot produced by evaporation and precipitation in the equatorial region and by freezing effects in high southern latitudes. Such instances complicate the picture but result in a diversity of compositions of sea water which are most useful for studying oceanic processes.

A start has been made on characterizing the isotopic composition of the principal water masses, especially of the deep waters (table 3). The core waters are of course remarkably uniform, but with the increased precision of measurement such features as the mixing of North Atlantic Deep Water with the underlying Antarctic Bottom Water, resulting in a range of little more than 0.1 permil in δO^{18} in the NADW, can be seen. Such measurements are potentially useful for deep water studies because of the conservative character of the isotopic composition at the lower boundary of the sea where enthalpy changes result from the heat flux.

A simple model for the isotopic-salinity correlations in the surface waters has been developed. We show that contrary to

what has been assumed, the mean composition of the evaporating water flux from the sea, the resultant of the exchange process, cannot be equilibrium vapor in single-stage equilibrium with the sea water. We show first that this follows from the simple material balance with the precipitation, whose weighted mean composition over the earth has been reasonably well established. We then show that a very simple model, in which it is assumed that the variation of the isotopic composition of the evaporating vapor is rather small over the oceans, coupled with a simple mixing model for balancing the E—P deficit or surplus in different regions, serves in a general way to explain the isotopic correlations with salinity in the surface waters Of course exact agreement cannot be expected, as we show later that the isotopic composition of the evaporate does vary as a function of the atmospheric humidity and other parameters. In a gross way, however, it is clearly seen that the surface water variations are simply the result of the evaporation and the marine precipitation over the sea.

We also show that the principal cause of the isotopic variations in surface sea waters cannot be the interaction of the permanent ice regions of the earth with the atmosphere and the sea, because of the small magnitude of the effects. To first order, the ocean simply acts as if there were no continents and permanent ice regions, because of the small areas and low precipitation rates in these regions. The surface water isotopic effects can only be understood by examining the effects of precipitation over the sea, and especially the effects of evaporation, very carefully.

This leads us to the ocean-atmosphere interaction and the kinetics of the exchange process. We show first of all that there are *three* types of water vapor which must be considered and clearly distinguished in discussing the sea:

(1) The net evaporate, or vapor flux, from the sea surface.

(2) The vapor which would be in isotopic equilibrium with the sea surface,

(3) The actual vapor over the sea which can be collected and analyzed.

These three vapor types have quite different characteristic isotopic compositions; the heavy isotope concentration *decreases* in the order: (1), (2), (3). Vapor type (2) is in fact hypothetical; it has been universally assumed to exist at sea but it never occurs outside of laboratories, except perhaps in brief intervals of temperature inversions over the sea surface.

The vapor relationships are well shown in a $\delta D - \delta O^{18}$ diagram of the type in which we show the relationship we have previously established for the meteoric waters of the earth (figure 1). In such a diagram, the deviation of the actual vapor, type (3), from the hypothetical vapor, type (2), is the resultant of two vectors representing different processes: a humidity effect, which insures that type (2) vapor can never occur unless the humidity is at saturation value (almost never the case over the sea), and a kinetic effect resulting from the differing isotopic transport rates in the exchange process. Even in the absence of the kinetic effect, the humidity effect insures the absence of vapor type (2).

The difference of the vectors in the $\delta D - \delta O^{18}$ diagram for these two effects is shown by the following conclusion: the kinetic effect produces an *offset* of the meteoric water line (figure 1) from the point (or narrow range) in the diagram occupied by the surface waters representing the moisture sources. The humidity effect does not produce an offset; it is similar to a multi-stage distillation process in that the vapor and liquid phases are simply pushed apart along the equilibrium meteoric water line. A four component diagram can be plotted in $\delta D - \delta O^{18}$ space, showing the relationships between the three vapor types listed above and the surface sea water. In a simplified model in which the precipitation is related to the vapor type (3) by single-stage isotopic equilibrium, these four components occupy the corners of a parallelogram whose sides have slopes of 8.0, corresponding to the equilibrium slope of the meteoric water line, and about 5.5, corresponding to the slopes in $\delta D - \delta O^{18}$ space taken up by evaporating water bodies on the continents relative to their input waters. The lengths of these sides of slope 5 reflect the magnitude of the kinetic effect.

The CGH experiments showed that the rapid molecular exchange with the atmosphere, which produces a stationary isotopic state in an evaporating liquid with no input, is characterized by

a kinetic effect which cannot be explained by the differences in molecular diffusion coefficients of the isotopic species, nor by the effects of hypothetical fractionation by turbulence. This is shown by the fact that deuterium is characterized by an *excess* transport resistence which cannot be accounted for by diffusion as the diffusion effect is too small. More important is the fact that the magnitude of the effect relative to the oxygen 18 effect is quite different from that predicted from straightforward diffusion theory.

The nature of the effect has been developed in terms of an interfacial disequilibrium in which an important contribution to the isotopic fractionation is produced by the differences in isotopic « condensation coefficients », or activation energies needed to surmount the energy barrier for evaporation. From the oceanic effects, crude limits can be set on the mean condensation coefficient, which can be interpreted as the sticking probability or barrier penetration probability, for water molecules on the sea surface. It is found that the effect is only of the order of a percent of the total condensation resistance which can be produced by the action of certain organic monolayers on a fresh water surface.

One is led to the suspicion that it might be worthwhile to study the possible variation of the oceanic condensation coefficient in different regions by these isotopic techniques, because of the implications for climatic effects if the interfacial resistance is an important part of the total resistance to evaporative transport over the sea.

The contribution of molecular diffusion to the isotopic fractionation in the exchange process can be calculated on the basis of a hydrodynamically smooth surface (the model in figure 13), with a fixed laminar layer, or from a statistical « micro-eddy » model for a rough surface which is directly in contact with turbulent eddies and supplies vapor to these eddies by diffusion. Assuming no turbulent contribution (from diffusional exchange *between* eddies) to the isotope effects, and assuming the turbulent transport resistance itself to be small in the experiments done to date, the statistical rough-surface model predicts the H_2O^{18} fractionation in these experiments (figure 14) but not the effects for HDO. The HDO effects are always larger than predicted, indicating that the condensation coefficient for this molecule differs significantly from

that for H_2O^{16} and this effect coupled with a significant undersaturation of vapor at the interface contributes an additional fractionation effect for HDO. The interfacial contribution for H_2O^{18} fractionation seems to be very small relative to the molecular diffusion effects in these experiments. The validation of these conclusions, however, depends on carrying out further experiments in which the turbulent resistance to transport of vapor is varied over a wide range, so that possible fractionation effects in turbulent transport, as proposed by PASQUILL, which could also produce the observed oxygen-18 fractionations, can be definitely evaluated.

From the theory of the isotopic evaporation and exchange rates, we develop the dependence of the isotopic composition of the evaporating flux, type (1), on the composition of the vapor phase, type (3), the humidity, and other variables. From this relationship the quasi-stationary isotopic state in the vapor over the sea, and in the liquid, is shown to follow directly from the feedback nature of the dependance of the isotopic composition of the evaporate on the other variables. A very simple model of the atmosphere-sea moisture balance over the sea is constructed, using the physical characteristics of the lower troposphere, below the trade-wind inversion, in the tropical oceans. In this model, it is found that the isotopic composition of marine precipitation, as observed, can only result from convective transport initiated in the upper part of homogeneous layer below the cloud layer, and cannot result from convective transport initiated up in the cloud layer. This of course is well known to be the actual case, so the result is not unexpected.

The moisture exchange with the continents is discussed, together with the major differences in our ideas about the oceanic moisture balance and in the well-known FRSH theory which attributes a major role in the oceanic isotopic variations to the interaction with the continents. We again emphasize our view that, to first order the continents do not exist for oceanic effects, and support this with a quantitative assessment of the amount of moisture involved with the land.

Finally, we show how the actual variation of the isotopic composition of the evaporating vapor over the sea is to be taken into account in the regional isotopic-salinity correlations discussed earlier, on the basis of a roughly constant composition, and discuss the number of variables and equations involved in such studies. We then use the equations developed for the isotopic flux between atmosphere and sea to calculate the ratio of the tritium flux by molecular exchange to the flux by precipitation into the sea, and show that the tritium input by molecular exchange is several times higher than the precipitative input in both the pre-nuclear and nuclear eras.

ACKNOWLEDGEMENTS

Many individuals have helped us very greatly throughout the course of this work. Professor Roger Revelle first explained the mysteries of the oceanic circulation to us, encouraged the work from its inception, and was a continuous source of enthusiasm. Professor Y. Horibe developed the Horibe traps, made a detailed study of the vapor at La Jolla, and measured the equilibrium isotopic fractionation factors. W. Dowd collected the N. Atlantic vapor samples on Expedition Zephyrus, and aided the senior author in many ways on Expedition Carrousel. Norman Anderson did the hydrographic work and salinity measurements on expeditions Monsoon and Zephyrus, and Fred Dixon helped us rig sampling gear and aided us in countless ways on both these expeditions. R. Fisher obtained the Proa trench samples for us. We are also grateful to the scientific staff and crew of the Antarctic Research Ship *Eltanin* for their willing cooperation in obtaining important samples for us, and to the Antarctic Research branch of the National Science Foundation for making this possible. In the laboratory Everett Hernandez has been responsible for the care and feeding of the spec trometers Samson and Delilah, and Miss Bea Hom and Mrs. Sara Drais have done outstandingly careful analytical work. The senior author gratefully acknowledges the tenure of a Guggenheim fellowship while visiting at the University of Pisa, the hospitality of Professor Tongiorgi in the Laboratorio di Geologia Nucleare in Pisa where many of these ideas were generated, and very helpful discussions with Profs. Athos Ferrara, Porthos Longinelli, and Aramis Gonfiantini in that institution. Professor Giovanni Boato of the University of Genoa was a willing and helpful listener to many problems. Our research has been supported by the National Science Foundation, grants GP-1885 and GP-3347, and grants G-24479 and GP-3140 which supported Expeditions Zephyrus and Carrousel; by the Office of Naval Research on grant no. 2216 (23); and locally by the Water Resources Institute of the University of California, which has supported the research on evaporation problems, and by the Marine Life Research Program over the past year. To all of these agencies we record our gratitude.

REFERENCES

ANDERSON E. R., ANDERSON L. J. and MARCIANO J. J. 1950. A review of evaporation theory and development of instrumentation. *Interim report*: Lake Mead Water Loss Investigations. *U.S. Nav. Electronic Laboratory Report 159*, San Diego, Cal.

BENTON G. S. and ESTOQUE M. A. 1954. Water vapor transfer over the North American continent. *J. Meteorology* 11:462.

BIERI R., KOIDE M. and GOLDBERG E. D. 1964. Noble gases in sea water. *Science* 146:1035.

BOLIN B. and STOMMEL H. 1961. On the abyssal circulation of the world ocean. - IV. Origin and rate of circulation of deep ocean water as determined with the aid of tracers. *Deep-Sea Research* 8:95.

BONNER F. T., ROTH E., SCHAEFFER O. A. and THOMPSON S. O. 1961. Chlorine-36 and deuterium study of Great Basin lakes. *Geochim. Cosmochim. Acta* 25:261.

BULL C. 1958. Snow accumulation in North Greenland. *J. Glaciology* 3:237.

BUNKER A. F., HAURWITZ B., MALKUS J. S. and STOMMEL H. 1949. Vertical distribution of temperature and humidity over the Caribbean Sea. Papers *Phys. Ocean. Met., M.I.T. - WHOI*, Vol. 11, no. 1.

CRAIG H. 1954. Carbon 13 in plants and the relationships between carbon 13 and carbon 14 variations in nature. *J. Geology* 62:115.

— 1957a. Isotopic standards for carbon and oxygen and correction factors for mass-spectrometric analysis of carbon dioxide. *Geochim Cosmochim. Acta* 12:133.

— 1957b. The natural distribution of radiocarbon and the exchange time of carbon dioxide between atmosphere and sea. *Tellus* 11:1.

— 1957c. Distribution, production rate, and possible solar origin of natural tritium. *Phys. Rev.* 105:1125.

— 1958. A critical evaluation of radiocarbon techniques for determining mixing rates in the oceans and the atmosphere. *Second U.N. Conf. Peaceful Uses Atomic Energy*, Conf. 15/P/1979, U.N. Publication.

— 1961a. Isotopic variations in meteoric waters. *Science* 133:1702.

— 1961b. Standard for reporting concentrations of deuterium and oxygen-18 in natural waters. *Science* 133:1833.

— 1963. The natural distribution of radiocarbon: Mixing rates in the sea and residence times of carbon and water. *Earth Science and Meteoritics, F. G. Houtermans anniversary volume*, Ed. J. Geiss and E. D. Goldberg, North-Holland.

— 1965. The measurement of oxygen isotope paleotemperatures. This volume.

— Isotopic exchange effects in the evaporation of water: 2. Theory of the exchange process. (to be published in JGR).

CRAIG H., GORDON L. I. and HORIBE Y. 1963. Isotopic exchange effects in the evaporation of water: 1. Low-temperature experimental results. *J.G.R.* 68:5079.

CRAIG H. and DEVENDRA LAL. 1961. The production rate of natural tritium. *Tellus* 13:85.

DANSGAARD W. 1954. The O^{18} abundance in fresh water. *Geochim. Cosmochim. Acta* 6:241.

DANSGAARD W. 1961. The isotopic composition of natural waters. *Medd. om Grønland* 165:99.

DEFANT A. 1961. Physical Oceanography, Vol. 1. Pergamon Press.

EPSTEIN S. 1959. Variations of O^{16}/O^{18} ratio in nature and some geologic implications. *Researches in Geochemistry*, ed. P. Abelson, Wiley Press.

EPSTEIN S. and MAYEDA T. 1953. Variation of O^{18} content of waters from natural sources. *Geochim. Cosmochim. Acta* 4:213.

FOFONOFF N. P. 1956. Some properties of sea water influencing the formation of Antarctic bottom waters. *Deep-Sea Research* 4:32.

FRIEDMAN I. 1953. Deuterium content of natural water and other substances. *Geochim. Cosmochim Acta* 4:89.

FRIEDMAN I., REDFIELD A. C., SCHOEN B. and HARRIS J. 1964. The variation of the deuterium content of natural waters in the hydrologic cycle. *Revs. Geophysics* 2:177.

GONFIANTINI R. and LONGINELLI A. 1962. Oxygen isotopic composition of fogs and rains from the North Atlantic. *Experientia* 18:222.

JACOBS W. C. 1951. The energy exchange between sea and atmosphere and some of its consequences. *Bull. Scripps Inst. Oceanography* 6, no. 2, 27-122.

KIRSHENBAUM I. 1951. Physical properties and analysis of heavy water. McGraw Hill.

LEE A. 1963. The hydrography of the European arctic and subarctic seas. *Oceanogr. Mar. Biol. Ann. Rev.* 1:47.

LOEWE E. 1960. Notes concerning the mass budget of the Antarctic inland ice. *Antarctic Meteorology*, pp. 361-369. Pergamon Press.

MAZOR E., WASSERBURG G. J. and CRAIG H. 1964. Rare gases in Pacific ocean water. *Deep-Sea Research* 11:929.

MALKUS J. S. 1962. Large-scale interactions. Chapter 4, *The Sea*, Vol. 1, Interscience.

MARCIANO J. J. and HARBECK G. E. 1952. Mass-transfer studies. US Geol. Survey Circular 229: Water-loss investigations: Vol. 1 - Lake Hefner Studies, 46.

MERLIVAT L., BOTTER R. and NIEF G. 1963. Fractionment isotopique au cours de la distillation de l'eau. *J. Chim. Phys.* 60:56.

MONTGOMERY R. B. 1940. Observations of vertical humidity distribution above the ocean surface and their relation to evaporation. *Pap. Phys. Ocean. Met., MIT-WHOI*, Vol. 7, n. 4.

MONTGOMERY R. B. 1959. Salinity and the residence time of subtropical oceanic surface water. *C-G Rossby Memorial Volume*, Oxford University Press.

PASQUILL F. 1943. Evaporation from a plane, free-liquid surface into a turbulent air stream. *Proc. R. Soc. London A* 182:75:

RIEHL H. 1954. *Tropical Meteorology*. McGraw-Hill.

SCHRAGE R. W. 1953. A theoretical study of interphase mass transfer. *Columbia Univ. Press.*

SUTTON O. G. 1934. Wind structure and evaporation in a turbulent atmosphere. *Proc. R. Soc. London A* 146:701.

SUTTON W. G. L. 1943. On the equation of diffusion in a turbulent medium *Proc. R. Soc. London A* 182:48.

SVERDRUP H. U. 1937. On the evaporation from the oceans. *J. Marine Res.* 1:1.

SVERDRUP H. U. 1951. Evaporation from the oceans. *Compendium of Meteorology* :1077. American Meteorological Society.

SVERDRUP H. U., JOHNSON M. W. and FLEMING R. H. 1946. *The Oceans*, Prentice-Hall.

WIBERG K. B. 1955. The deuterium isotope effect. *Chem. Revs.* 55:713.

ZUBENOK L. I. 1956. The water cycle of continents and oceans. *Doklady Akademii Nauk* 108:829.

Some results of oxygen isotope studies of marine waters

J. C. FONTES *, R. LETOLLE *, A. MARCÉ **

* *Laboratoire de Géologie Dynamique de la Sorbonne - Paris*
** *Present adress: Bureau de Recherches Géologiques & Minières - Paris*

INTRODUCTION

After the preliminary work by EPSTEIN and MAYEDA (1953), oxygen isotope analysis of sea water was carried out by various authors, such as CRAIG (1957, 1961a, 1961b), CRAIG and GORDON (1965), DANSGAARD (1961), LLOYD (1964). The data show that one can hope to get a better view of such phenomena as slow diffusion between different marine masses, upwellings or local pulsations. These phenomena are difficult to characterize.

DATA AND PROBLEMS

The Villefranche bay, about 4 km East of Nice, with an NNE-SSW axis, is a notch carved in the Jurassic limestones of the Nice Alpin arc (fig. 1). The isobaths go from 20 m in the Northern part of the bay, to some 300 m off Cape Ferrat. The bay opens on a submarine canyon bearing NE-SW, which is a tributary of the Baie des Anges canyon (BOURCART, 1957). This part of the coast is characterized by the lack of continental shelf: depths of more than 100 meters are found some 5 km off shore.

No rivers enter the bay, and no evidence exists of submarine karst fresh water springs. The annual pluviometry calculated on the last four years is 687 mm, measured at Cape Ferrat meteorological station.